Spring 2012

The effect of supercritical water on crude glycerin solution

Jared Bouquet

Department: Chemical and Biochemical Engineering

THE EFFECT OF SUPERCRITICAL WATER ON CRUDE GLYCERIN SOLUTION

by

JARED SCOTT BOUQUET

A DISSERTATION

Presented to the Faculty of the Graduate School of the

MISSOURI UNIVERSITY OF SCIENCE AND TECHNOLOGY

In Partial Fulfillment of the Requirements for the Degree

DOCTOR OF PHILOSOPHY

in

CHEMICAL ENGINEERING

2012

Approved
Sunggyu Lee, Advisor
Douglas Ludlow, Co-advisor
Yangchuan Xing
John Sheffield
Fatih Dogan

PUBLICATION DISSERTATION OPTION

This dissertation has been prepared in the style utilized by Energy and Fuels Pages 15-103 and the style utilized by Energy Sources, Part A: Recovery, Utilization and Environmental Effects pages 104-135. The content of those pages will be submitted for publication in those journals.

ABSTRACT

Crude glycerin solution, a principal byproduct of the conventional biodiesel process, was reacted in supercritical water using a specially designed Haynes® Alloy 282 reactor system for the production of hydrogen rich syngas. The effects of temperature, pressure, water-to-carbon molar ratio, reactor residence time, and glycerin-to-methanol weight ratio on the extent of carbon gasification and gas composition were explored. Based on the results, the extent and selectivity of reactions that concurrently occur when methanol and glycerin are in the presence of supercritical water were analyzed.

A decomposition reaction pathway for glycerin conversion to syngas was hypothesized, and then utilizing the results of the crude glycerin solution experiments, as well as experiments using pure methanol and pure glycerin with supercritical water, the hypothesized decomposition pathway was evaluated. Also an empirical equation was formulated to predict the gas composition and carbon gasification of crude glycerin using the reaction conditions of temperature and reactor residence time.

To gain a better understanding of how the functional groups of different hydrocarbon molecules react when exposed to supercritical water, experiments were also conducted to determine the effect of hydroxyl groups on hydrocarbons in supercritical water. These experiments used isopropanol, propylene glycol, and glycerin as monohydric, dihydric, and trihydric alcohol feeds. The effect that the number and the position of hydroxyl groups in the molecular structures had on carbon gasification and gas composition were determined at multiple temperatures, of hydroxyl groups were shown to have a great impact on the decomposition mechanism of hydrocarbons.

ACKNOWLEDGMENTS

I would first like to thank my advisor, Dr. Sunggyu Lee. Through his guidance, patience, and encouragement he has shaped me into the person I am today, and I cannot think of anyone I would have rather had as my advisor. It has been an honor to have been one of his students.

I would also like to thank Dr. Douglas Ludlow, Dr. Fatih Dogan, Dr. John Sheffield, and Dr. Yangchuan Xing for agreeing to be on my advisory committee and for the time and effort they have spent aiding me in my endeavors.

The help of my fellow graduate students, at both MS&T and Ohio University, is greatly appreciated. My special thanks go to Mick Stever, Jason Picou, and Dr. Jonathan Wenzel who helped in the construction of the experimental unit, and to Ryan Tschannen and Aaron Gonzales who aided me in the operation of the reactor system.

I would also like to thank everyone at Ohio University for accommodating me as a visiting scholar, especially David McCandlish for assistance provided in the GC/MS analysis of my liquid samples, and Oludamilola Daramola for his help with Gaussian.

For their financial support, I would also like to thank the Department of Education for their GAANN Fellowship and the Korea Institute of Science and Technology (KIST) for their partial support of the project.

Finally, I would like to thank my parents and my sisters for their moral support and encouragement throughout graduate school and all other parts of my life. I would also like to thank Blake, Matt, Lindsay, James, and Dan for being such great friends.

TABLE OF CONTENTS

LIST OF ILLUSTATIONS

LIST OF TABLES

1. INTRODUCTION

Discovering and utilizing alternative fuels as replacements for traditional fossil fuels has been a focus of the scientific community for many decades. From 2004 to 2009, global renewable energy capacity for many technologies grew 10-60 percent annually.[1] Still, in 2009 the United States used 6.04 quadrillion BTUs of fossil fuels, compared to 0.563 quadrillion BTUs of renewable fuel.[2] With the amount of fossil fuels utilized annually being over ten times that of renewable fuels, new innovation in the development and uses of alternative fuels is still required as a high priority.

One type of alternative fuel that shows promise is biodiesel. Biodiesel is a renewable biofuel produced from the oils of a variety of different crops, such as soybean oil, rapeseed oil, canola oil, sunflower oil, palm oil, flax oil, safflower oil, corn oil, algae oil, and many others. From 2004 to 2009 biodiesel production has increased 51 percent, with 16.6 billion liters produced globally in 2009.[1] One of the biggest advantages of biodiesel is the ability to be used in current diesel engines with little to no modification, allowing it to be used with current transportation fuel infrastructure.

Biodiesel is produced through the transesterification of triglycerides with primary alcohols, usually methanol or ethanol. This reaction between one mole of triglyceride and three moles of methanol makes three moles of biodiesel esters, and one mole of glycerin. This process normally uses a base such as potassium hydroxide or sodium hydroxide as a catalyst, but there is a catalyst free, continuous version of the process that utilizes supercritical methanol as a reactant.[3] In both processes excess alcohol reactant is used to drive the transesterification reaction to completion.

Unfortunately the production of biodiesel has some disadvantages. To remain profitable, most biodiesel industries must sell or get the best value of the glycerin byproduct that is produced. Since glycerin is non-toxic and sweet, it has many commercial uses such as being an ingredient in food additives, cosmetics, baby care products, embalming fluid, adhesives, and explosives.[4] Unfortunately the amount of glycerin being produced far exceeds the market demand. In 2005, replacing just two percent of diesel with biodiesel would have produced an extra 325,000 tons of glycerin, almost doubling the demand of 350,000 tons of glycerin a year based on the previous five years.[5] In addition the crude glycerin solution, which is typically a mixture of glycerin and excess methanol reactant, must undergo an energy-intensive purification process before it can be used commercially.

One solution is to use the crude glycerin with supercritical water for hydrogen production without going through any of the purification process. Reacting crude glycerin in supercritical water for hydrogen production not only provides a novel outlet for the excess glycerin being produced by biodiesel plants, but also allows for an increased amount of transportation fuel to be produced from the triglyceride feedstock. Using crude glycerin with supercritical water also has the advantage of not having to undergo an energy intensive separation process.

A chemical species becomes a supercritical fluid when it is above its critical temperature and pressure. Water's critical temperature and pressure are 374°C and 217.7 atm, respectively.[6] A supercritical fluid has properties similar to both liquids and gases. In addition non-polar molecules such as aliphatic hydrocarbons become more readily soluble in supercritical water than they are in ambient water.

One use of supercritical water is for the reformation of hydrocarbons into hydrogen and carbon monoxide. Due to the highly energetic nature of supercritical water as well as its highly solubilizing/homogenizing property, no catalyst is necessary for the reaction process, rendering the process great versatility as to the number of different feedstocks it can take. Supercritical water reformation has been used to make hydrogen from hydrocarbons such as jet fuel, sucrose, and ethanol.[7-13] While glycerin and methanol in the presence of supercritical water produce hydrogen and carbon monoxide, it is believed that they undergo decomposition instead of traditional reformation.[14, 15]

With such a wide variety of hydrocarbon fuels that can be used to produce hydrogen with supercritical water, mixtures of fuels besides glycerin and methanol may be used. However, since different hydrocarbons undergo different types of reactions based on their molecular structures, determining the impact of different functional groups in the molecular structure of the fuel is of the utmost importance. In this study, the role and effect of hydroxyl groups on the supercritical water reformation and decomposition of hydrocarbons in supercritical water environment were examined. The hydrocarbon fuels used to accomplish this objective were glycerin, propylene glycol, and isopropanol, all of which are C_3-alcohols.

The water gas shift (WGS) reaction is another prominent reaction when crude glycerin solution is in the presence of supercritical water. Carbon monoxide produced from the decomposition of glycerin and decomposition of methanol can further react with supercritical water by the forward WGS reaction to produce hydrogen and carbon dioxide. The water gas shift reaction is a reversible reaction, and the forward reaction is thermodynamically favored at temperatures below 815°C. [16]

The focus of the first paper presented in this work is the effect of different operating variables on the gas and liquid compositions and carbon gasification yield when a crude glycerin solution is reacted in a supercritical water medium. Specific operational variables examined include temperature, pressure, water-to-carbon molar ratio, space time, and glycerin-to-methanol weight ratio. Analyzing the results, the extent and selectivity of different chemical reactions that take place in the system were determined.

The first paper also focuses on the construction of the mechanistic reaction pathways of glycerin in supercritical water, which were elucidated from analysis of the gaseous and liquid products, and supported with findings from literature. An empirical equation was also formulated using the linear trends in gas composition found by varying temperature and space time. Using these equations, the relative amounts of product gases from crude glycerin decomposition can be determined.

The second paper presented in this work shows the effects hydroxyl groups in the molecular structure of hydrocarbon fuels have on the gas composition and carbon gasification when reacted in supercritical water. The effects of hydroxyl groups were determined across a range of temperatures to show their effect at different run conditions. The changes in gas composition and carbon gasification were analyzed to determine how the presence of hydroxyl groups influenced the decomposition or reformation of the different hydrocarbons.

2. REVIEW OF LITERATURE

2.1 BIODIESEL AND CRUDE GLYCERIN PRODUCTION

The process by which biodiesel is produced has a large amount of variation between biodiesel plants. As such, there is great variation in the resultant crude glycerin produced as a byproduct. The composition of the crude glycerin depends on a number of factors such as the oil that is used as the triglyceride, the type and amount of excess alcohol used, and the amount of type of catalyst used.[17] Figure 0 shows a general reaction for the production of biodiesel using methanol.

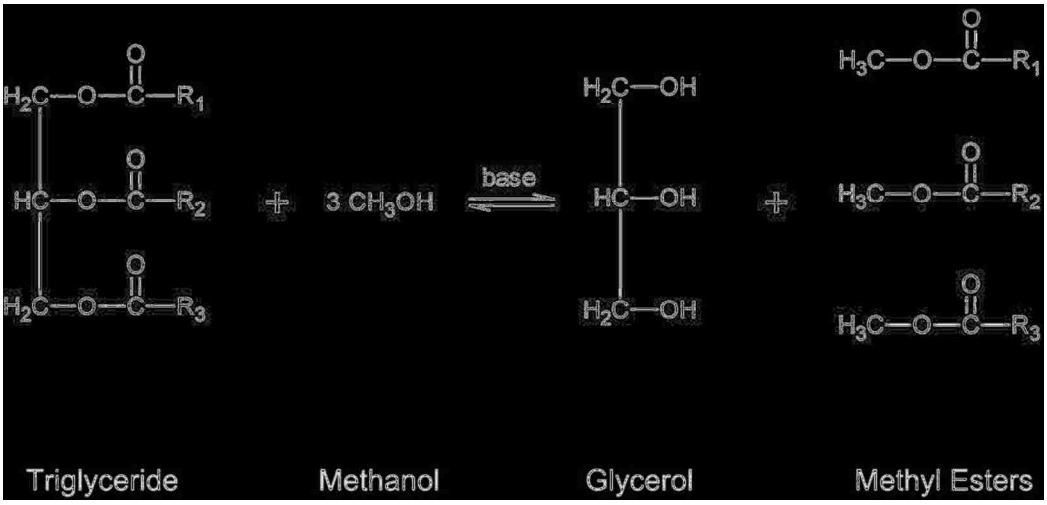

Figure 0 General transesterification reaction to produce biodiesel

Biodiesel is produced through a base catalyzed transesterification reaction between an alcohol and a triglyceride to make glycerin and biodiesel. Many types of triglyceride oils are used as a feedstock for biodiesel production. Table 0 shows the

compositions of various oils and fats that can be used for biodiesel feedstock. The table shows the lengths and number of double bonds in the carbon chains in each triglyceride, which correspond to what the molecular structure of the ester that will be produced.

Table 0 Composition of various oils and fats[18]

	Chain Length: Number of Double Bonds							
Oil or Fat	14:0	16:0	18:0	18:1	18:2	18:3	20:0	22:1
Soybean	0	6-10	2-5	20-30	50-60	5-11	0	0
Corn	1-2	8-12	2-5	19-49	34-62	trace	0	0
Peanut	0	8-9	2-3	50-65	20-30	0	0	0
Olive	0	9-10	2-3	73-84	10-12	trace	0	0
Cottonseed	0-2	20-25	1-2	23-35	40-50	trace	0	0
Hi Linoeic Safflower	0	5.9	1.5	8.8	83.8	0	0	0
Hi Oleic Safflower	0	4.8	1.4	74.1	19.7	0	0	0
Hi Oleic Rapeseed	0	4.3	1.3	59.9	21.1	13.2	0	0
Hi Erucic Rapeseed	0	3	0.8	13.1	14.1	9.7	7.4	50.7
Butter	7-10	24-26	10-13	28-31	1-2.5	0.2-0.5	0	0
Lard	1-2	28-30	12-18	40-50	7-13	0-1	0	0
Tallow	3-6	24-32	20-25	37-43	2-3	7-13	0	0
Linseed Oil	0	2-4	2-4	25-40	35-40	25-60	0	0
Yellow Grease (Typical)	2.43	23.24 16:1=3.79	12.96	44.32	6.97	0.67	0	0

The most commonly used alcohol in this process is methanol, since it limits water content that can interfere with the reaction, can lower yields, or create soaps as a product.[18] Usually methanol is fed at a 6:1 molar ratio instead of the stoichiometric 3:1 to drive the reaction to completion.[18] Using such excess quantities of reactant, methanol can constitute up to 40 weight percent of the crude glycerin solution leaving the process.[17]

Common base catalysts used for making biodiesel include sodium hydroxide, potassium hydroxide, and sodium methoxide, though acid-catalyzed processes and catalyst free processes using supercritical methanol exist as well. [3, 18] A relatively small amount of catalyst is needed, usually 0.3 kg of sodium hydroxide per 100 kg of oil.[18] After the reaction the base catalyst is neutralized with an acid, usually hydrochloric acid.

2.2 METHANOL DECOMPOSITION

There are number of reactions that methanol can undergo in the presence of supercritical water. The main reaction is methanol decomposition which is shown in Equation 1. The water gas shift reaction, which takes the carbon monoxide produced from decomposition and water to produce carbon dioxide and hydrogen, is shown in Equation 2. According to N. Boukis, another important reaction is methanation, which is shown in Equations 3 and 4.[15]

$$CH_3OH \rightarrow 2H_2 + CO \quad (1)$$

$$H_2O + CO \leftrightarrow H_2 + CO_2 \quad (2)$$

$$3H_2 + CO \rightarrow H_2O + CH_4 \quad (3)$$

$$4H_2 + CO_2 \rightarrow 2H_2O + CH_4 \quad (4)$$

According to Van Bennekom et al.[19] increasing temperature and space time increases carbon gasification, while increasing the weight percent of methanol in the solution decreases gasification. This has been shown in other work, as well as showing

that methane production increases with temperature and increasing concentration of methanol in the solution, with little to no methane production at temperatures below 600 degrees Celsius.[15, 20] The presence of base catalyst for biodiesel production in the methanol was shown to increase carbon conversion and inhibit the production of methane.[19, 21] In contrast, the presence of base catalyst had very little effect on the extent of water gas shift reaction occurring.[19]

2.3 GLYCERIN DECOMPOSTION

While methanol decomposition in supercritical water is fairly straightforward, the decomposition of glycerin is much more complicated. Glycerin decomposes through a series free radical and ionic mechanisms which produce a large number of intermediates, which in turn leads to a large number of chemical products.[14] At temperatures near the critical point of water, the ionic decomposition is important, while at higher temperatures the free radical decomposition becomes prominent.[14] Also primarily liquid products are produced near the critical point, and gaseous products produced at higher temperatures.[14]

There are a variety of liquid intermediates that are produced from glycerin decomposition in supercritical water. The first step of glycerin decomposition involves glycerin dehydrating into hydroxyacetone if a primary hydroxyl group is removed from glycerin or 3-hydroxypropanal if a secondary hydroxyl group is removed. Removal of the primary alcohol is more favorable unless in the presence of a catalyst.[22, 23] Other liquid intermediates include acetic acid, propanoic acid, acetaldehyde, propionaldehyde, allyl alcohol, ethanol, 1-propanol, formaldehyde, phenols, and acrolein.[14, 19, 24-27] Figure

shows a partial mechanistic pathway that produces 3-hydroxylpropanal, acetaldehyde, formaldehyde, and acrolein from glycerin.

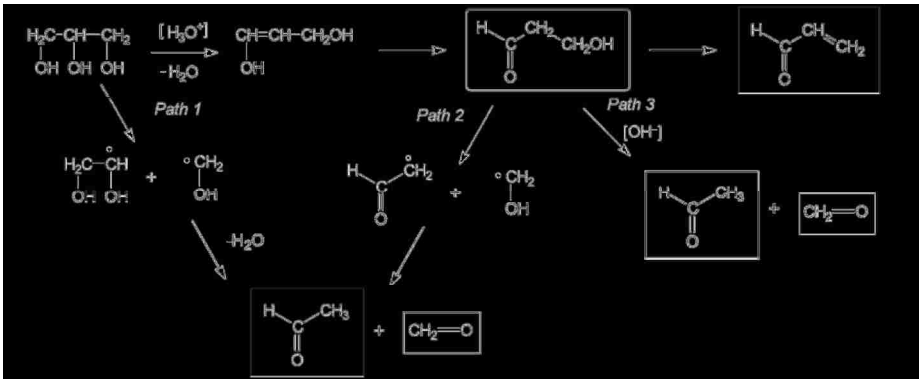

Figure 2.2 Glycerin decomposition pathways[14, 28, 29]

Gaseous products from glycerin decomposition in supercritical water include hydrogen, carbon monoxide, methane, carbon dioxide, ethane, ethylene, propane, and propylene. [14, 19] At temperatures below 500°C, gaseous products are minor.[14] However, increased temperatures leads to the liquid intermediates further decomposing into gaseous products.

A number of different reaction systems have been used for glycerin decomposition to make hydrogen. Some processes use near-critical and supercritical

water without catalysts. Other process use a packed bed or fluidized bed of catalysts ranging from nickel, platinum in γ-alumina, ruthenium, quartz, silicon carbide, copper, sulfuric acid, and others.[30-32] These catalysts can help increase gasification at lower temperatures and pressures, or improve the selectivity of certain reactions to favor the production of certain products and intermediates. Even with catalysts, these reaction systems sometimes carry out their reactions in supercritical water to achieve better conversion and gasification.[32]

2.3.1 Acetaldehyde Decomposition. The one of the primary intermediates species produced in glycerin decomposition is acetaldehyde. Acetaldehyde decomposes into methane and carbon monoxide through a free radical mechanism.[33] The mechanism is known as the Rice-Hersfield Mechanism and is detailed in the Equations 5-10. The entire process produces primarily carbon monoxide and methane, with hydrogen and ethane as minor byproducts. Propagation steps one and two, shown as Reactions (8) and (9), are the major reactions that account for a majority of the acetaldehyde decomposition. This mechanistic pathway also explains the mechanistic steps leading to methane and ethane formation.

$$\text{Initiation Step 1:} \quad CH_3CHO \rightarrow CH_3\bullet + CHO\bullet \tag{5}$$

$$\text{Chain Transfer Step 1:} \quad CHO\bullet \rightarrow H\bullet + CO \tag{6}$$

$$\text{Chain Transfer Step 2:} \quad H\bullet + CH_3CHO \rightarrow CH_3CO\bullet + H_2 \tag{7}$$

$$\text{Propagation Step 1:} \quad CH_3\bullet + CH_3CHO \rightarrow CH_3CO\bullet + CH_4 \tag{8}$$

$$\text{Propagation Step 2:} \quad CH_3CO\bullet \rightarrow CH_3\bullet + CO \tag{9}$$

$$\text{Termination Step 1:} \quad 2CH_3\bullet \rightarrow C_2H_6 \tag{10}$$

2.3.2 Formaldehyde Decomposition. The formaldehyde produced from glycerin decomposition breaks down further into hydrogen and carbon monoxide.[14] The formaldehyde is almost immediately broken down by other free radicals into carbon monoxide, and hence little to no formaldehyde comes out in the liquid effluent.[14, 32] In other words, formaldehyde may be regarded as a short-lived "fleeting" species in this reaction environment.

2.3.3 Acrolein Decomposition. Another intermediate produced from glycerin decomposition is acrolein. Acrolein is produced from the dehydration of 3-hydroxypropanal, which is the product of the dehydration of glycerin on the secondary alcohol.[24] While the dehydration of the primary alcohol on glycerin is preferred, the presence of an acid such as sulfuric acid, or of certain metal catalysts increases the selectivity of acrolein products.[14, 22, 26, 27] Acrolein decomposes into carbon monoxide and ethylene.

2.4 ISOPROPANOL DECOMPSOTION

Having two fewer hydroxyl groups than glycerin, isopropanol decomposition proceeds very differently from glycerin decomposition. Isopropanol thermally decomposes via dehydrogenation into hydrogen and acetone.[34, 35] The acetone may then further decompose into methane and ethanone.[36] The ethanone can then undergo one of

two decomposition routes. Two ethanone molecules can combine for bimolecular decomposition to produce ethylene and two carbon monoxides.[36, 37] Ethanone produced may also undergo hydration to acetic acid.[38] Acetic acid may then decompose into carbon dioxide and methane.[39] The chemical stoichiometric equations of all of the decomposition reactions described above are shown below.

$$\text{Isopropanol Decomposition:} \quad CH_3CHOHCH_3 \rightarrow CH_3COCH_3 + H_2 \qquad (11)$$

$$\text{Acetone Decomposition:} \quad CH_3COCH_3 \rightarrow CH_2CO + CH_4 \qquad (12)$$

$$\text{Ethanone Decomposition:} \quad 2CH_2CO \rightarrow C_2H_4 + 2CO \qquad (13)$$

$$\text{Ethanone Hydration:} \quad CH_2CO + H_2O \rightarrow CH_3COOH \qquad (14)$$

$$\text{Acetic Acid Decomposition:} \quad CH_3COOH \rightarrow CH_4 + CO_2 \qquad (15)$$

Any acetone produced by isopropanol dehydrogenation may also undergo free radical decomposition. In this free radical decomposition, acetone breaks up into a methyl radical and an acetyl radical.[40] This free radical decomposition can lead to higher order hydrocarbons as methyl groups add on to other acetone molecules.

Isopropanol may also undergo dehydration to produce propylene.[41, 42] Propylene then decomposes by a series of free radical reactions, which produce primarily hydrogen, methane, and ethylene, as well as small amounts of higher hydrocarbons.[43] This propylene may also react with hydrogen produced by other reactions to make propane, which undergoes decomposition by a different series of free radical reactions. [44]

It is also possible that in addition to the reactions given above, isopropanol may also undergo supercritical water reformation directly to hydrogen and carbon monoxide. Unfortunately there is currently no literature information on the subject. The proposed chemical equation for this direct reformation is shown below.

$$\text{Isopropanol SCW Reformation: } CH_3CHOHCH_3 + 2H_2O \rightarrow 6H_2 + 3CO \qquad (16)$$

2.5 PROPYLENE GLYCOL DECOMPOSTION

Propylene glycol in supercritical water has been shown to dehydrogenate to produce hydroxyacetone, also known as acetol.[45] Hydroxyacetone may then undergo decomposition into acetaldehyde and formaldehyde, or steam reformation to produce hydrogen and carbon monoxide.[26, 46] The chemical equations for propylene glycol dehydrogenation and hydroxyacetone decomposition and reformation mechanisms are shown in Equations 17-19.

$$\text{Propylene Glycol to Acetol: } CH_3CHOHCH_2OH \rightarrow H_2 + CH_3COCH_2OH \qquad (17)$$

$$\text{Acetol Decomposition: } CH_3COCH_2OH \rightarrow CH_3CHO + CH_2O \qquad (18)$$

$$\text{Acetol SCW Reformation: } CH_3COCH_2OH + H_2O \rightarrow 4H_2 + 3CO \qquad (19)$$

Another possible mechanism is the dehydration of propylene glycol to propionaldehyde.[47] The propionaldehyde may then decompose into ethane and carbon monoxide.[48] The chemical equations for this decomposition pathway are shown below in Equations 20 and 21.

$$\text{Prop. Glycol Dehydration}: \quad CH_3CHOHCH_2OH \rightarrow H_2O + CH_3CH_2COH \qquad (20)$$

$$\text{Propionaldehyde Decomposition}: \quad CH_3CH_2COH \rightarrow CO + C_2H_6 \qquad (21)$$

The first pathway involves the formation of aldehydes, viz., acetaldehyde and formaldehyde, as intermediates and/or byproducts, whereas the second pathway produces ethane as byproduct.

PAPER

1. DETERMINTATION OF A COMPREHENSIVE MECHANISTIC REACTION PATHWAY AND THE EFFECTS OF REACTION PARAMETERS ON THE DECOMPOSTION OF A CRUDE GLYCERIN SOLUTION IN SUPERCRITICAL WATER

1.1 ABSTRACT

Glycerin is a substantial byproduct of the transesterification reaction to produce biodiesel. With the expanded use of biodiesel as a renewable transportation fuel, the amount of glycerin produced has begun to greatly exceed the market demand. In order to offer the glycerin on the conventional chemical market, the crude glycerin solution containing excess methanol reactant must undergo an energy intensive purification. One possible alternative to this problem is utilizing the crude glycerin solution for hydrogen production through decomposition in supercritical water. This process would not only allow for an outlet where the excess crude glycerin can be used, but would also increase the amount of renewable transportation fuel produced from the triglyceride feedstock used in biodiesel production. Using a specially designed Haynes® Alloy 282 reactor system, the effects of temperature, space time, water-to-carbon molar ratio, pressure, and glycerin-to-methanol weight ratio on the decomposition of a crude glycerin solution in supercritical water were explored. Experimental reaction conditions were varied between temperatures of 500 to 700 °C, space times of 30 to 60 seconds, water-to-carbon molar ratios of 1.58 to 6.47, pressures of 3250 to 3750 psi, and glycerin-to-methanol weight ratios of 1.5 to 4. From the experimental results, a comprehensive mechanistic pathway for glycerin-to-syngas conversion was proposed and evaluated, and empirical equations

showing the linear trends in the production of the gaseous species of glycerin decomposition were formulated using temperature and space time.

1.2 INTRODUCTION

Biodiesel is an important renewable transportation fuel due to its ability to be used in conventional diesel engines with little to no modification. With approximately ten pounds of glycerin being produced for every hundred pounds of biodiesel, the supply of glycerin far exceeds the demand.[18] Using this excess crude glycerin for hydrogen production via decomposition in supercritical water has a number of advantages. One advantage is that the process is catalyst free and does not require the glycerin to be purified of the excess methanol beforehand. Another advantage is increasing the total amount of renewable transportation fuel produced per unit of triglyceride feedstock. Further, the process can be effectively operated on a small scale.

There are many types of triglycerides used in the production of biodiesel. With such a diverse feedstock, there are variations in the process that lead to variations in the resultant crude glycerin. In general, if the transesterification process uses 6:1 methanol to bio-oil ratio the resulting crude glycerin is between 60 and 80 percent glycerin with the balance being methanol.[17]

Water above its critical point of 374°C and 217.7 MPa becomes supercritical, and exhibits drastically different physical properties than ambient water.[6] Supercritical water has properties that are both liquid water-like and steam-like, and has an outstanding potential to serve as a very energetic reaction medium. In addition, organic molecules and

oxygen become readily miscible in supercritical water, which is not possible in ambient or subcritical water.

In the presence of supercritical water, glycerin and methanol both undergo separate decomposition reactions.[14, 15, 19] In methanol decomposition, methanol breaks down into carbon monoxide and hydrogen gas. The water gas shift (WGS) reaction can then utilize the carbon monoxide produced with water to produce carbon dioxide and more hydrogen gas.[16] Another reaction that is claimed to occur with methanol in supercritical water is methanation, though significant methane production was found to only occur at temperatures above 600˚C.[15, 20]

The mechanism for glycerin decomposition in supercritical water is more complicated than that of methanol. In supercritical water, glycerin first dehydrates to form either hydroxyacetone or 3-hydroxypropanal.[24] The hydroxyacetone can then decompose into acetaldehyde and formaldehyde. The formaldehyde readily decomposes further into hydrogen and carbon monoxide in the reactor's prevailing conditions, which may subsequently undergo the water gas shift reaction to produce carbon dioxide and more hydrogen.[14, 32] Acetaldehyde decomposes through a free radical mechanism that produces primarily carbon monoxide and methane, with trace of ethane and hydrogen.[49]

3-hydroxypropanal that is produced is relatively unstable, and is readily dehydrated into acrolein.[24] Acrolein can further decompose into carbon monoxide and ethylene.[50, 51] Acrolein can also be hydrogenated to produce propionaldehyde, which further decompose into ethane and carbon monoxide, or reacts with hydrogen to produce 1-propanol. In addition, due to the large number of carbonyl groups in the liquid

intermediates, higher order carbons can also be produced through aldol condensation and similar reactions.[24, 27]

1.3 EXPERIMENTAL

1.3.1 Materials. The chemicals used for the experiments were deionized water, 99.7 percent pure glycerol from the chemistrystore.com, and over 99 percent pure histological grade methanol from Fisher Scientific. Glycerin is hygroscopic and can readily absorb atmospheric water until it is only about 80 percent pure by weight.[52] To prevent an unknown quantity of water from getting absorbed into the glycerin, freshly unsealed glycerin was immediately diluted down to 75 percent purity. The water, glycerin, and methanol for the experiments were then mixed into solutions that had water-to-carbon molar ratios of 6.47, 4.22, and 1.58. A water-to-carbon molar ratio was used to ensure that the crude glycerin solution would be diluted equally for each experiment even though the solutions have varying amount of glycerin and methanol. These solutions contained glycerin-to-methanol weight ratios of 4, 2.33, and 1.5, corresponding glycerin-to-methanol molar ratios to 1.403, 0.812, and 0.520, respectively. This also corresponds to crude glycerin solutions of 80, 70, and 60 weight percent glycerin. Based on the glycerin-to-methanol weight ratio being used, the total moles of carbon in a glycerin/methanol mixture were calculated, and that solution was diluted down with the appropriate amount of water. Table 1 shows the compositions of the different solutions used in these experiments, as well as the critical points of the starting mixtures which were calculated in Aspen-Plus® using the property method of Peng-Robinson with Wong-Sandler mixing rules.

1.3.2 Reactor System. The supercritical water reaction system used in these experiments consists of a solution feed system, a solution preheating system, a Haynes® Alloy 282 high pressure reactor with heater, a liquid effluent collection system and a gas sampling system. The entire process operation is controlled by a Labview® data acquisition and control system.

The feed system uses an Eldex piston pump to continuously feed crude glycerin solution to the reactor system. The feed then enters an integrated heat exchanger and is heated by the high-temperature effluent leaving the reactor. Next is a preheating section that uses heat tapes to raise the temperature even higher. The solution then enters the Haynes® Alloy 282 reactor which is a high-nickel alloy with chromium, cobalt, molybdenum, titanium, aluminum, and iron.[53]

After exiting the reactor, the effluent goes back through the integrated heat exchanger to pre-heat the incoming feed, and then through a water-cooled heat exchanger. A control valve then brings the effluent back to atmospheric pressure, and the liquid and gaseous products separate. Samples of the liquid effluent are collected for each experimental run. The gaseous effluent goes through the gas sampling system and a wet-test meter to record the volumetric flow rate before being vented. Figure 1 shows a diagram of the entire reactor system.

Samples of the liquid effluent were collected at ambient conditions and stored in screw-top bottles. The samples were then analyzed using a Thermo Scientific ISQ gas chromatograph/mass spectrometer system. Before analysis, each sample was diluted using methanol to a 1/5 sample-to-methanol solution to reduce the relative amount of water in the sample, and also increase separation and reduce noise peaks.

1.3.3 Analytical. The samples collected of the gaseous effluent at ambient conditions were analyzed using a HP 5890 Series A gas chromatograph with a thermal conductivity detector. The chromatograph uses argon as a carrier gas, and was calibrated with a standard gas mixture from Praxair to detect hydrogen, air, carbon monoxide, methane, carbon dioxide, ethylene, ethane, propylene, and propane.

1.3.4 Procedure. The reactor system was regularly cleaned with sub- and supercritical water at the beginning and end of day's experiments were being conducted. An experimental run was considered complete when steady-state was achieved for the reactor system. An experimental run was considered to be at steady-state when two gas samples, taken over the course of an hour, had matching compositions and there were no significant changes in the gas volumetric flow rate.

The effects of many different process parameters were explored in this study. Process operating parameters explored include temperature (500-700°C), reactor space time (30-60 seconds), water-to-carbon molar ratio (1.58-6.47), pressure (3250-3750 psi), and glycerin-to-methanol weight ratio (1.5-4). Table 2 shows a list of the experimental runs and their run conditions.

1.3.5 Definitions. The temperatures specified for an experiment were measured by thermocouples in a thermowell running down the interior of the Haynes® Alloy 282 reactor. The space times were defined as 101ml internal volume of the reactor divided by the volumetric flow rate entering the reactor. The volumetric flow entering the reactor was calculated using Aspen® simulation software using the Peng-Robinson equation of state with Wang-Sandler mixing rules. This ensures that a uniform volumetric flow rate is

entering the reactor that takes into account the density changes of the crude glycerin solution that occur with different temperatures and pressures.

The carbon gasification was calculated as the moles of gaseous carbon leaving the system divided by the moles of carbon entering. The carbon in the gaseous effluent was determined using the average gas flow rate and average gas composition for the experimental run. Using the gas effluent flow rates, the carbon gasification percentages were normalized so that the highest carbon gasification would become 100 percent. The amount of carbon entering the reactor system was calculated using the feed mass flow rate with the weight percent of glycerin and methanol in the solution.

Hydrogen conversion is defined as the mole of hydrogen gas produced divided by the theoretical maximum number of moles of hydrogen gas that could be produced from the flow rate and composition of that experiment. The theoretical maximum mole of hydrogen assumes the complete conversion of glycerin and methanol into carbon monoxide and hydrogen, and all carbon monoxide subsequently undergoing the water gas shift reaction to produce more hydrogen gas. The theoretical maximum is seven moles of hydrogen per mole of pure glycerin, and three moles of hydrogen per mole of pure methanol. For the crude glycerin solutions, the theoretical maximum of hydrogen for the mixture was determined using the maximums for each of the pure species and the fractions of each species in the solution. Equations 1-5 show the stoichiometric equations used to calculate the theoretical maximums for hydrogen production.

$$\text{Glycerin Decomposition:} \quad C_3H_5(OH)_3 \rightarrow 3CO + 4H_2 \tag{1}$$

$$\text{Water Gas Shift:} \quad CO + H_2O \rightarrow CO_2 + H_2 \tag{2}$$

$$\text{Glycerin Decomposition + WGS:} \quad C_3H_5(OH)_3 \rightarrow 3CO_2 + 7H_2 \tag{3}$$

$$\text{Methanol Decomposition:} \quad CH_3OH \rightarrow CO + 2H_2 \tag{4}$$

$$\text{Methanol Decomposition + WGS:} \quad CH_3OH + H_2O \rightarrow CO_2 + 3H_2 \tag{5}$$

The gas composition of all experiments is given as moles of the gaseous species in the effluent per mole of carbon fed into the reactor. Because two different chemical species as source reactants were producing these gaseous products, it was not possible to non-dimensionalize the product gas results using moles of reactant fed. Using a basis of carbon fed ensured gas results would be comparable between all experiments, even those with different glycerin-to-methanol feed ratios.

1.4 RESULTS AND DISCUSSION

Table 3 shows a summary of the results of the experimental runs. The major gaseous species produced in the decomposition of crude glycerin are hydrogen, carbon monoxide, methane, carbon dioxide, and ethane. Some experiments in this investigation did show ethylene production, but it was only produced in trace quantities of less than 0.01 moles of ethylene per moles of carbon fed and therefore will be disregarded in the current analysis. There was no noticeable production of any gaseous C_3 hydrocarbons in any of the experiments performed for this investigation.

1.4.1 Analysis of Liquid Intermediates.

The liquid effluent leaving the reactor was analyzed using a gas chromatograph system with a mass spectrometer detector.

Figures 2-9 show the results of the liquid analysis for experiments at a range of temperatures, pressures, water-to-carbon molar ratios, and glycerin-to-methanol weight ratios. Each figure shows the residence times and relative abundance of each peak, as well as identifying the species that corresponds with each peak. Figures 11-18 show a sample total ion chromatogram (TIC) for each of the major species found in the liquid samples.

Figure 2 shows the liquid composition of experimental run WCG-112M, which was conducted at 600°C, 3500 psi, a 4.22 water-to-carbon molar ratio, a 70/30 glycerin-to-methanol weight ratio, and a 45 second space time. The primary liquid species produced in experiment WCG-112M were acetic acid, methyl propionate, hydroxyacetone, and propanoic acid. Other liquid species detected include 2-butanone, 1-propanol, allyl alcohol, cyclopentanone, propylene glycol, glycerin, and various phenolic compounds. Because methanol was used as a solvent to dilute the sample, it does not appear in the liquid analysis. Acetaldehyde and propionaldehyde do not appear in the liquid analysis because they readily undergo oxidation with atmospheric oxygen at room temperature and were converted into acetic acid and propanoic acid.[54]

Figure 3 shows the liquid species present in WCG-140M, which was conducted at the same experimental operating conditions as WCG-112M. Both experiments had similar values for carbon gasification (70.6% and 76.7%), so the amount of carbon present in the liquid samples should be approximately the same. Hydroxyacetone is the most prominent product, followed by a substantial amount of methyl propionate and 2-butanone. Acetic acid, propanoic acid, 1-propanol, allyl alcohol, cyclopentanone, propylene glycol, and phenols were also detected. So while WCG-112M and WCG-

140M produced the same liquid species, they were present in much different proportions. This is due to much less of the hydroxyacetone decomposing in experiment WCG-140M, while WCG-112M had a much greater amount of hydroxyacetone decompose to produce acetaldehyde, which was later oxidized to acetic acid.[24] The increased extent of carbon gasification in WCG-112M can be attributed to its further decomposition from hydroxyacetone to acetaldehyde and formaldehyde.

The liquid species present in experiment WCG-116M are shown on Figure 4. WCG-116M had a more concentrated water-to-carbon ratio of 1.58, but was otherwise operated at identical conditions as WCG-112M and WCG-140M. Due to the increased concentration of carbon in the starting solution, WCG-116M achieved a carbon gasification of only 48.6%. Overall, the chromatogram of WCG-116M looks very similar to that of WCG-140M, but with a slightly less prominent hydroxyacetone peak, and a larger relative abundance of acetic acid and propanoic acid.

Experiment WCG-122M has a more dilute 6.47 water-to-carbon ratio, but otherwise has the same run conditions as WCG-112M, WCG-140M, and WCG-116M. The gas chromatography and mass spectrometry results for WCG-122M are shown in Figure 5. While similar to the results of the previous liquid samples, the biggest difference is the decrease in the relative amount of 2-butanone, cyclopentanone, and phenols, while more acetic acid and propanoic acid are produced. The reason for this is because 2-butanone, cyclopentanone, and phenols, are all products of condensation reactions between two liquid hydrocarbon intermediates, and a more dilute solution would inhibit the MW-increasing reactions between liquid hydrocarbons.

Figure 6 shows the liquids that were produced in experimental run WCG-139M, which was conducted at 600°C, 3500 psi, a 4.22 water-to-carbon molar ratio, a 60/40 glycerin-to-methanol weight ratio, and a 45 second space time. The results are similar to WCG-140M, with the exceptions of a slightly higher relative abundance of methyl propionate and very small acetic acid peak. The higher abundance of methyl propionate can be attributed to an increase in the amount of methanol, which reacts with propanoic acid via esterification reaction to create methyl propionate.

The liquid analysis results for experiment WCG-138M are displayed in Figure 7. WCG-138M has a glycerin-to-methanol weight ratio of 80/20, but otherwise has the same run conditions as WCG-112M, WCG-140M, and WCG-139M. All experiments had similar carbon gasification, and the most noticeable difference in the liquid analysis results of WCG-138M is the decreased relative abundance of methyl propionate. Again, the amount of methyl propionate appears to correspond with the excess amount of methanol in the starting solution.

Figure 8 shows the liquid analysis for experiment WCG-109M, which was conducted at 600°C, 3250 psi, a 4.22 water-to-carbon molar ratio, a 70/30 glycerin-to-methanol weight ratio, and a 45 second space time. At this lower pressure the carbon gasification was only around 56.2%, and with the exception of the high relative abundance of methyl propionate, the results were otherwise similar to that of other experiments.

Experimental run WCG-119M, which is displayed in Figure 9, was conducted at 550°C, 3500 psi, a 1.58 water-to-carbon molar ratio, a 70/30 glycerin-to-methanol weight

ratio, and a 45 second space time. WCG-119M reached only a low carbon gasification of 14.9%, and hence most of the carbon from the solution still remains in the liquid effluent. This is evidenced by the large relative abundance of glycerin in the liquid sample analysis. The presence of hydroxyacetone, acetic acid, and propanoic acid is still relatively large, with peaks for 2,3-butadione and cyclopentanone present as well. The analysis result matches with the low reactivity of the glycerin decomposition as well as the incomplete reactions following the mechanistic pathway.

The liquid analysis results for experimental run WCG-111M, which was conducted at 700°C, 3500 psi, a 4.22 water-to-carbon molar ratio, a 70/30 glycerin-to-methanol weight ratio, and a 60 second space time was a run that reached 99.8% carbon gasification. The liquid sample reflects this by having no peaks for liquid species other than a small one for hydroxyacetone. The liquid analysis also verifies that the desired decomposition reaction of crude glycerin in supercritical water could reach a state of complete conversion, if the operating conditions are set accordingly.

1.4.2 Elucidation of a Glycerin-to-Syngas Mechanistic Pathway. Based on the liquid analysis of the samples from all of the experimental conditions, a conclusion can be drawn that basically the same set of liquid species is present in all samples. The primary liquid species detected in each of these experiments were hydroxyacetone, acetic acid, propanoic acid, and methyl propionate. Other substantial products included 2-butanone, 1-propanol, and phenols. Minor products include allyl alcohol, cyclopentanone, and propylene glycol.

Based on of the molecular species present analyzed in the liquid effluent, a comprehensive mechanistic pathway for the reactions of glycerin in supercritical water was elucidated. While a wide variety of intermediate liquid species are present, all of the reactions occurring can be summarized as one of the following four reactions: dehydration, hydrogenation, decomposition/pyrolysis, or condensation. With only those reactions, all of the liquid species found in the liquid effluent can be adequately accounted for.

The first reaction of glycerin in supercritical water is dehydration, which can produce one of two products depending on the hydroxyl group that is removed during the dehydration. If a primary alcohol group is removed, then hydroxyacetone is produced. If glycerin is dehydrated removing the secondary hydroxyl group, then 3-hydroxypropanal is the resulting product.

The 3-hydroxypropanal produced as an intermediate is relatively unstable at prevailing operating conditions and will either decompose into acetaldehyde and formaldehyde, or dehydrate further to form acrolein.[55] Any acrolein produced can further undergo a number of reactions. One of those reactions is decomposition into the gaseous products of carbon monoxide and ethylene.[50] Another possible reaction pathway is hydrogenation, either of the carbon-carbon double bond, or of the carbon-oxygen double bond. Thermodynamically, hydrogenation of the carbon-carbon double bond is more favored over hydrogenation of the carbon-oxygen double bond, so the conversion of acrolein to propionaldehyde is preferred over the production of allyl alcohol.[56] This corresponds to the results in the liquid analysis, where propionaldehyde was a relatively major product and the relative abundance of allyl alcohol was very small.

The hydroxyacetone produced from the dehydration of glycerin can also decompose into acetaldehyde and formaldehyde.[26, 57] Any formaldehyde produced is quickly converted into carbon monoxide and hydrogen.[14] Acetaldehyde decomposes via a free radical mechanism into primarily methane and carbon monoxide.[49]

Other reaction pathways of hydroxyacetone include hydrogenation to propylene glycol, which can then be dehydrated into acetone or propionaldehyde.[24, 47] Propionaldehyde produced from either the hydroxyacetone pathway or acrolein pathway can further undergo decomposition, where the primary products are carbon monoxide and ethane.[48] Hydrogen can react with the carbon-oxygen double bond in propionaldehyde to produce 1-propanol. Dehydration of 1-propanol results in propylene, and decomposition of 1-propanol results in acetaldehyde and methane.[58]

Acetone produced from propylene glycol thermally decomposes into methane and ethanone, and two ethanone molecules can react to produce two carbon monoxide and ethylene.[37] Hydrogenation of acetone results in isopropanol, which can be subsequently dehydrated to produce propylene.[35, 41, 42] Propylene produced from both 1-propanol and isopropanol can be converted to propane with the addition of hydrogen, and propane can decompose in methane and ethylene.[44]

Most of the liquid products produced with more than three carbons are the result of aldol condensation reactions, where the carbonyl group of one molecule reacts with the enol conjugate form of another ketone or aldehyde. While relatively minor products in the liquid samples, they still have a notable presence in each sample. The primary species involved with these condensation reactions is acrolein, which can react with acetaldehyde

to make cyclopentenone. The carbon-carbon double bond in cyclopentenone reacts with hydrogen to produce cyclopentanone, which is seen in the liquid samples. Acrolein can also react with propionaldehyde to produce 2-methyl cyclopentenone, which can be converted to 2-methyl cyclopentanone through hydrogenation. Phenol is created through the reaction of acrolein with acetone.[23] 2-Butanone is produced through the condensation reaction of acetaldehyde molecules, and methyl-phenols are the result of 2-butanone reacting with acrolein.

Because propionaldehyde and acetaldehyde are oxidized to propanoic acid and acetic acid at ambient conditions, it is unable to be determined whether propanoic acid and acetic acid are mechanistically occurring products of glycerin decomposition. Upon review of literature, sources that used metallic catalysts in the conversion of glycerin produced carboxylic acids, such as acetic acid and propanoic acid, while those sources that did not use metal catalysts reported little or no production of carboxylic acids.[14, 19, 23, 26, 27, 59] Because of this, it is believed no substantial quantities of carboxylic acid were produced during glycerin decomposition in supercritical water, and were only produced from atmospheric oxidation afterward. Methyl propionate found in the liquid samples was the product of the esterification of propanoic acid made from propionaldehyde oxidation and unreacted methanol.

Figure 19 illustrates the full reaction pathway of glycerin to its final gaseous products, and Table 4 summarizes the comprehensive list of decomposition reactions occurring, and Table 5 shows all of the possible pathways from glycerin to it final gaseous products and water. Because only trace ethylene was found in the gas effluent,

the assumption that all ethylene produced was hydrogenated by product hydrogen to ethane was made.

Using Gaussian simulation software, the enthalpies of reaction and Gibbs free energies of reaction were calculated for each of the reactions in the proposed mechanism. Table 6 shows the results of those simulations. Each quantum simulation was modeled at 600°C and 3500 psi, and was performed in an environment of zero dielectric constant to create an environment similar to supercritical water.[60] Specifically Gaussian 09 was used with B3LYP hybrid functional and the aug-cc-pVDZ basis set, and the calculations were carried out at the default levels of convergence in Gaussian. Analysis of the results reveals that dehydration reactions have largely negative ΔG values, and are exothermic unless the dehydration produces a carbon-carbon double bond, in which case the dehydration is endothermic. Reactions that hydrogenate a carbon-oxygen bond have positive ΔG values and are non-spontaneous, while hydrogenation of a carbon-carbon double bond is spontaneous. All decomposition reactions are endothermic and spontaneous, except the acetaldehyde decomposition which is slightly exothermic, and reactions involving ethanone. The decomposition of acetone to produce ethanone is non-spontaneous, and the decomposition of ethanone is spontaneous and exothermic, suggesting that the production of ethanone is unfavorable.

Using the ΔG of reaction, the mechanistic pathway in Figure 19 was reduced down to only those pathways from glycerin to gaseous products that only included spontaneous reactions. Figure 20 shows just these preferred reaction pathways occurring in glycerin decomposition into gaseous products. This preferred mechanism produces

primarily hydroxyacetone, acetaldehyde, and propionaldehyde as liquid intermediates, which matches the primary liquid intermediates found in the liquid samples.

Comparing this glycerin decomposition mechanism to the mechanism for supercritical water reformation, there are some key points verifying that decomposition is what is occurring when glycerin is in supercritical water. The first is that the bonds primarily broken in the decomposition mechanism are carbon-carbon bonds or carbon-oxygen bonds, which have substantially weaker bond energies than the hydrogen-oxygen and carbon-hydrogen bonds broken in reformation. Table 7 lists the typical bond energies for each type of bond. The second factor that shows reformation is not as feasible as decomposition is the methanation reaction, which is the source of methane production in the reformation mechanism.[61] Methanation is a reversible reaction, where hydrogen and carbon monoxide react to produce methane and water. Using the Gibbs free energies of formation, the equilibrium of the methanation reaction shifts in favor of hydrogen production at temperatures above ~750 K, or ~477°C.

1.4.3 Temperature. The first variable that will be examined is the effect of temperature on the decomposition of a crude glycerol solution in supercritical water. Figures 21-23 show the effect of temperature with different space times and water-to-carbon molar ratios. While the effect of temperature was determined at different space times and water-to-carbon molar ratios, all of the experiments used a constant pressure of 3500 psi and a glycerin-to-methanol weight ratio of 7:3, which is equivalent to a 0.812 glycerin-to-methanol molar ratio. The graphs show the trend in carbon gasification as well as the changes in gas composition with respect to temperature.

All three figures show similar trends for carbon gasification, with less than 15 percent gasification at 500°C to almost full conversion at 700°C. Similar trends also seen in the gas composition with the amount of all gases being produced steadily increasing with temperature, except carbon monoxide which begins to decrease around 650°C. The decrease in carbon monoxide is due to increased water gas shift reaction, which becomes very active at 650°C and showing a sharper temperature dependence than decomposition. This is not surprising, since in most syngas reaction environments the water gas shift reaction has shown stronger temperature dependence than the hydrocarbon decomposition reaction. Because carbon gasification is constantly increasing through the range of temperatures, determining the selectivity of reactions is difficult since the amount of all product gases are increasing. To better determine the selectivity of different products, the gas was also shown with respect to the amount of carbon reacted, rather than the carbon fed. To convert the basis from moles of carbon fed to moles of gaseous carbon reacted, all of the gas composition results were divided by the gaseous carbon conversion. The results are shown in Figures 24-26.

The gas composition based on moles of gaseous carbon reacted show a steady decrease in carbon monoxide production with increasing temperature, while methane, carbon dioxide and ethane increase. The hydrogen being produced per gaseous carbon with increasing temperature seems somewhat erratic by decreasing at first, then increasing. The initial decrease is due to the creation of more liquid intermediates that can be hydrogenated, thus removing hydrogen from the gaseous effluent. The increase in hydrogen at higher temperatures is due to increased reactivity of water gas shift reaction, as well as more complete gasification of liquid intermediates.

Since carbon dioxide is produced primarily through the water gas shift reaction and not from the decomposition of methanol or glycerin, the pre-WGS gas composition can be determined. This is achieved by taking the gas composition results per gaseous carbon and eliminating the carbon dioxide, and subtracting an equal amount from the hydrogen composition and adding the same value to carbon monoxide composition. By undoing the water gas shift reaction, the gas composition resulting from just the decomposition of glycerin and methanol can be obtained as shown. The pre-WGS gas compositions are shown in Figures 27-29.

Without the water gas shift reaction, the amount of carbon monoxide in the effluent gas is decreasing linearly with increasing temperature. Likewise, the amount of methane and ethane increase with increasing temperature. The moles of hydrogen per gaseous carbon decline steadily with increasing temperature after removing the water gas shift reaction. This is indicative that at higher temperatures there is relatively less hydrogen produced from formaldehyde decomposition due to an increase in acetaldehyde decomposition (and thus more carbon accounted for in the gaseous effluent), as well as an increase in other glycerin decomposition pathways that do not produce formaldehyde and acetaldehyde.

One last examination that can be done on the gas composition results is to take out the predicted gas results for methanol so just the gas composition of glycerol remains. Previous experiments show that at similar conditions, methanol decomposes into carbon monoxide and hydrogen, except at higher temperatures and water-to-methanol ratios where methane formation starts to occur.[20] To take the methanol out of the crude glycerin

gas results, the assumption that both methanol and glycerol decompose at similar rates at the same temperature must be made, which is fairly accurate.[19]

To remove the gas composition coming from methanol decomposition from the overall confounded gas results, the mole fraction of carbon coming from methanol was first determined, which is 29.1 mole percent methanol for a solution containing 7:3 glycerin-to-methanol weight ratio (0.812 glycerin-to-methanol molar ratio). Overall gas results are then reduced by the appropriate amount based on the mole fraction and predicted gas results from previous work at similar experimental conditions. For most experimental runs the carbon monoxide value was reduced by close to 29 percent of the total gaseous carbon accounted for, and hydrogen was reduced by twice as much. If the experiment was at a condition where methanol would produce substantial methane, the values were adjusted accordingly to match the gas results. The effect of temperature on the gas composition results with methanol removed are shown in Figures 30-32

With the gas results from the methanol removed, just the gas composition resulting from glycerin decomposition remains. Figures 30-32 all show increasing methane and ethane with increasing temperature, while carbon monoxide and hydrogen produced per gaseous carbon decrease with increasing temperature. Using these results, some insight on the effect of temperature on just glycerin decomposition can be obtained.

Utilizing the pathways for glycerin-to-final products shown in Table 5, it was hypothesized that due to the large amount of hydrogen seen in the gas results, those reactions pathways that produced hydrogen or consumed only a single mole of hydrogen occurred preferentially. Those pathways which involved multiple hydrogenation

reactions that consumed multiple moles of hydrogen before reaching their final products, were thought to not occur as often. That is to say that a majority of glycerin decomposition proceeded through pathways 1-5 as opposed to pathways 6-11 on Table 5. The stoichiometry of pathways 1-5 also correspond to the reactions present in the preferred pathway shown in Figure 20.

To verify that this is in fact the decomposition pathways primarily occurring, some stoichiometric calculations were conducted. Using the two independent stoichiometric equations in pathways 1-5 on Table 5, an equation was determined to calculate the moles of carbon monoxide that would be produced in the experiment using based on the amount of other gases present. Based on the Equation 1 below, Figures 33-35 show what the actual carbon monoxide produced is versus the carbon monoxide predicted by the sum of the other gases produced.

$$CO_{calculated} = [H_2] + [CH_4] + 2[C_2H_6] \quad (1)$$

Figures 33 and 34 show the calculated carbon monoxide values and actual values are relatively close, while Figure 35 matches up at higher temperatures, but not at lower temperatures. Points where the calculated and actual carbon monoxide values match show that the primary pathways of glycerin decomposition are the same as those shown in the preferred mechanistic pathway in Figure 20. Points that do not match up appear to follow the same trend as hydrogen, showing that inaccuracies in the calculated carbon monoxide value are the result of the experimentally determined hydrogen value. This is indicative of hydrogen gas created from glycerin decomposition hydrogenating other

liquid intermediates, and thus remaining in the liquid phase rather than appearing in the gas effluent.

Overall, when a crude glycerin solution decomposes in supercritical water, increasing temperature will result in increased carbon gasification and an increase in the amount of all gaseous species produced, except carbon monoxide. Also using moles of gaseous carbon to determine the selectivity of the different reactions that were occurring, it was determined that with increasing temperature the extent of forward water gas shift reaction occurring increased, and the amount of ethane being produced also increased with increasing temperature. The amount of hydrogen and carbon monoxide produced per gaseous carbon decreased with increased temperature due to an increase of decomposition of acetaldehyde and propionaldehyde, which produces less carbon monoxide and hydrogen per gasified carbon.

1.4.4 Space Time. The effect of space time was explored at three different temperatures of 550, 600, and 650°C with space time ranging from 30 to 60 seconds. For all of the experiments the water-to-carbon molar ratio, pressure, and glycerin-to-methanol molar ratio was kept at 4.22, 3500 psi, and 0.812, respectively. Figures 36-38 show the gaseous carbon conversion as well as the gas composition on a basis of carbon fed. The percentage of carbon gasification increases with longer space times, and the amount of each gaseous species produced increases with increased space time as well, except carbon monoxide at higher temperatures.

Like in the previous section, to get a better understanding of the selectivity of the different reactions the graphs were re-configured to a basis of moles of gaseous carbon produced rather than moles of carbon fed. Figures 39-41 show the effect of space time on

the gas composition on a basis of moles of gaseous carbon. At all temperatures the amount of methane and ethane seems to remain fairly constant with space time. With increasing space time, carbon monoxide decreases while carbon dioxide increases for Figures 40 and 41, while Figure 39 shows the amount of carbon monoxide staying relatively constant and carbon dioxide decreasing slightly. This means the relative extent of water gas shift reaction increases with increased space time, except at lower temperatures. Likewise, the amount of hydrogen produced at lower temperatures decreases with increasing space time, and at higher temperatures hydrogen production increases with increased space time. This is likely due to the inactivity of the water gas shift reaction at lower temperatures, and more hydrogen being produced from the water gas shift reaction at higher temperatures. At higher temperatures with a sufficiently long space time, the WGS reaction should go nearly to completion.

To examine what is happening regarding the decomposition of glycerin, reversing the water gas shift reaction from the experimental results, like what was done before with the temperature results, is necessary. Figures 42-44 show the effect of space time on the gas composition under a hypothetical situation where the water gas shift reaction had not occurred at all, i.e., mathematically subtracting the water gas shift reaction's contributions from the experimental results. With the water gas shift reaction undone, the only gaseous species to trend substantially with increasing space time is hydrogen which decreases at 550°C, stays fairly steady at 600°C, and increases at 650°C. At 550°C, the increased space time increases the amount of unsaturated liquid intermediates being produced while also giving hydrogen more time to react with them. At 650°C the solution gasifies quickly and more completely, so there is much less hydrogenation occurring.

After subtracting the predicted values for methanol decomposition so that just the gas results for glycerin decomposition remain, which is shown in Figures 45-47, the mechanism for decomposition was evaluated. This was done in the same manner as detailed in the temperature section, with the actual carbon monoxide production being checked against the predicted carbon monoxide production calculated from the other decomposition products. The results of the actual and calculated carbon monoxide values are shown in Figures 48-50. While some data points match nicely, meaning that glycerin decomposes to primarily acetaldehyde, formaldehyde, acrolein, and propionaldehyde as liquid intermediates, for other data points the calculated values start to diverge away from the actual carbon monoxide values. As was the case in the temperature results, the divergence in the space time results seems to follow the same trend as hydrogen. This again coincides with some hydrogen reacting directly with a liquid intermediates and not appearing in the gaseous effluent. The experiments at 550°C show an especially wide divergence at increased space times, which supports the assumption that at low gasification percentages and longer space times hydrogenation of liquid samples occurs more readily.

In summary, the effect of space time has a few effects on the decomposition of crude glycerin in supercritical water. With increasing space time the amount of carbon gasification increases. The extent of water gas shift reaction changes with space time, though at 550°C it decreases slightly with increasing space time, which suggests that the water gas shift reaction is not yet active at that temperature. At 600 and 650°C the extent of water gas shift reaction increases with increasing space time. Increasing space time seems to have little effect on the selectivity of the decomposition of glycerin, with little

change in the amounts of carbon monoxide, methane, and ethane being produced per gaseous carbon. However, at small carbon gasification percentages and increased space times, more hydrogenation of liquid intermediates occurs.

1.4.5 Water-to-Carbon Molar Ratio. The effect of water-to-carbon (W/C) molar ratio was also explored at temperatures of 550, 600, and 650°C. The W/C molar ratios used for these experiments were 1.58, 4.22, and 6.47, respectively. Table 1 shows the compositions of the different solutions in weight percents of glycerin and water. The space time, pressure, and glycerin-to-methanol weight ratio for these experiments were 45 seconds, 3500 psi, and 7:3, respectively.

Figures 51-53 show the effect of W/C ratio on the decomposition of a crude glycerin solution in supercritical water. The extent of carbon gasification increases with a higher W/C ratio, though at 600 and 650°C diluting from a 4.22 to a 6.47 solution seems to have no extra effect on the carbon gasification. The production of hydrogen slightly decreases over that same range, but that is likely the result of small decreases in the extent of the water gas shift reaction and carbon gasification. Otherwise the amounts of all gaseous species produced increases with increased water dilution.

Analyzing the gas composition on a basis of gaseous carbon exiting the reactor instead of carbon fed, the selectivity of reactions becomes more apparent. These results are shown in Figures 54-56. With increasing W/C ratio, hydrogen increases going from a 1.58 ratio to 4.22, then decreases slightly going to a 6.47 ratio. Carbon monoxide shows noticeable decrease with increasing W/C ratio, while carbon dioxide increases over the same period. This is directly indicative of increased water gas shift reaction with increased dilution. Increasing W/C ratio seems to have little effect on methane and

ethane, since they are produced from carbon-carbon bond cleavage and not a reaction with water.

The results with the water gas shift reaction undone are shown on Figures 38-40. With no water gas shift reaction, the only species showing a noticeable change with increasing W/C ratio is hydrogen. Figures 60-62 show the results with the predicted products for methanol removed. Again with increased W/C ratio, hydrogen increases at first, and then decreases. This trend is the result of more hydrogenation occurring with more concentrated glycerin solution, and more gasification of non-formaldehyde species in more dilute solutions. At 650°C, increasing W/C ratio shows a noticeable decrease in carbon monoxide while methane increases, indicating the decomposition of more acetaldehyde.

Figures 63-65 show the actual carbon monoxide verses the predicted carbon monoxide based on the decomposition mechanism mentioned in Equation 1. While some points match up closely with less than a 10 percent difference in values, others are very far off due to lack of hydrogen. This again indicates that some hydrogen is not accounted for and is reacting with a liquid intermediates.

Overall, the effect of W/C ratio on the decomposition of a crude glycerin solution seems varied. Increasing W/C ratio increases carbon gasification up to a point, after which further dilution has no effect and may even decrease carbon conversion. Likewise, with increasing W/C ratio hydrogen production increases to a point, and then begins to decrease. This is the result of increased hydrogenation in concentrated solutions and increased gasification of species that do not produce hydrogen in more dilute solutions.

The water gas shift reaction reactivity shows a slight increase with increasing dilution, while methane and ethane production remains constant. When checking if the glycerin decomposition mechanism was accurate, points with lower hydrogen did not match well. The lack of hydrogen is the result of hydrogen consumption by hydrogenation of a liquid intermediate, causing its deficiency in the gaseous effluent.

1.4.6 Pressure. Another experimental variable important to the decomposition of a crude glycerin solution in supercritical water is pressure. The critical point of water is 374°C and 217.7 atm (or 3199.3 psi), and the experiments showing the effect of pressure were performed at 3250, 3500, and 3750 psi so that they were all above the critical pressure of water. These experiments were performed at 600°C, a space time of 45 seconds, and a solution with a 4.22 water-to-carbon molar ratio and 7:3 glycerin-to-methanol weight ratio (0.812 molar ratio).

Figure 66 shows the effect of pressure on the carbon gasification and gas composition from crude glycerin decomposition per carbon fed. With increasing pressure, the carbon gasification increases about 10 percentage points going from 3250 to 3500 psi, and then decreases 5 percentage points going up to 3750 psi. The gas compositions all follow a similar trend of increasing and then decreasing with increasing pressure.

Looking at the gas composition per gaseous carbon leaving the reactor system, as shown in Figure 67, hydrogen decreases slightly with increased pressure. The amount of other gaseous species being produced stays relatively constant with increasing pressure. Figure 68 shows the gaseous results with the water gas shift reaction artificially undone. Again the only gas with any significant trend with increasing pressure is hydrogen, which is decreasing. The gas composition with the predicted methanol decomposition results

removed were shown in Figure 69, and Figure 70 shows the real carbon monoxide produced against that predicted from the expected glycerin decomposition mechanism. At lower pressure the suggested mechanism fits nicely, while at higher pressure the calculated carbon monoxide starts to deviate from the actual carbon monoxide due to the lack of hydrogen. This is likely due to increased pressures increasing the amount of hydrogenation of liquid intermediates occurring.

In summation, pressure seems to have relatively little effect on the decomposition of crude glycerin in supercritical water. Increasing pressure at first increases carbon gasification, but then begins to decrease after 3500 psi. Pressure seems to have little effect on the selectivity of reactions occurring, with only gaseous species to show any trend being hydrogen decreasing with increasing pressure. This decrease in hydrogen caused the decomposition mechanism for glycerol to deviate from the actual results, which is again due to an increase in hydrogen reacting with liquid intermediates.

1.4.7 Glycerin-to-Methanol Weight Ratio. The glycerin-to-methanol (G/M) weight ratios examined in these experiments were 1.5, 2.33, and 4. These correspond to crude glycerin solutions made up of 60, 70, and 80 weight percent glycerin and the balance methanol, and correspond to glycerin-to-methanol molar ratios of 0.520, 0.812, and 1.403. These solutions encompass the wide range of G/M ratios commonly found in biodiesel production before the glycerin undergoes purification.[17] These experiments were performed at 600°C, 3500 psi, 45 second space time, and a 4.22 water-to-carbon molar ratio.

Figure 71 shows the effect of increasing G/M ratio on gas composition and carbon gasification. Increasing the G/M ratio seems to have very little impact on carbon

conversion, with all solutions having conversions within 3 percentage points of each other. The similar carbon gasification with varying G/M ratios also demonstrates that the assumption of glycerin and methanol decomposing at the same rates is accurate. With increasing weight percent of glycerin, the amount of hydrogen decreases, carbon dioxide decreases then stays steady, and carbon monoxide increases and then decreases, which is due to increased amount of the water gas shift reaction for the experiment with 60 weight percent crude glycerin solution. Methane and ethane show little change with increasing weight percent glycerin.

The gas composition on a gaseous carbon basis is shown in Figure 72. The results seem similar to Figure 71, which makes sense due to the similar carbon conversions for each solution. Figure 73 shows gas composition with the water gas shift reaction undone. Besides hydrogen, which decreases with increasing G/M ratio, all other gas compositions stay constant with increasing G/M ratio. The decrease in hydrogen can be attributed to the increase in glycerin concentration in the starting solution, which in turn results in a higher concentration of liquid intermediates to hydrogenate.

The gas results with the predicted methanol decomposition taken out are shown on Figure 74. The data points in Figure 74 were normalized to take into account the differing amounts of glycerin and methanol between points. With increasing weight percent of glycerin, only hydrogen shows significant change increasing and then decreasing. To test the decomposition mechanism of crude glycerin, the actual carbon monoxide values were compared to the calculated values, and the results were shown on Figure 75. Like previous comparisons of the decomposition mechanism to the actual

results, some points are close while others fall short due to lack of hydrogen coming out in the gas.

Overall, the G/M ratio has little effect on the amount of decomposition occurring with carbon gasification being almost equal for all solutions. The extent of water gas shift reaction is slightly higher with lower G/M ratios, but otherwise there is little change in the gas composition. The increase in the WGS reaction at lower G/M ratios is likely the result of an increase in the amount of carbon monoxide produced per carbon, since methanol produces more carbon monoxide than glycerin. This is due to methanol producing one carbon monoxide mole per mole of carbon, where glycerin at most can produce two moles of carbon monoxide and a mole of methane per every three carbon atoms, or 2/3 moles of carbon monoxide per mole of carbon. The decomposition matches for some experimental runs, but there seems to be hydrogen that is unaccounted for, like in previous results.

1.4.8 Empirical Equation. The trends of the different gaseous species being produced with increasing space time and temperature appear to be linear. This is very evident on Figures 45-47, which show the effect of increasing space time on the amount of each gaseous species being produced per gaseous carbon coming out in the effluent after the water gas shift reaction is undone (mathematically taken out) and the methanol results are removed. Using the data in Figures 45-47, an empirical correlation showing the combining the effects of temperature and space time on glycerin decomposition was formulated. All experiments used for the empirical equation had a reactor pressure of 3500 psi, and used solutions with 4.22 water-to-carbon molar ratios and 7:3 glycerin-to-methanol weight ratios.

First, the linear regression values for each of the carbon containing gaseous species were calculated. The regression values for hydrogen were not evaluated due to hydrogen reacting with liquid intermediates. Table 8 shows the slope, intercept, and correlation coefficient for carbon monoxide, methane, and ethane as a function of space time at each of the three temperatures. The correlation coefficient for all three gaseous species at 550°C is very good, with all species having a correlation coefficient above 0.99.

Then it was assumed that the slopes and intercepts shown in Table 8 were all functions of temperature, as shown in Equation 1. Assuming that the function with respect to temperature was linear, Equation 2 was formed. Table 9 shows the linear regression values of the slopes and intercepts from Table 8 with respect to temperature.

$$\frac{Moles\ of\ gas}{Moles\ of\ gaseous\ carbon} = m(T) \times \tau + b(T) \quad (1)$$

$$\frac{Moles\ of\ gas}{Moles\ of\ gaseous\ carbon} = (m_1 T + m_2) \times \tau + b_1 T + b_2 \quad (2)$$

Table 3 shows that the linear fit with respect to temperature works very well, with only one of the six correlation coefficients below 0.9. Plugging in the values from Table 3 into Equation 2, Equations 3-5 are created, where T is temperature in Kelvin and τ is space time in seconds. Using Equations 3-5, the gas compositions can be expressed in terms of temperature and space time as:

$$\frac{Moles\ of\ carbon\ monoxide}{Moles\ of\ gaseous\ carbon} = (1.28 \times 10^{-5} T - 0.0125) \times \tau - 0.00190T + 2.26 \quad (3)$$

$$\frac{Moles\ of\ methane}{Moles\ of\ gaseous\ carbon} = (-5.03 \times 10^{-6} T + 0.0053) \times \tau + 0.00093T - 0.524 \quad (4)$$

$$\frac{Moles\ of\ ethane}{Moles\ of\ gaseous\ carbon} = (-2.98 \times 10^{-6}T + 0.0028) \times \tau + 0.00042T - 0.531 \quad (5)$$

To test the accuracy of Equations 3-5, experiments with the correct water-to-carbon molar ratio, glycerin-to-methanol weight ratio, and pressure had their gas compositions compared to what was determined with the equations. Table 10 compares the results of the calculated gas values using the equations above to the experimental values. For experiments used to derive the formula, the values predicted by it are usually within 0.03 moles of gas per mole of gaseous carbon. Runs at 500˚C and 700˚C were also compared to see how accurate the equations were when extrapolated at temperatures above and below the experiments used to develop the equations. Only the methane values at higher temperatures shows a large discrepancy between the actual and calculated values. Overall the equations are fairly accurate, and the regression values indicate a strong linear relationship between space time, temperature, and the amount each gaseous product being formed.

1.5 CONCLUSION

The reaction parameters affecting the decomposition of crude glycerin in supercritical water were experimentally investigated with respect to the mechanistic and parallel reactions. For the experimental conditions and levels considered in this study, the two variables with the strongest effect for increasing carbon gasification are temperature and space time. Increasing the water-to-carbon ratio increases carbon gasification to a point, but after a certain dilution it does not have any additional effect. The highest carbon gasification was achieved at 3500 psi, with higher and lower pressures resulting in

less gaseous conversion of carbon. Glycerin-to-methanol weight ratio had no noticeable effect on carbon gasification, providing a justification of the mechanistic claim that methanol and glycerin have very similar kinetic behaviors of decomposition.

The relative amount of the water gas shift reaction occurring increased with increasing temperature, space time, and water-to-carbon molar ratio up to a certain ratio. Changes in pressure seemed to have no effect on the water gas shift reaction, while increasing glycerin-to-methanol weight ratio decreases the amount of forward water gas shift reaction, since less carbon monoxide is produced per carbon in the solution.

By undoing the water gas shift reaction in the results, the mechanism for crude glycerin decomposition was determined. Based on previous work, methanol was determined to decompose into mostly carbon monoxide and hydrogen under most experimental conditions, with substantial methane production only at higher temperatures and low water-to-carbon molar ratios.[20]

Based on the liquid analysis of multiple samples, a comprehensive mechanistic pathway of glycerin decomposition to its final gaseous products was determined. Also based on the results of the Gibbs free energies of reaction for each of the reactions in the pathway, a favored reaction pathway was hypothesized as one where formaldehyde, acetaldehyde, acrolein, and propionaldehyde were produced and gasified.

Using this thermodynamically favored reaction pathway, the amount of carbon monoxide being produced was compared to the amount of carbon monoxide that would theoretically be produced based on the amount of other gases exiting the reactor. The results correlated quite well for a number of experimental conditions, especially those

with high carbon conversion. For experiments where the carbon monoxide values did not match up, the reason was from lack of hydrogen in the gas. This suggests the hydrogen reacting with liquid intermediates, and thus not exiting in the gaseous effluent. Hydrogenation with a liquid intermediate would also explain why the mechanism fits better at higher carbon gasification, since there is much less carbon for the hydrogen to react with in the liquid effluent.

The equations formulated using the linear regression of space time and temperature show a good fit to the experimental data. This suggests a linear relationship of the decomposition pathways of glycerin with both temperature and space time. The equation finds a practical value in designing an optimal process system as well as in carrying out a process economic study.

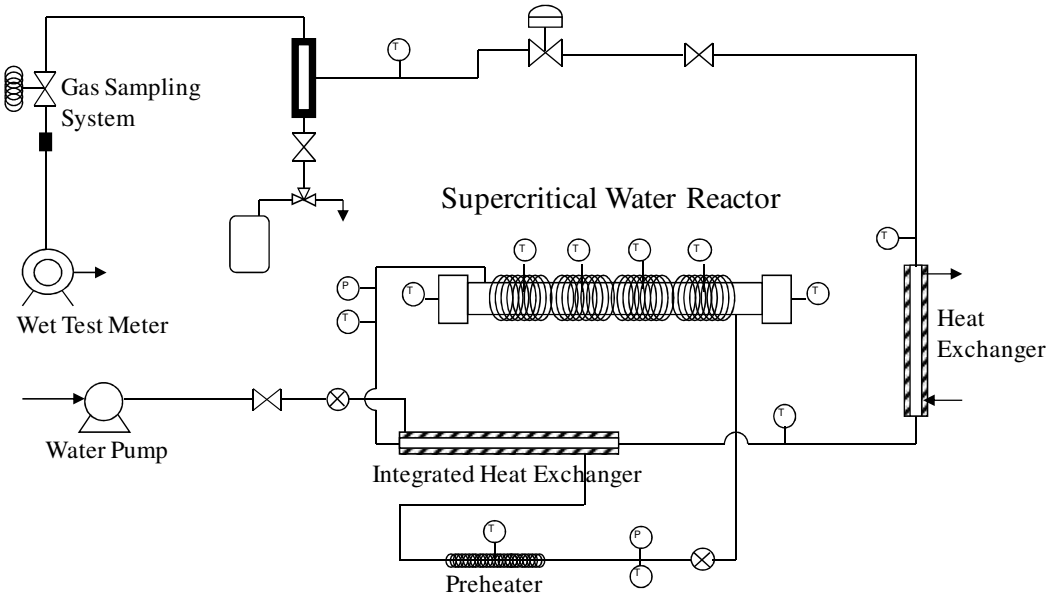

Figure 1. The multi-fuel reformation reaction system at Ohio University.

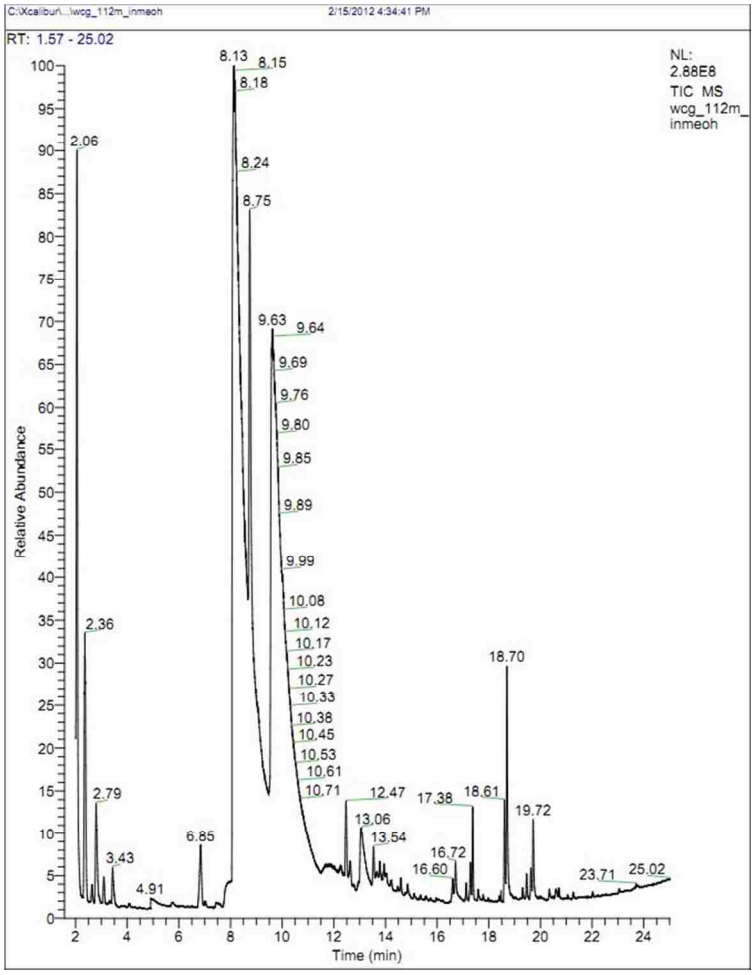

WCG-112M	
Residence time	Species
2.06	Methyl Propionate
2.36	2-Butanone
2.79	1-Propanol
3.43	Allyl Alcohol
6.85	Cyclopentanone
8.13	Acetic Acid
8.75	Hydroxyacetone
9.63	Propionic Acid
13.06	Propylene Glycol
18.70-19.72	Phenols
23.71	Glycerin
12.47, 13.54,16.72	Silicon Based Column Bleed

Figure 2. Gas chromatography/mass spectrometry results of liquid sample from experiment WCG-112M.

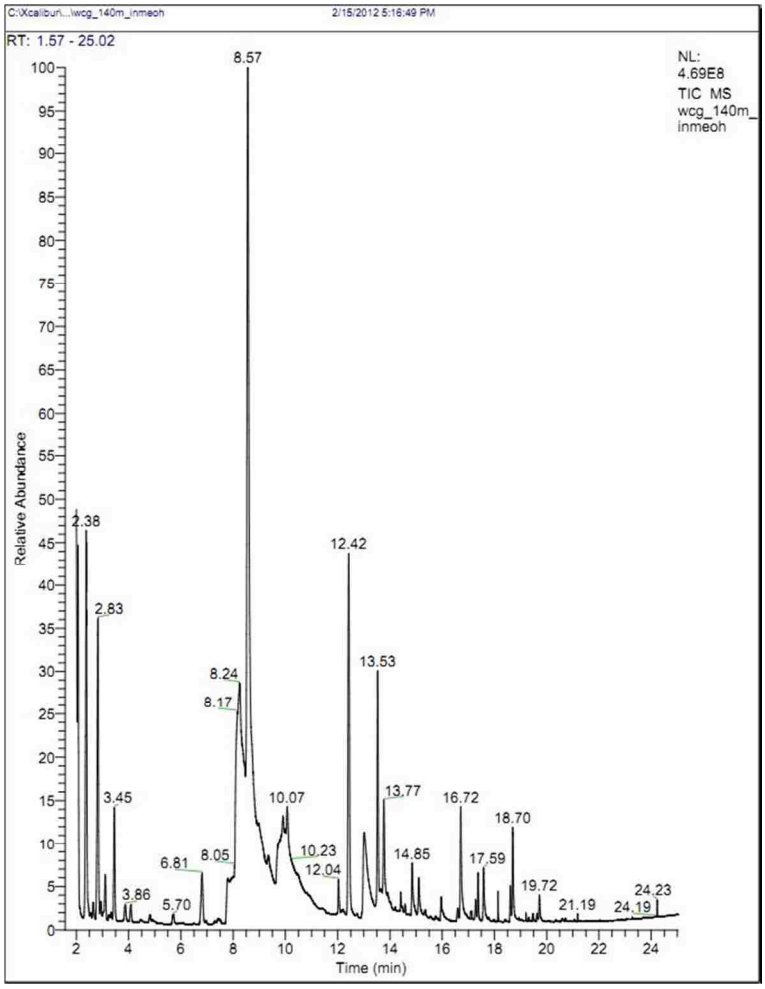

WCG-140M	
Residence time	Species
2.08	Methyl Propionate
2.38	2-Butanone
2.83	1-Propanol
3.45	Allyl Alcohol
6.81	Cyclopentanone
8.24	Acetic Acid
8.57	Hydroxyacetone
10.07	Propionic Acid
13.03	Propylene Glycol
18.70-19.72	Phenols
24.23	Glycerin
12.42,13.53,16.72	Silicon Based Column Bleed

Figure 3. Gas chromatography/mass spectrometry results of liquid sample from experiment WCG-140M.

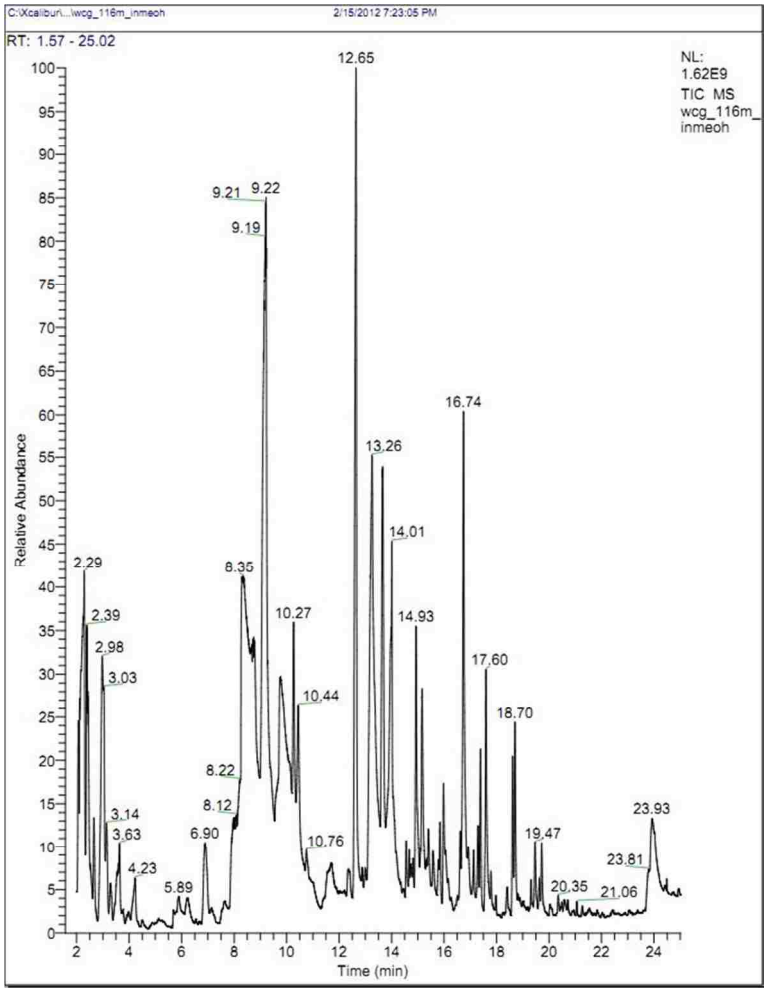

WCG-116M	
Residence time	Species
2.29	Methyl Propionate
2.39	2-Butanone
2.98	1-Propanol
3.63	Allyl Alcohol
6.9	Cyclopentanone
8.35	Acetic Acid
9.21	Hydroxyacetone
10.27	Propionic Acid
13.26	Propylene Glycol
18.70-19.72	Phenols
23.93	Glycerin
12.65,13.69,16.74	Silicon Based Column Bleed

Figure 4. Gas chromatography/mass spectrometry results of liquid sample from experiment WCG-116M.

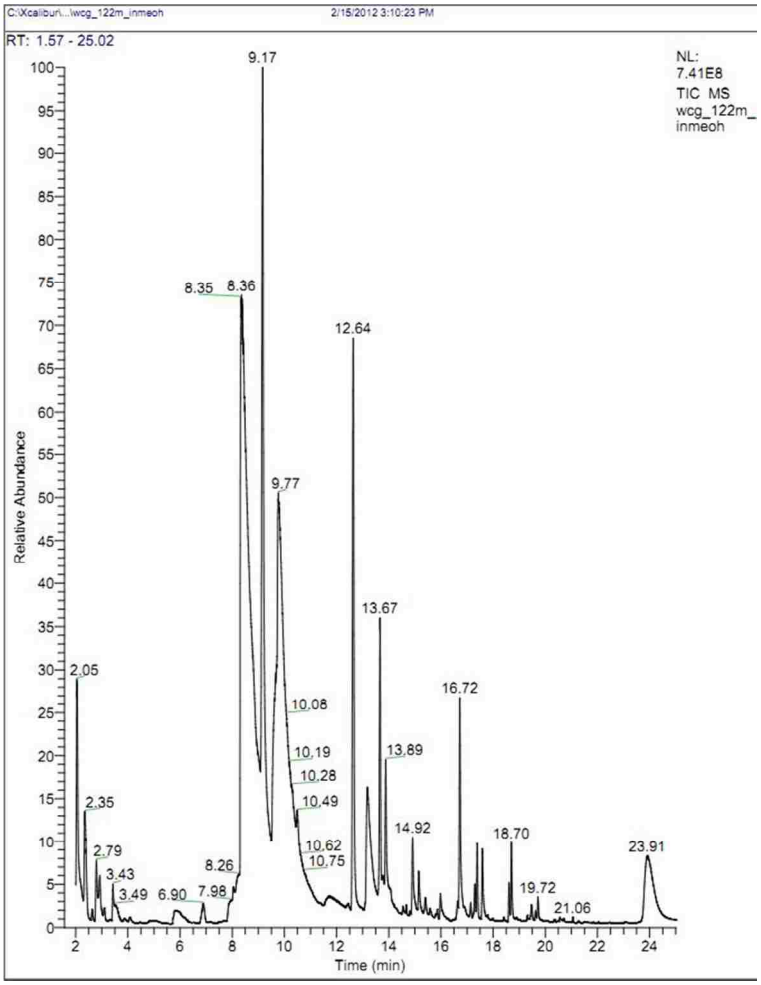

WCG-122M	
Residence time	Species
2.05	Methyl Propionate
2.35	2-Butanone
2.79	1-Propanol
3.43	Allyl Alcohol
6.9	Cyclopentanone
8.35	Acetic Acid
9.17	Hydroxyacetone
9.77	Propionic Acid
13.13	Propylene Glycol
18.70-19.72	Phenols
23.91	Glycerin
12.64,13.67,16.72	Silicon Based Column Bleed

Figure 5. Gas chromatography/mass spectrometry results of liquid sample from experiment WCG-122M.

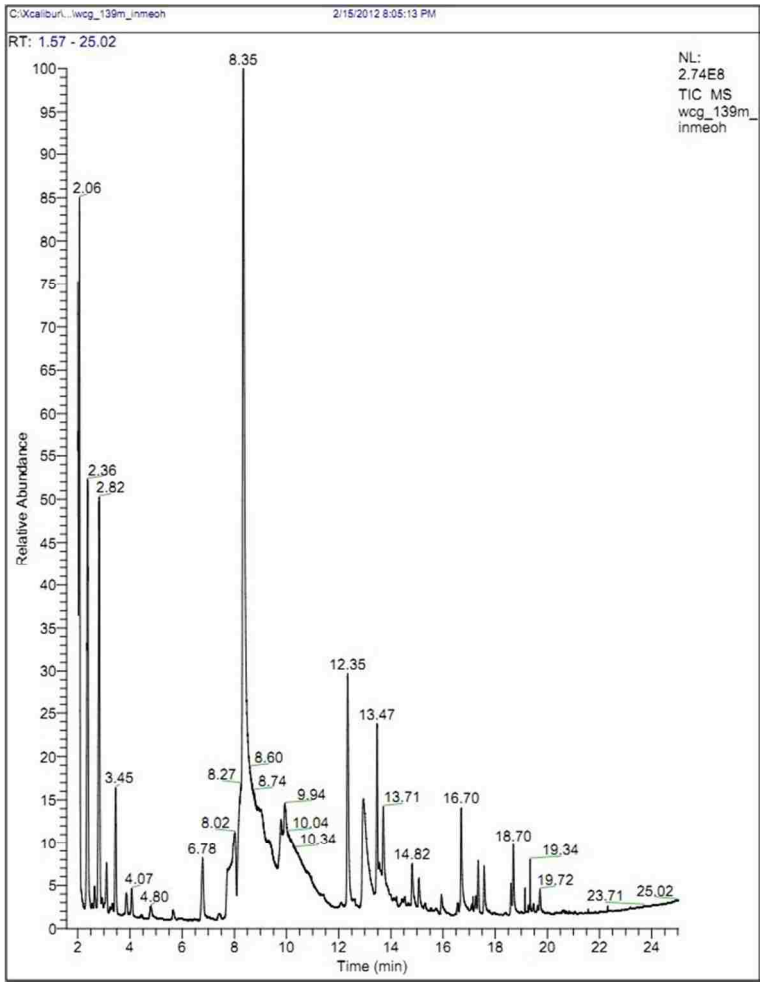

WCG-139M	
Residence time	Species
2.06	Methyl Propionate
2.36	2-Butanone
2.82	1-Propanol
3.45	Allyl Alcohol
6.78	Cyclopentanone
8.02	Acetic Acid
8.35	Hydroxyacetone
9.94	Propionic Acid
13.14	Propylene Glycol
18.70-19.72	Phenols
23.71	Glycerin
12.35,13.47,16.70	Silicon Based Column Bleed

Figure 6. Gas chromatography/mass spectrometry results of liquid sample from experiment WCG-139M.

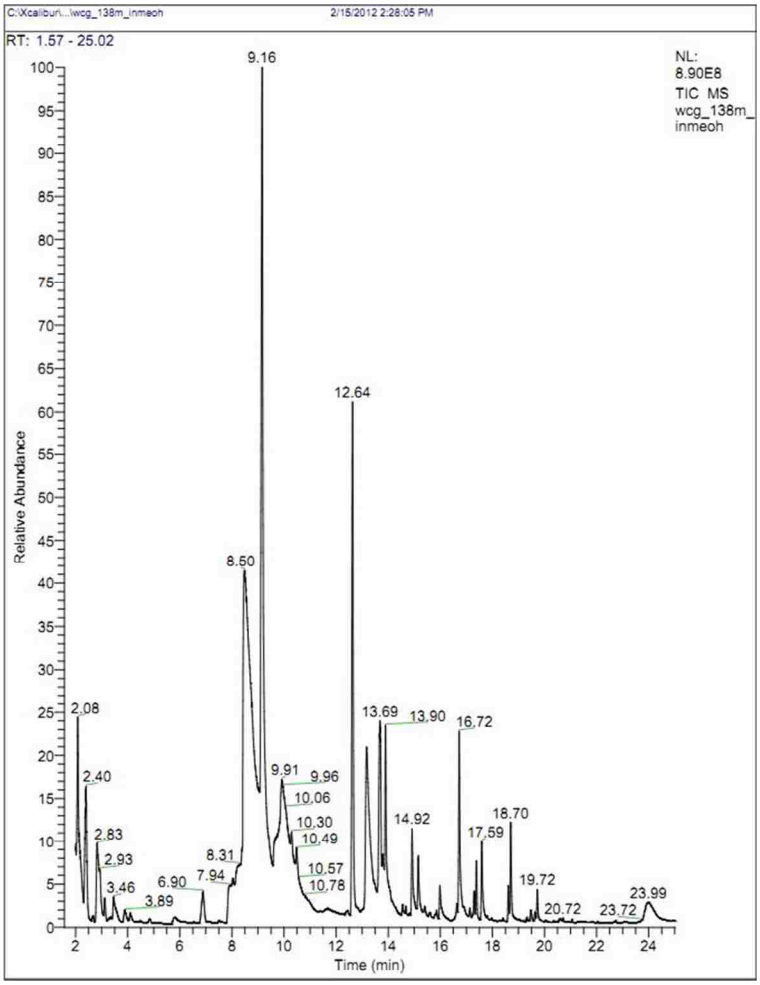

WCG-138M	
Residence time	Species
2.08	Methyl Propionate
2.4	2-Butanone
2.83	1-Propanol
3.46	Allyl Alcohol
6.9	Cyclopentanone
8.5	Acetic Acid
9.16	Hydroxyacetone
9.91	Propionic Acid
13.17	Propylene Glycol
18.70-19.72	Phenols
23.99	Glycerin
12.64,13.69,16.72	Silicon Based Column Bleed

Figure 7. Gas chromatography/mass spectrometry results of liquid sample from experiment WCG-138M.

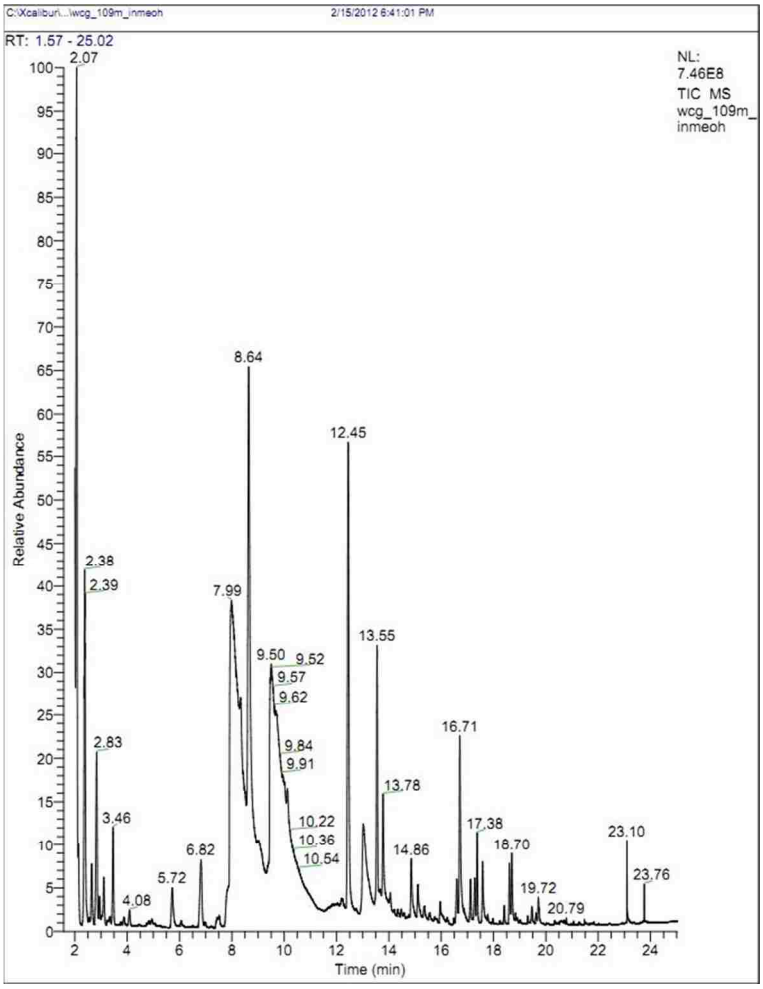

WCG-109M	
Residence time	Species
2.07	Methyl Propionate
2.38	2-Butanone
2.83	1-Propanol
3.46	Allyl Alcohol
6.82	Cyclopentanone
7.99	Acetic Acid
8.64	Hydroxyacetone
9.5	Propionic Acid
13.11	Propylene Glycol
18.70-19.72	Phenols
23.76	Glycerin
12.45,13.55,16.71	Silicon Based Column Bleed

Figure 8. Gas chromatography/mass spectrometry results of liquid sample from experiment WCG-109M.

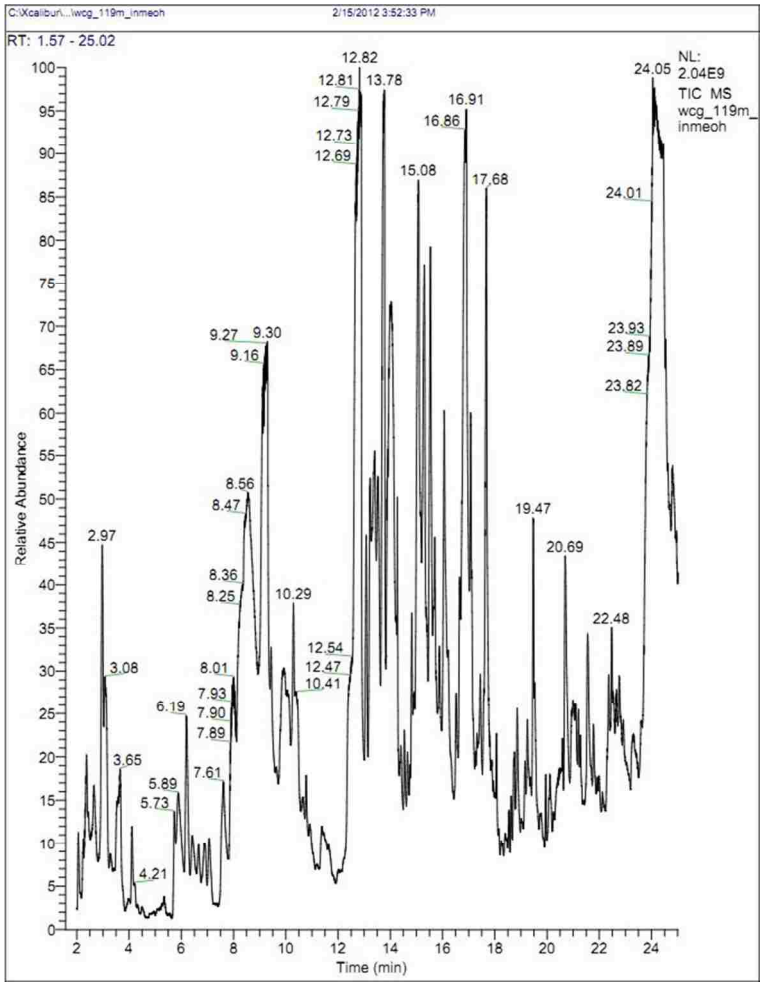

WCG-119M	
Residence time	Species
2.06	Methyl Propionate
2.97	2,3-Butanone
3.65	Allyl Alcohol
6.19	Cyclopentanone
8.56	Acetic Acid
9.3	Hydroxyacetone
10.29	Propionic Acid
13.36	Propylene Glycol
18.70-19.72	Phenols
24.05	Glycerin
12.82,13.78,16.91	Silicon Based Column Bleed

Figure 9. Gas chromatography/mass spectrometry results of liquid sample from experiment WCG-119M.

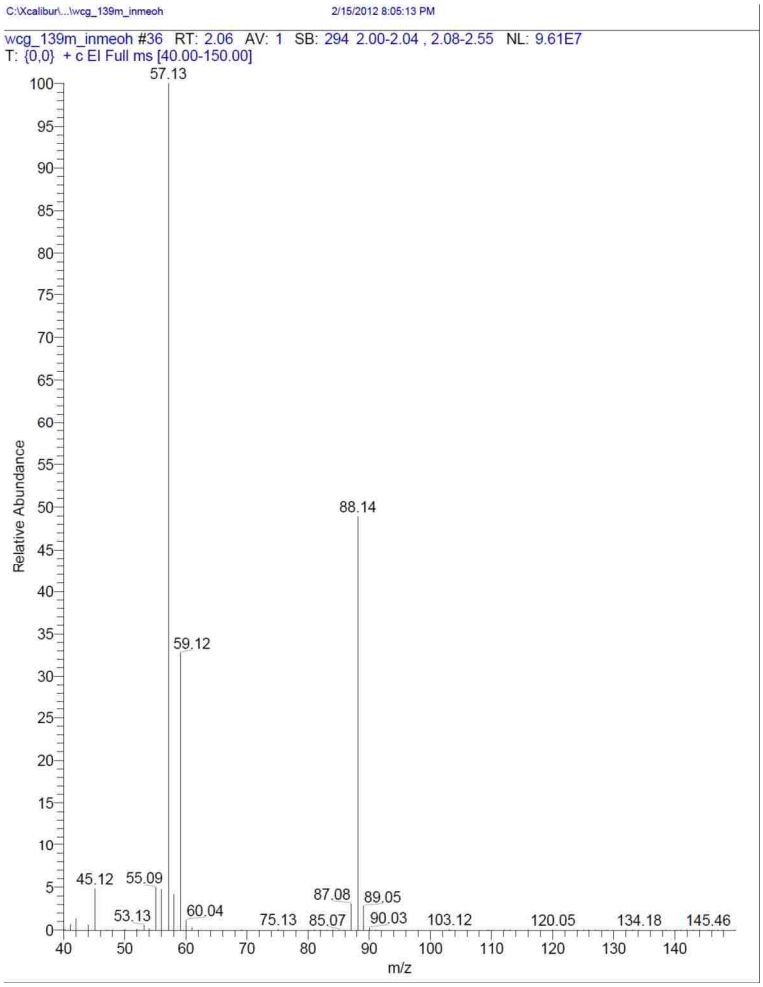

Figure 10. Total ion chromatograph of methyl propionate from WCG-139M.

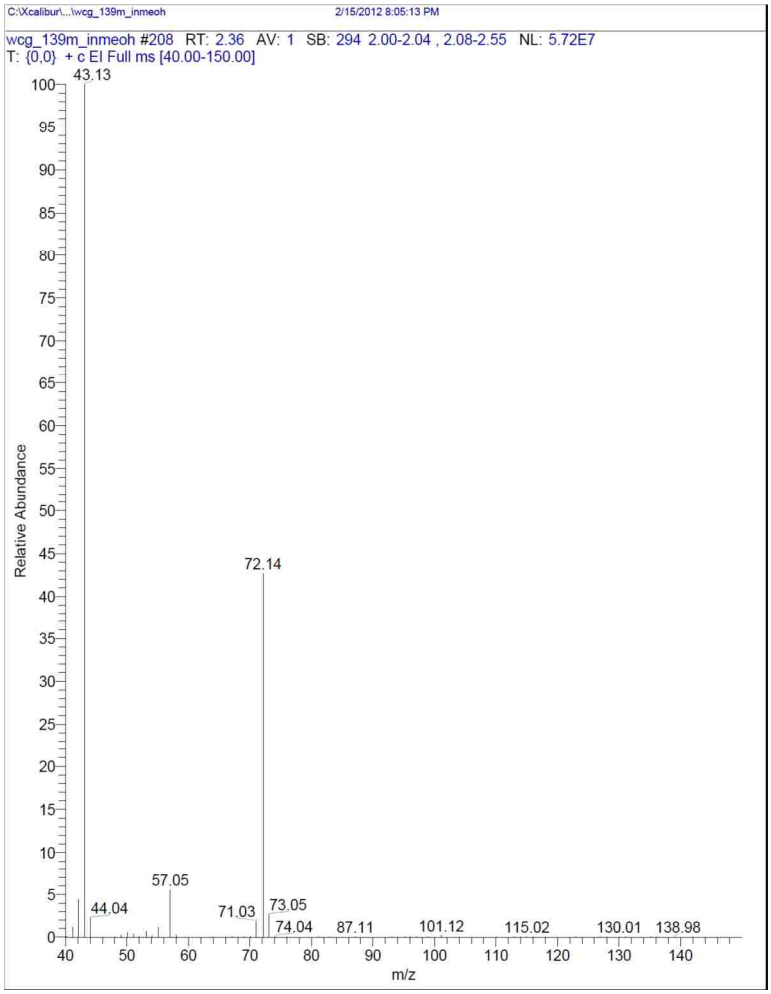

Figure 11. Total ion chromatograph of 2-butanone from WCG-139M.

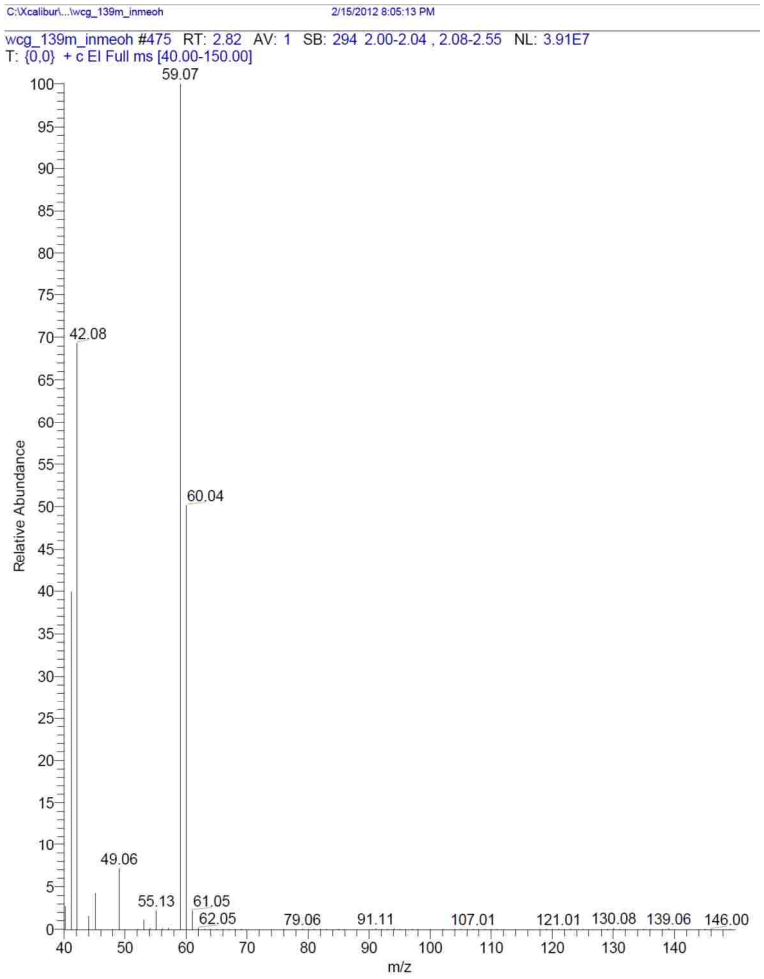

Figure 12. Total ion chromatograph of 1-propanol from WCG-139M.

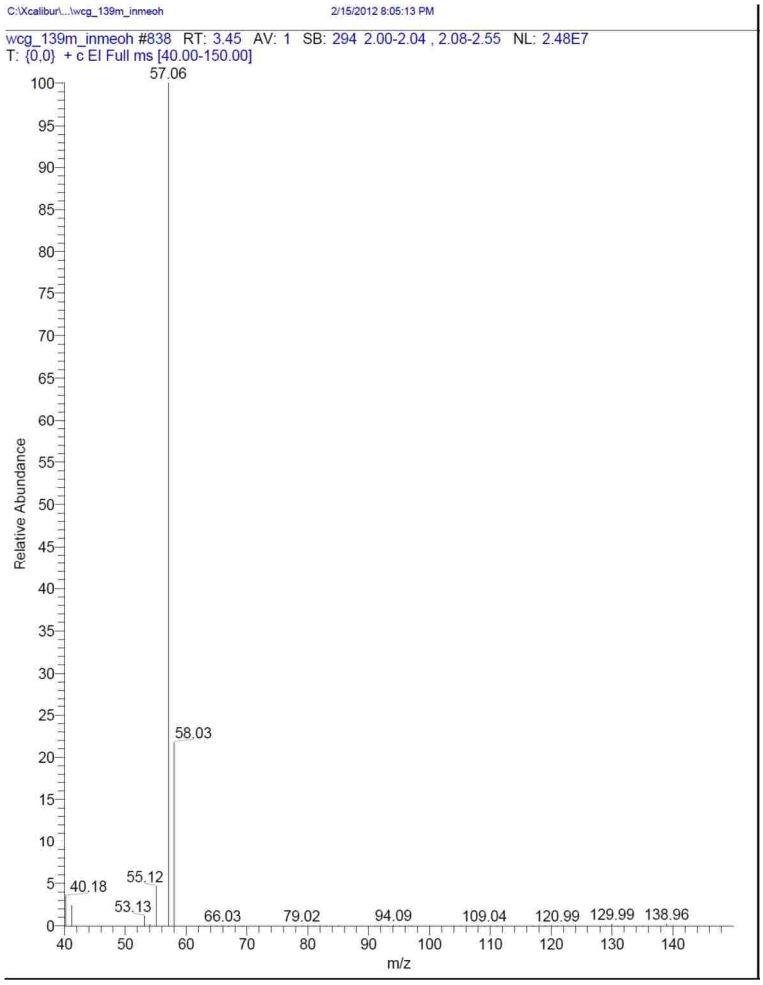

Figure 13. Total ion chromatograph of allyl alcohol from WCG-139M.

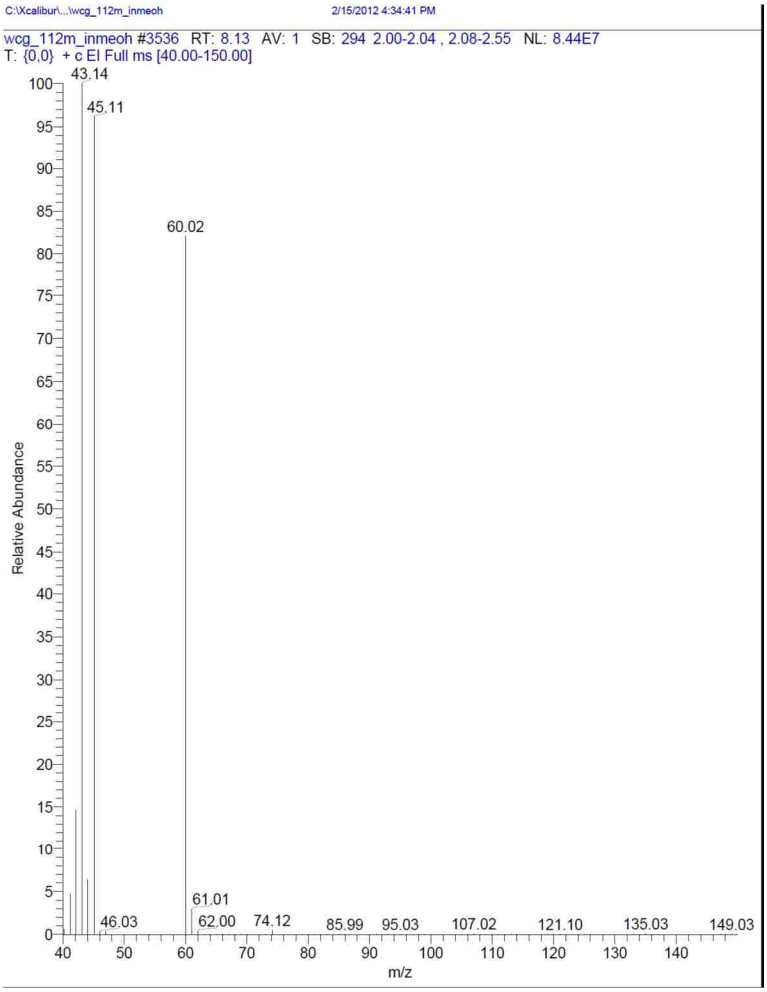

Figure 14. Total ion chromatograph of acetic acid from WCG-112M.

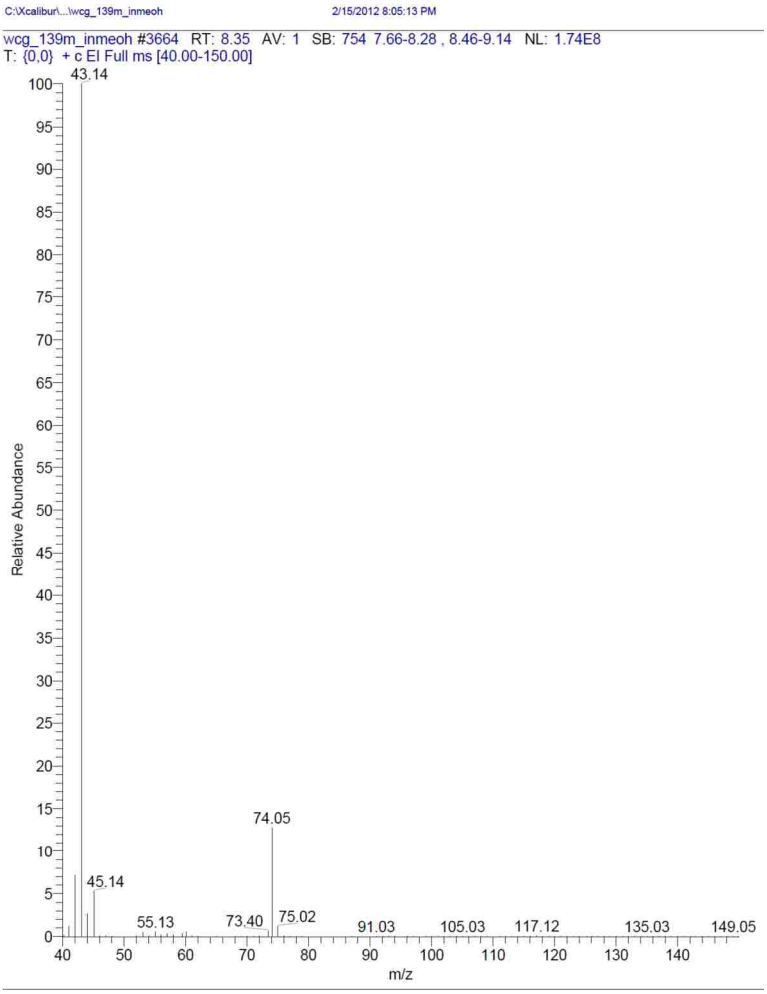

Figure 15. Total ion chromatograph of hydroxyacetone from WCG-139M.

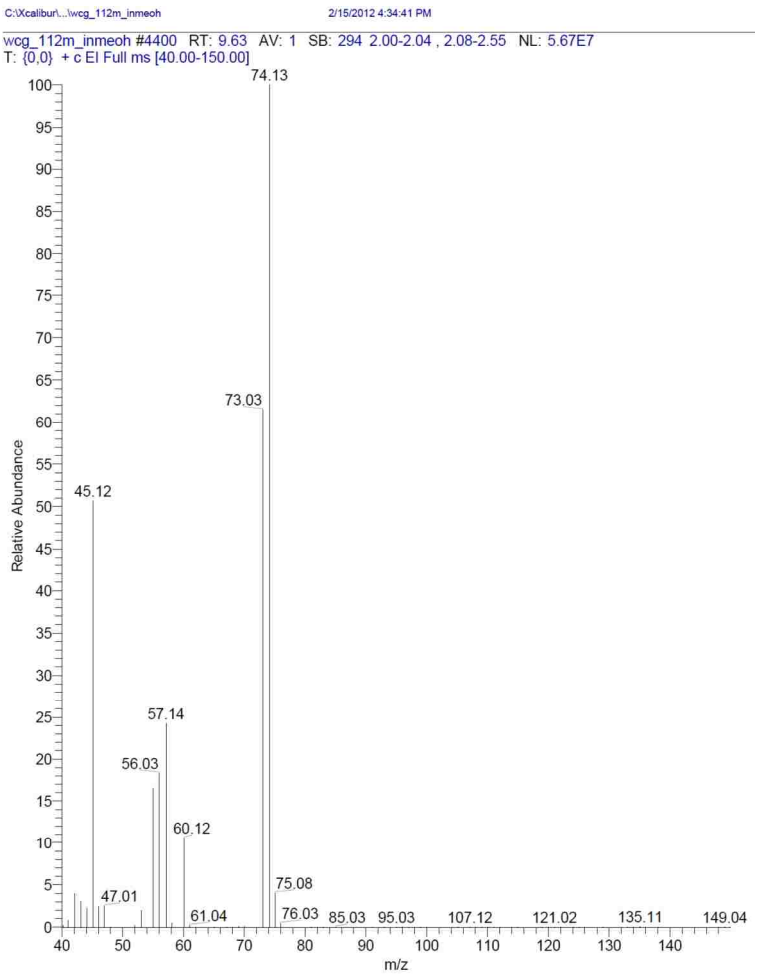

Figure 16. Total ion chromatograph of propanoic acid from WCG-112M.

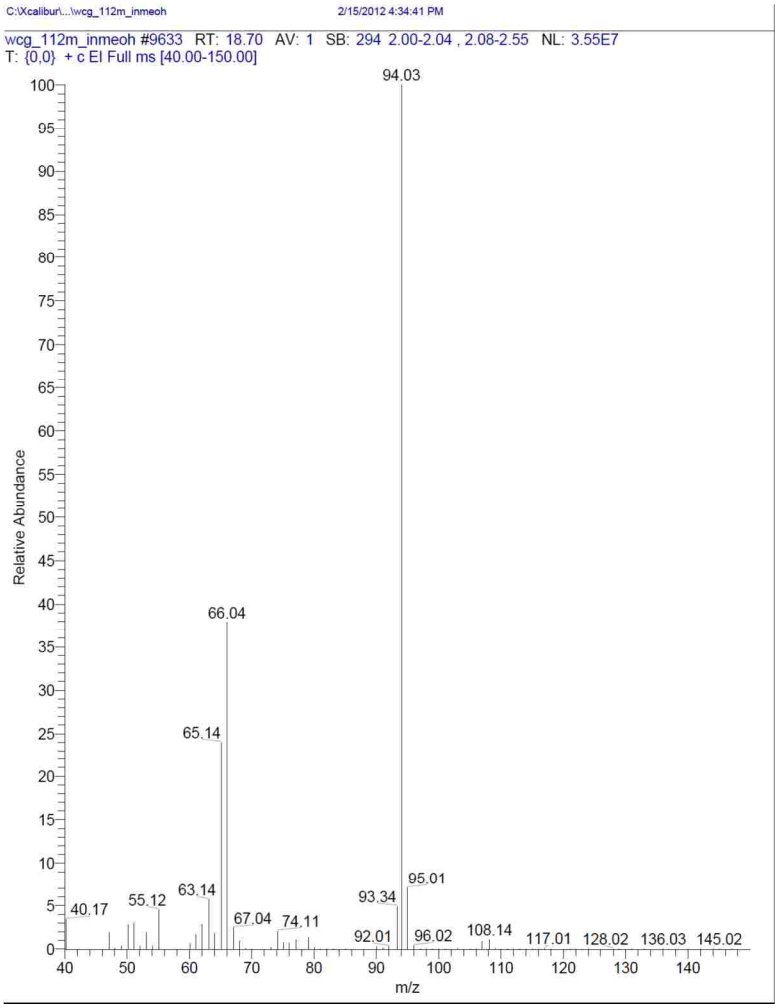

Figure 17. Total ion chromatograph of phenol from WCG-112M.

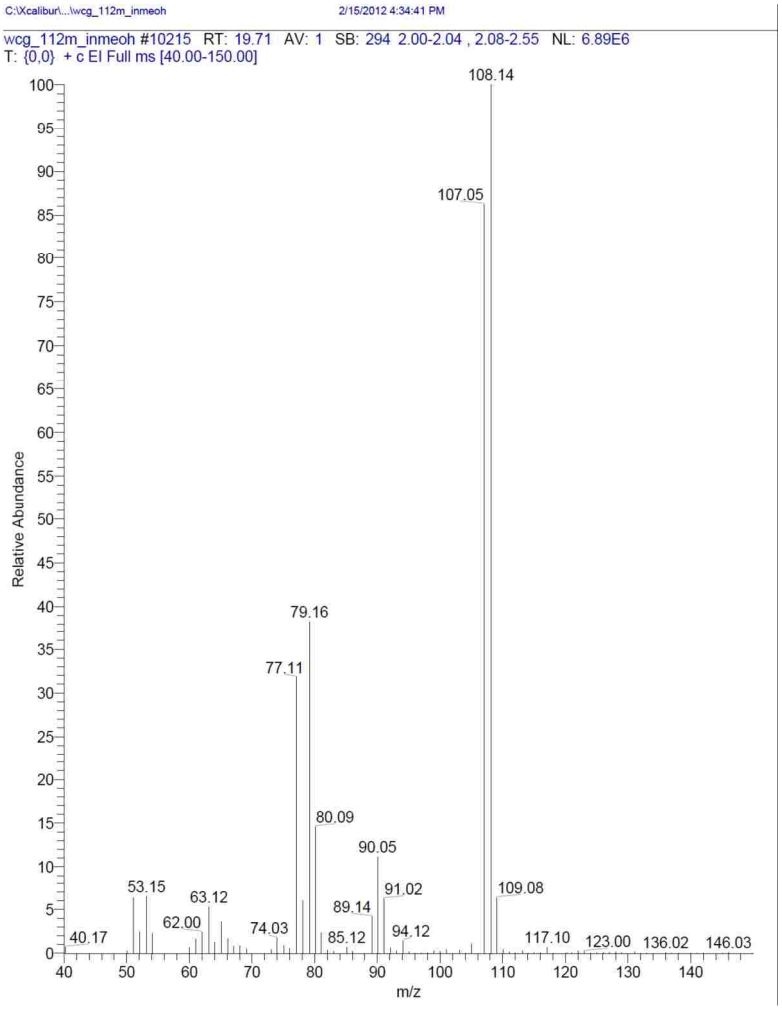

Figure 18. Total ion chromatograph of 2-methyl phenol from WCG-112M.

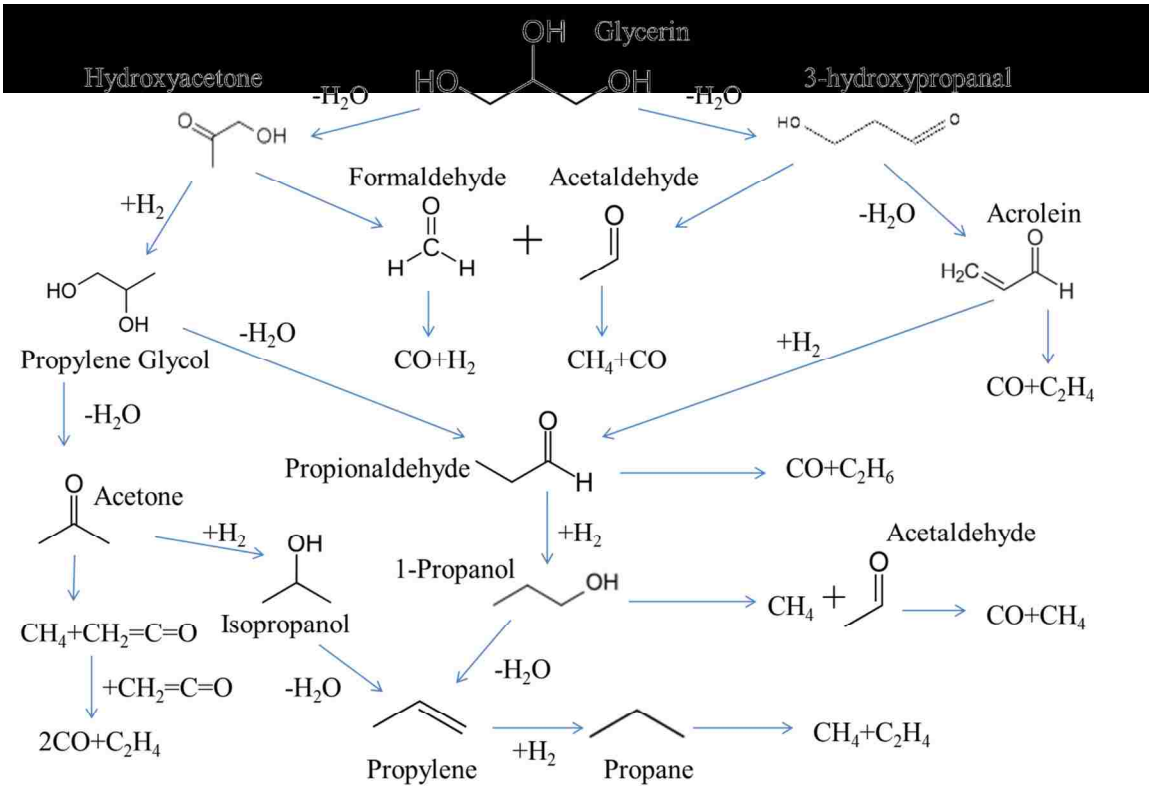

Figure 19. Comprehensive mechanistic pathway of glycerin decomposition in supercritical water.

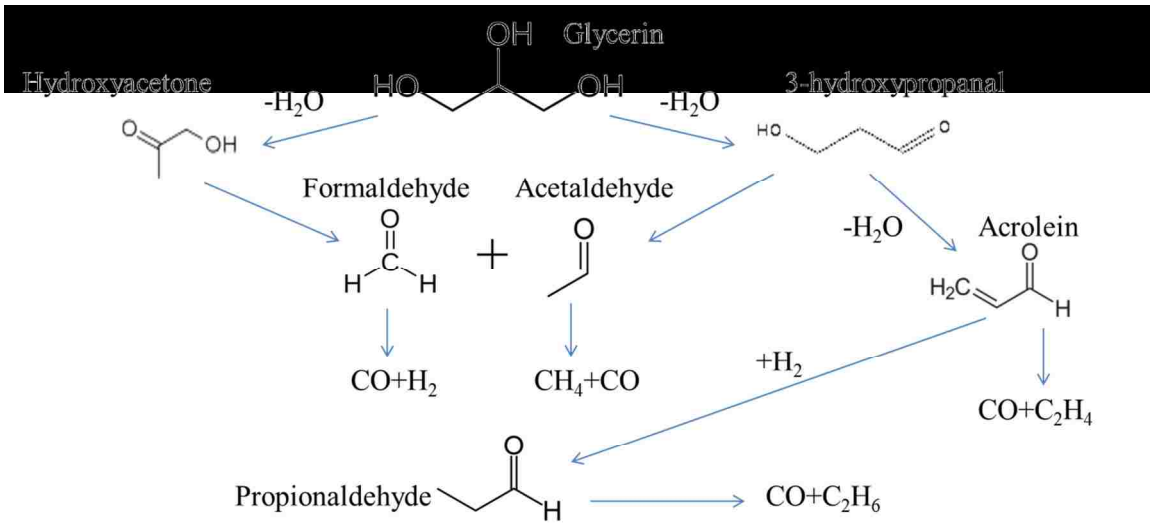

Figure 20. The thermodynamically favorable reaction pathways of glycerin decomposition based on ΔG analysis.

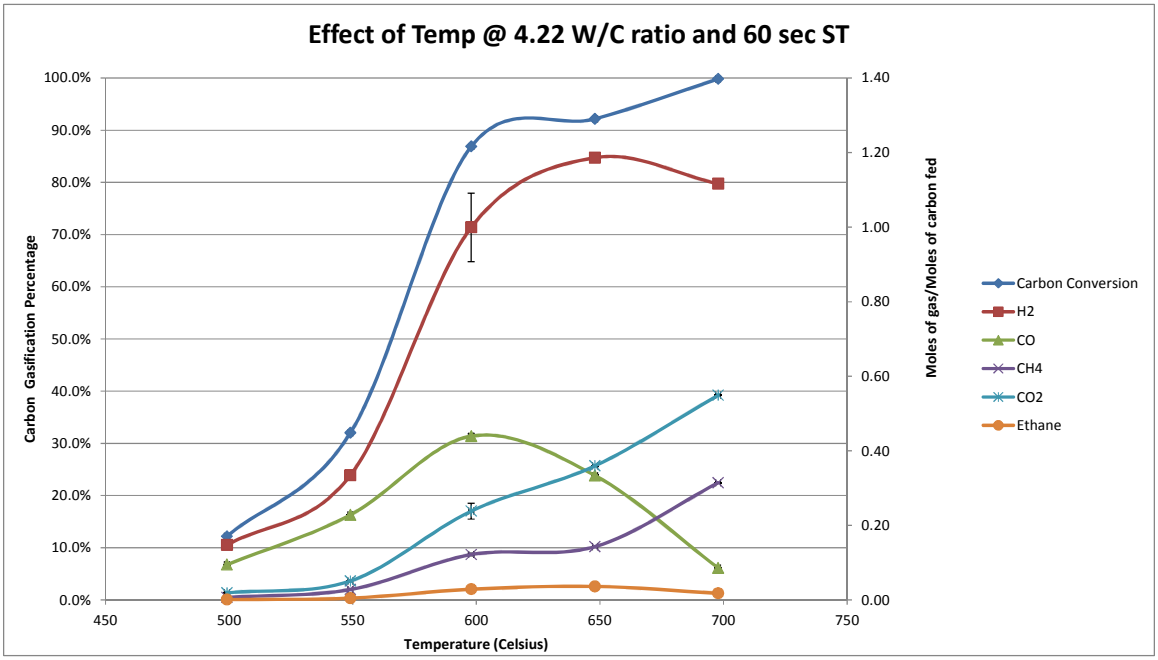

Figure 21. The effect of temperature at a 4.22 water-to-carbon molar ratio and 60 second space time on carbon gasification and gas composition (moles/moles carbon fed).

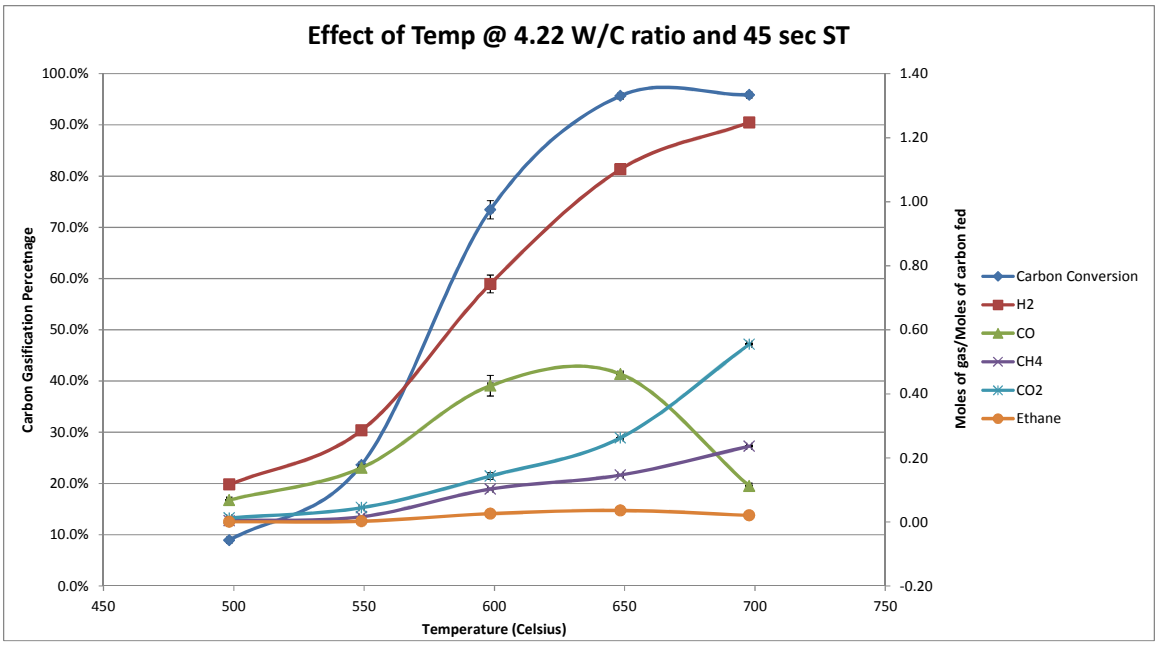

Figure 22. The effect of temperature at a 4.22 water-to-carbon molar ratio and 45 second space time on carbon gasification and gas composition (moles/moles carbon fed).

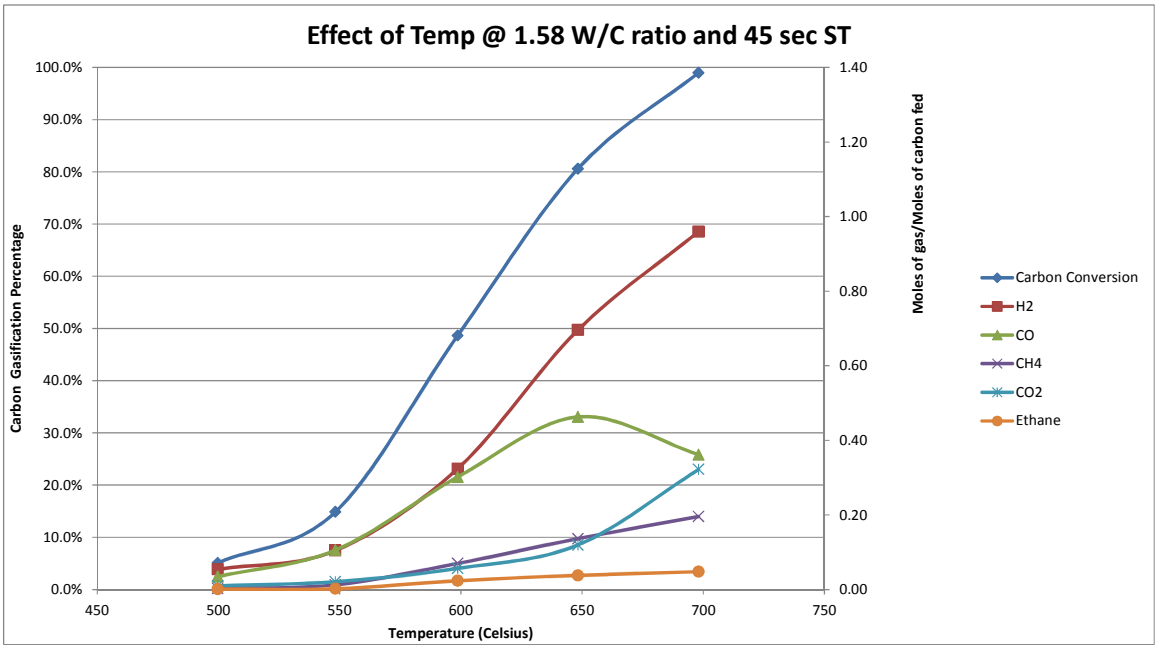

Figure 23. The effect of temperature at a 1.58 water-to-carbon molar ratio and 45 second space time on carbon gasification and gas composition (moles/moles carbon fed).

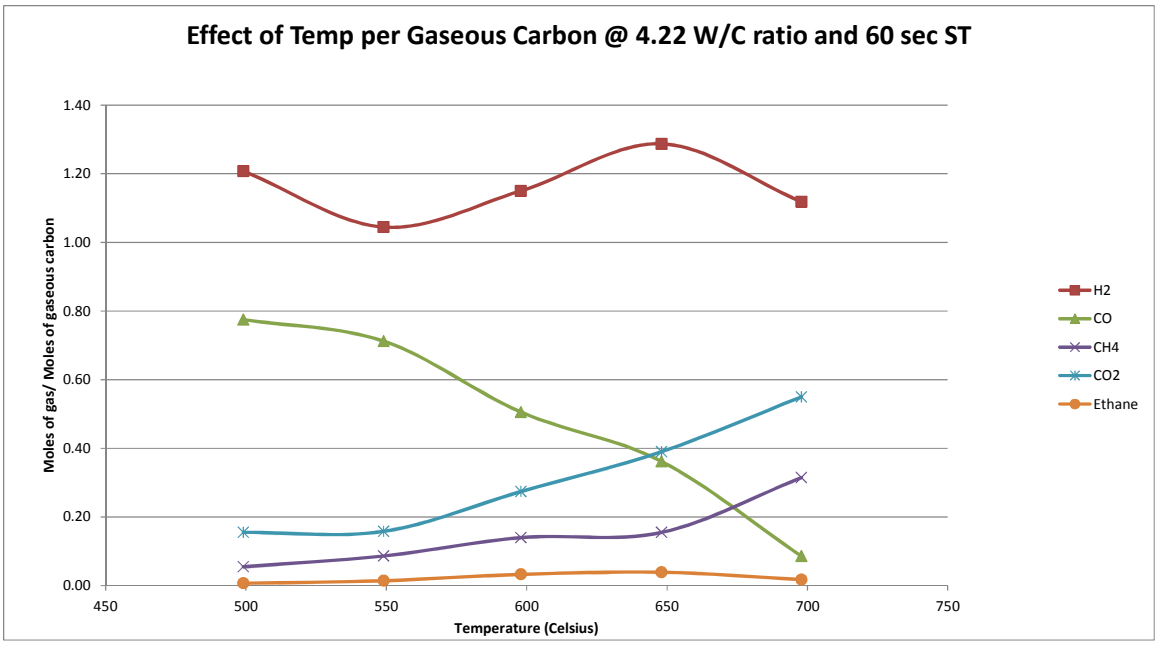

Figure 24. The effect of temperature at a 4.22 water-to-carbon molar ratio and 60 second space time on gas composition (moles/moles gaseous carbon).

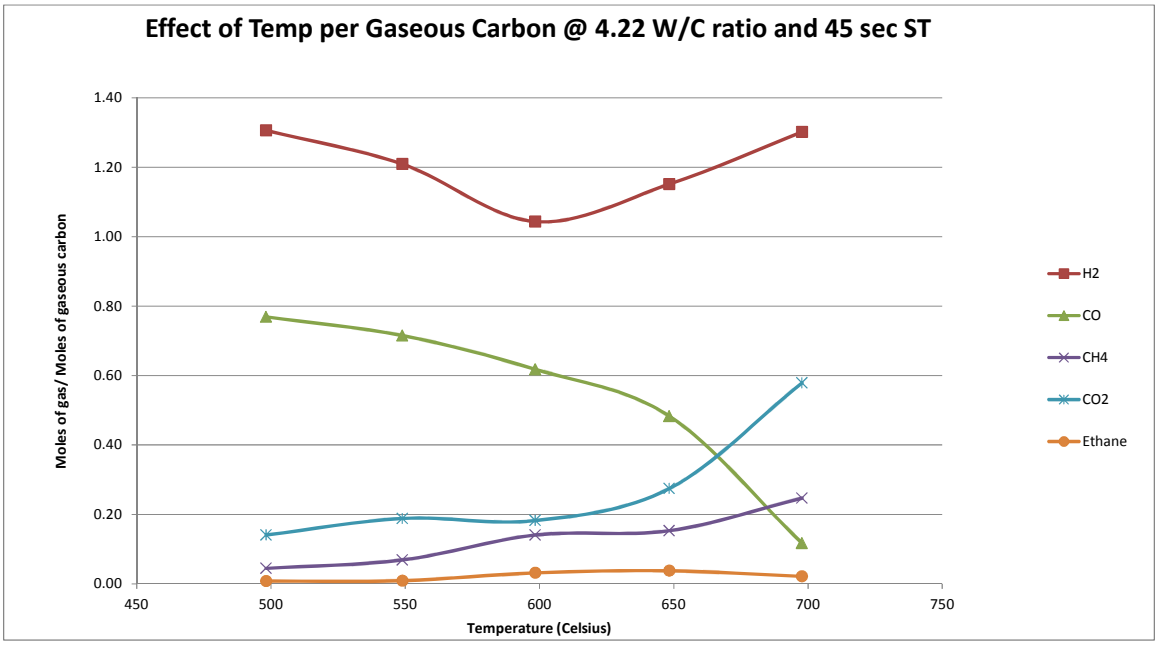

Figure 25. The effect of temperature at a 4.22 water-to-carbon molar ratio and 45 second space time on gas composition (moles/moles gaseous carbon).

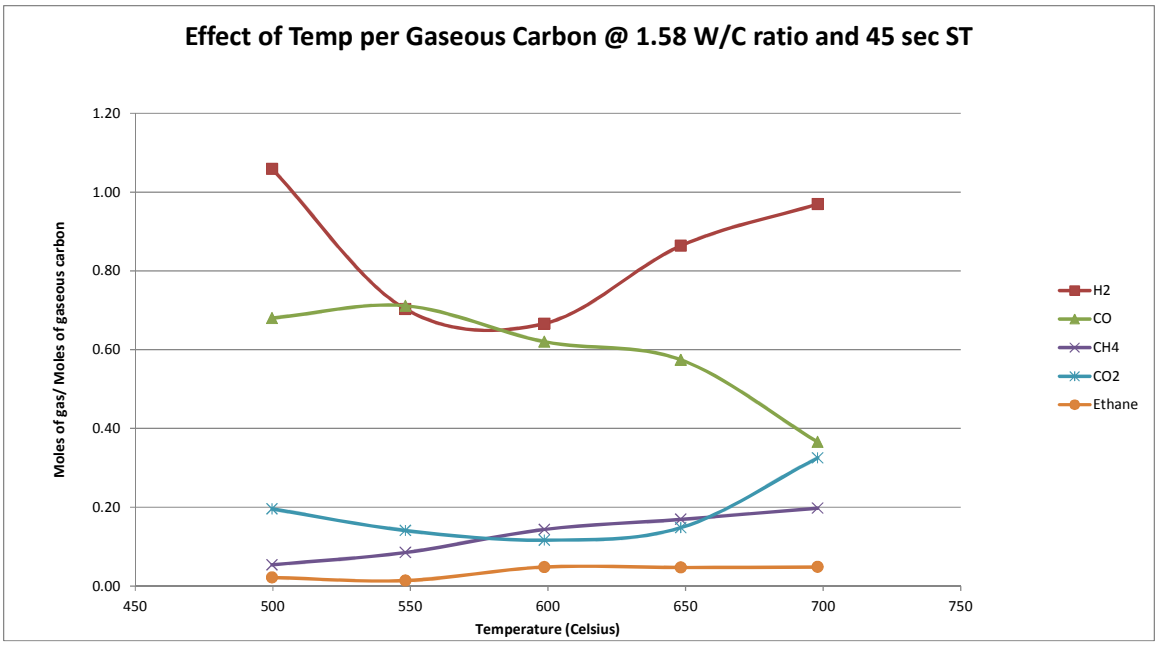

Figure 26. The effect of temperature at a 1.58 water-to-carbon molar ratio and 45 second space time on gas composition (moles/moles gaseous carbon).

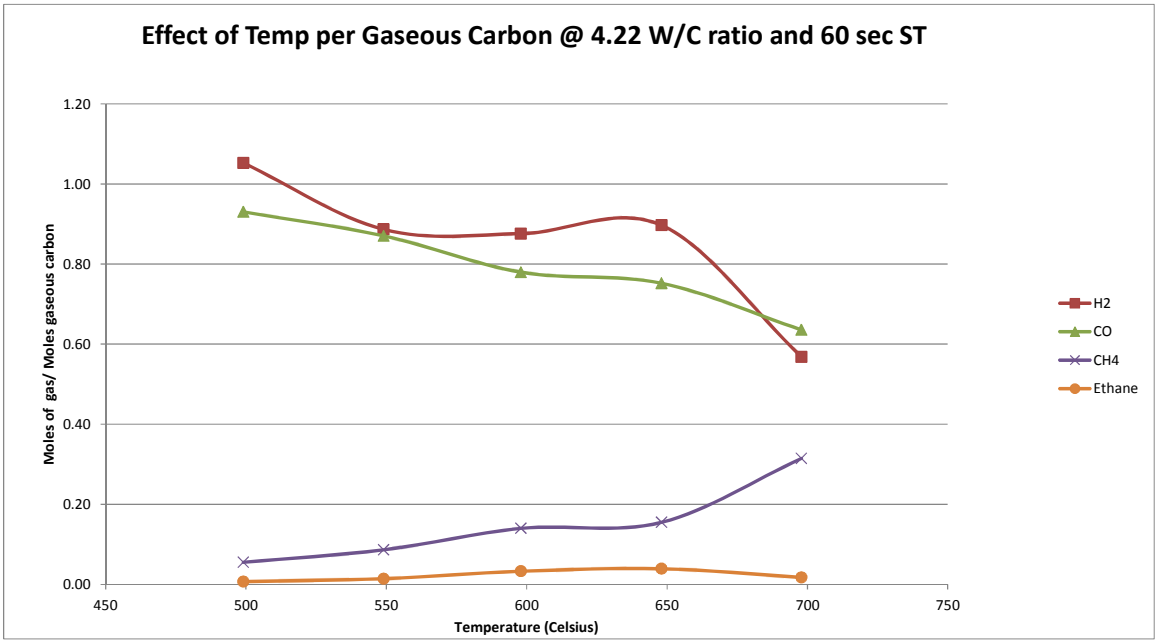

Figure 27. The effect of temperature at a 4.22 water-to-carbon molar ratio and 60 second space time on gas composition (moles/moles gaseous carbon) with the water gas shift reaction undone.

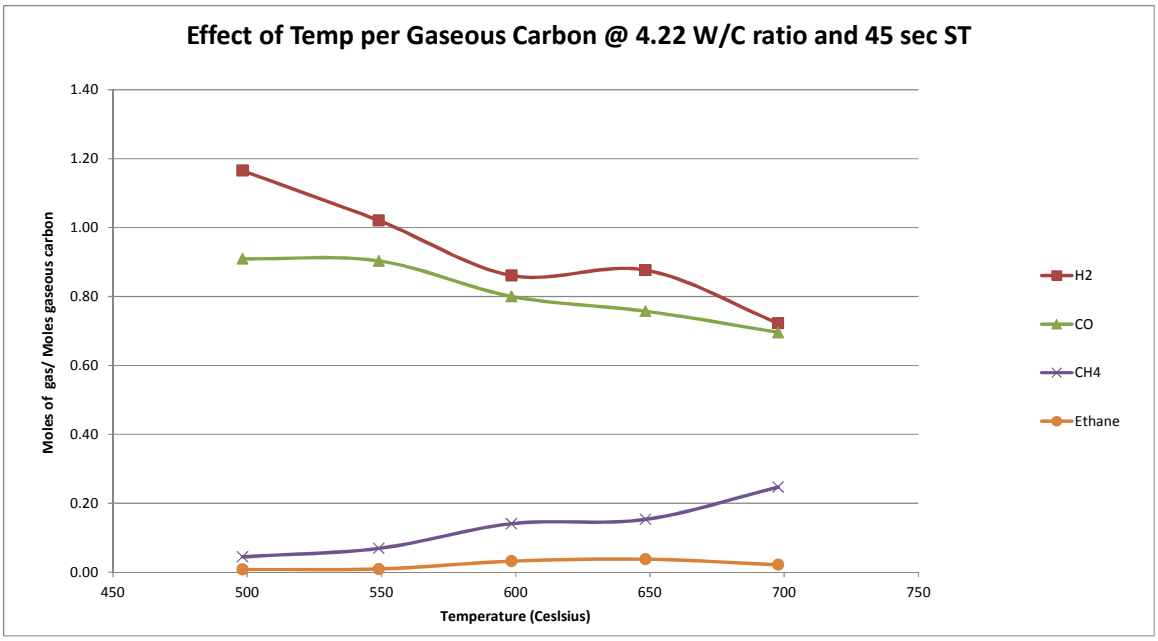

Figure 28. The effect of temperature at a 4.22 water-to-carbon molar ratio and 45 second space time on gas composition (moles/moles gaseous carbon) with the water gas shift reaction undone.

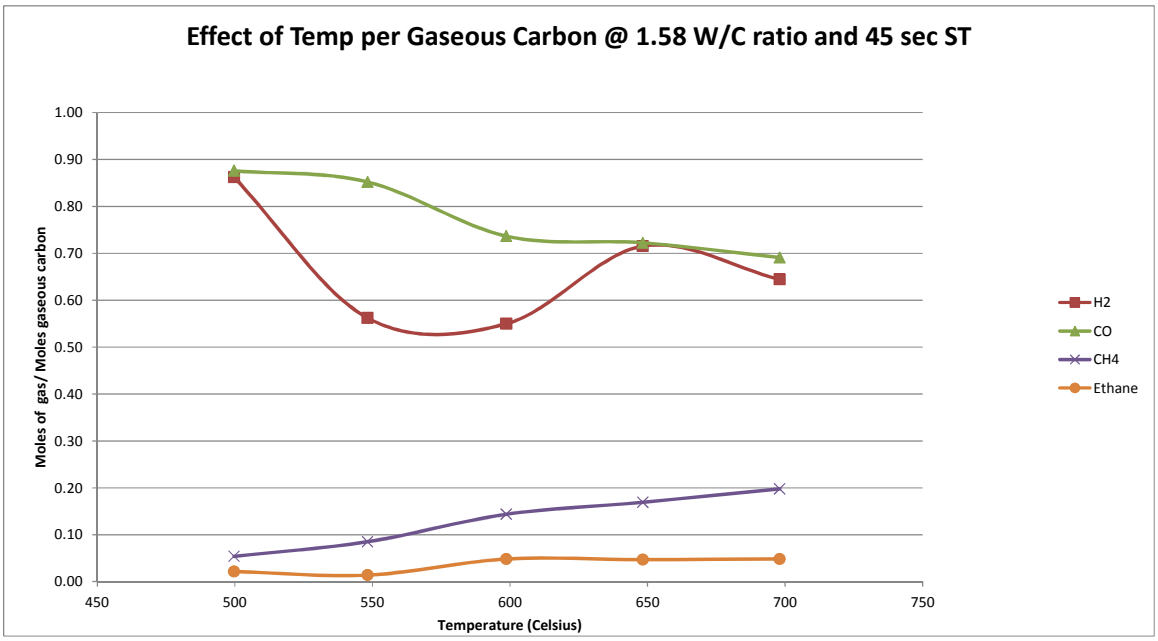

Figure 29. The effect of temperature at a 1.58 water-to-carbon molar ratio and 45 second space time on gas composition (moles/moles gaseous carbon) with the water gas shift reaction undone.

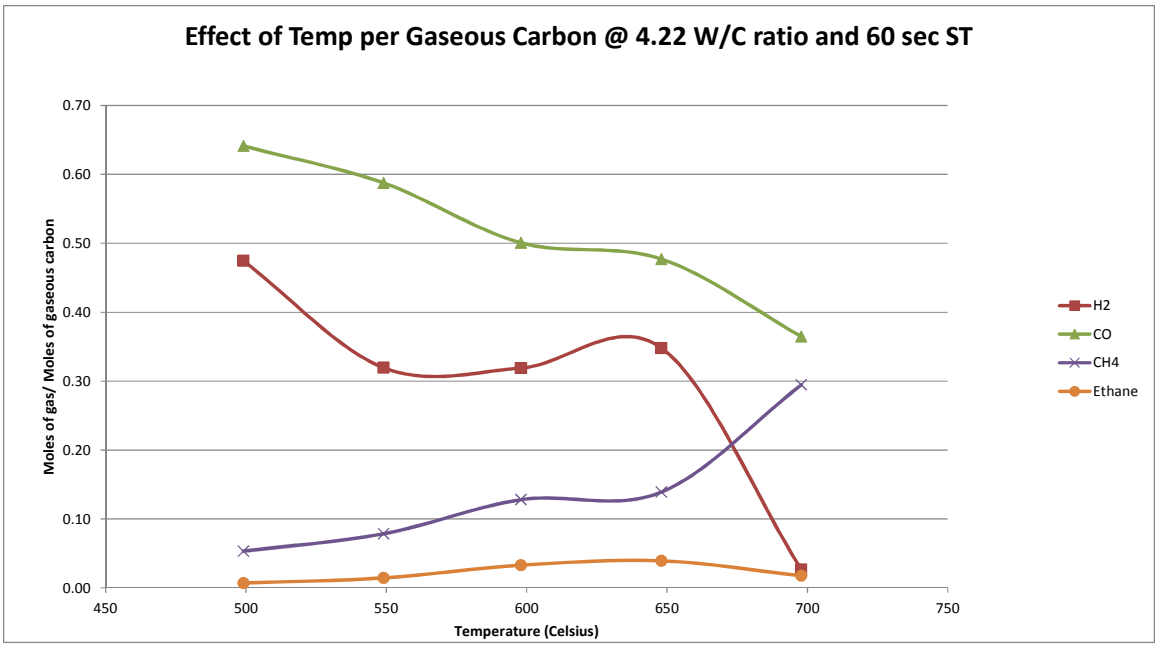

Figure 30. The effect of temperature at a 4.22 water-to-carbon molar ratio and 60 second space time on gas composition (moles/moles gaseous carbon) with the water gas shift reaction undone and predicted methanol decomposition results removed.

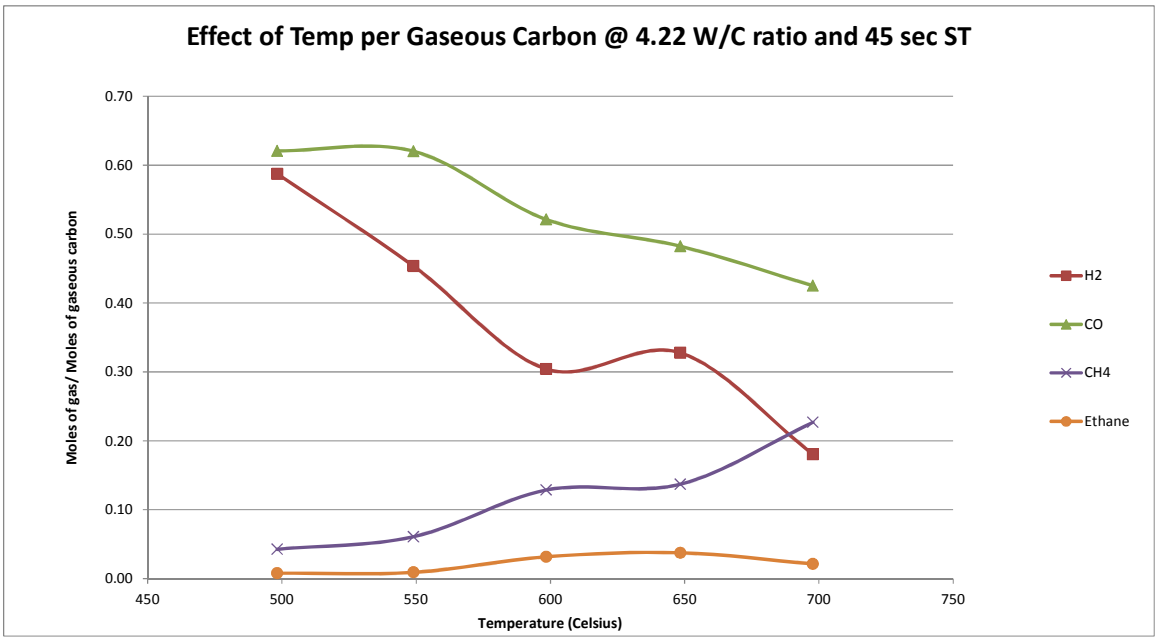

Figure 31. The effect of temperature at a 4.22 water-to-carbon molar ratio and 45 second space time on gas composition (moles/moles gaseous carbon) with the water gas shift reaction undone and predicted methanol decomposition results removed.

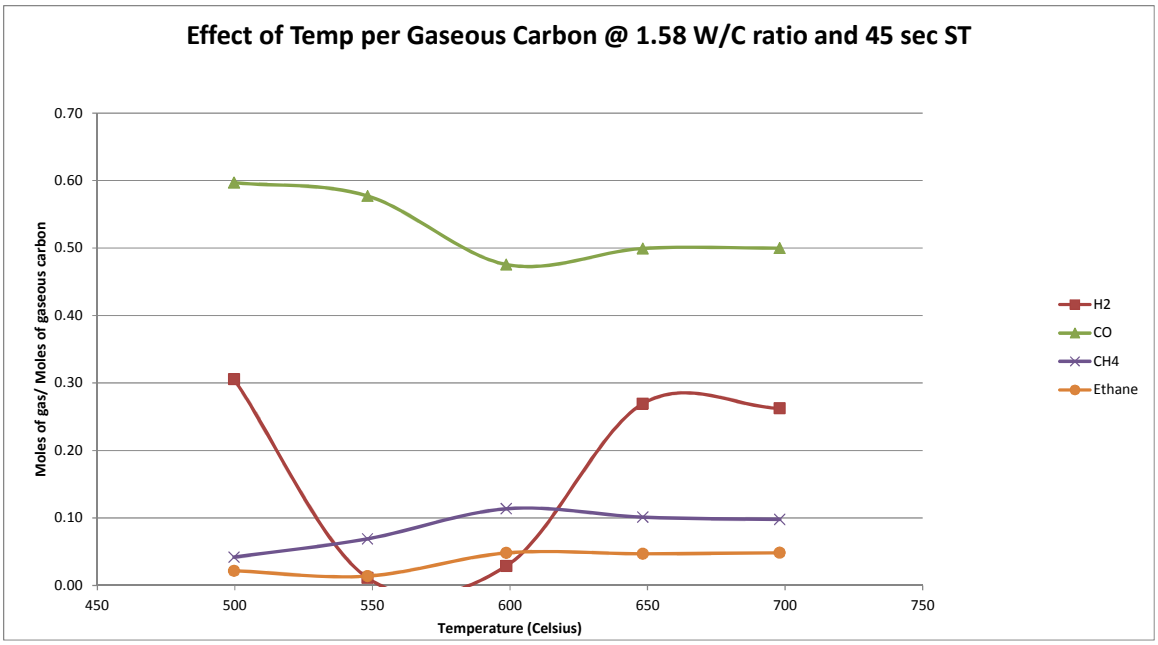

Figure 32. The effect of temperature at a 1.58 water-to-carbon molar ratio and 45 second space time on gas composition (moles/moles gaseous carbon) with the water gas shift reaction undone and predicted methanol decomposition results removed.

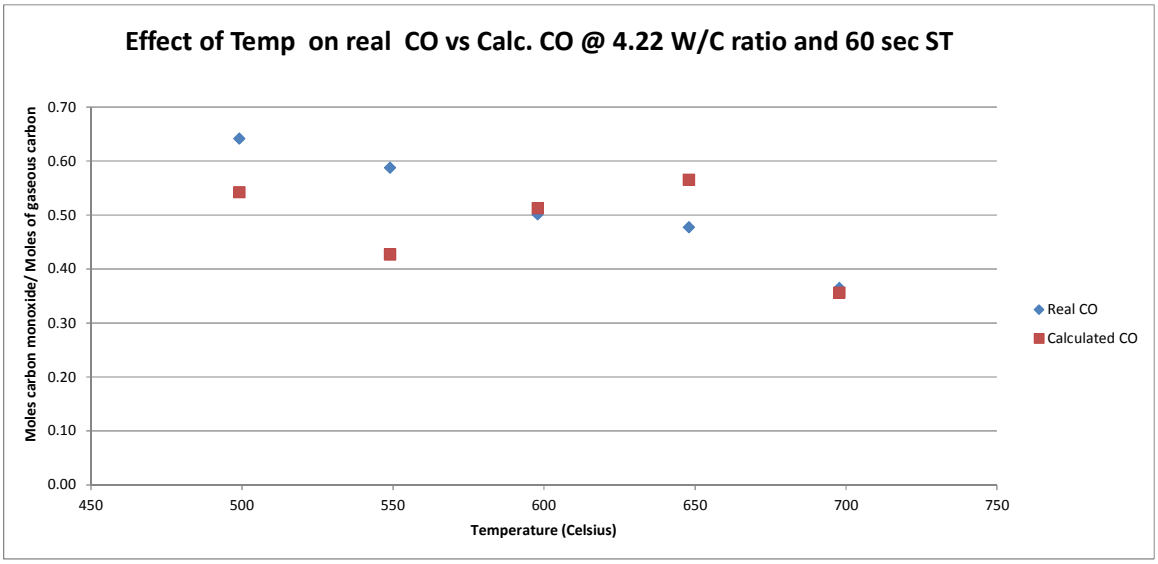

Figure 33. The effect of temperature at a 4.22 water-to-carbon molar ratio and 60 second space time on the accuracy of the glycerin decomposition mechanism.

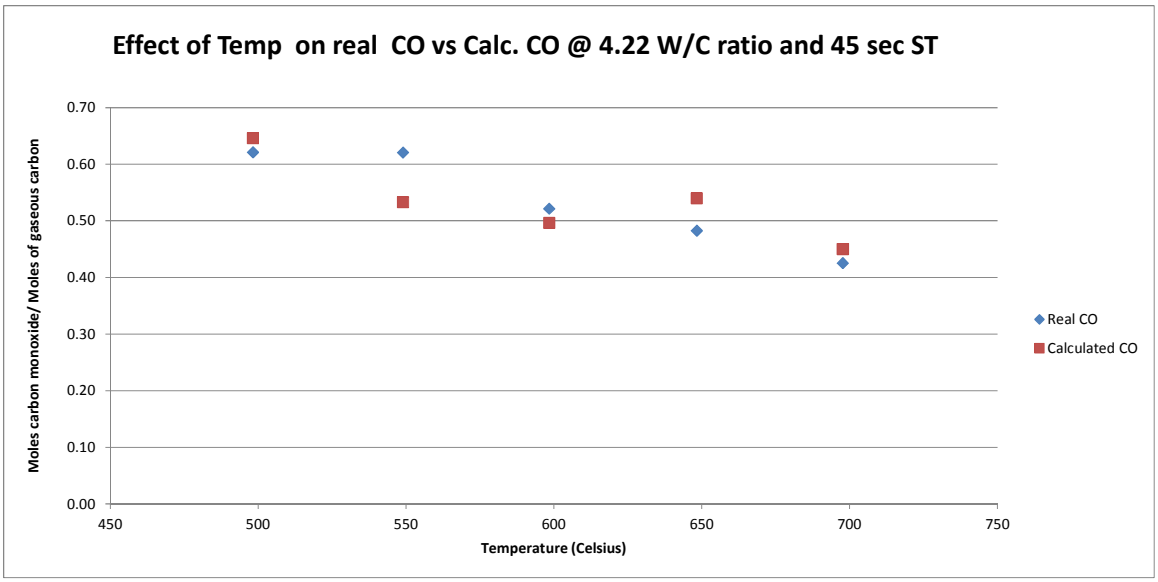

Figure 34. The effect of temperature at a 4.22 water-to-carbon molar ratio and 45 second space time on the accuracy of the glycerin decomposition mechanism.

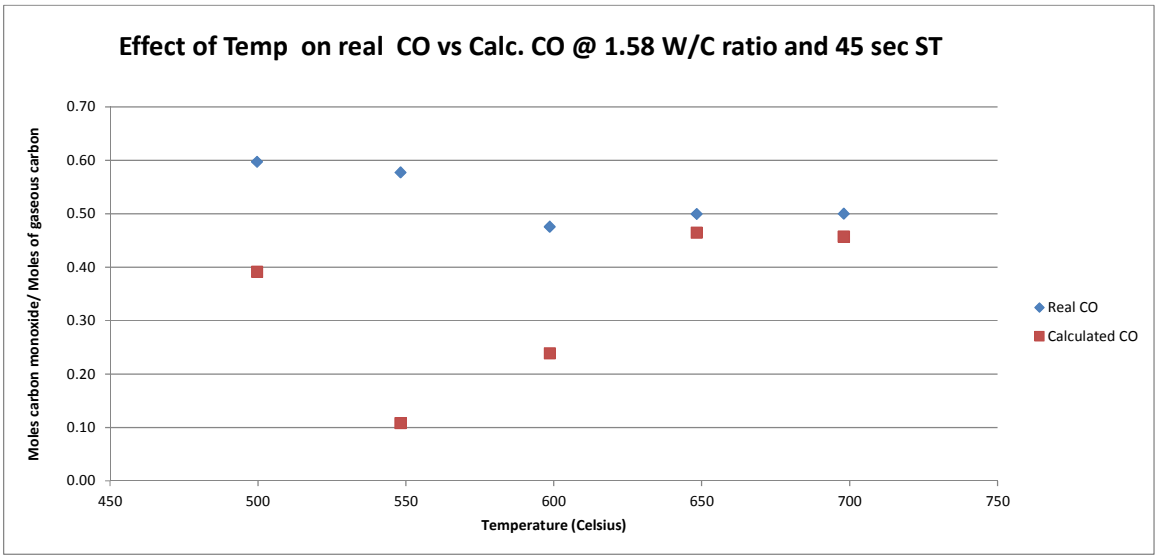

Figure 35. The effect of temperature at a 1.58 water-to-carbon molar ratio and 45 second space time on the accuracy of the glycerin decomposition mechanism.

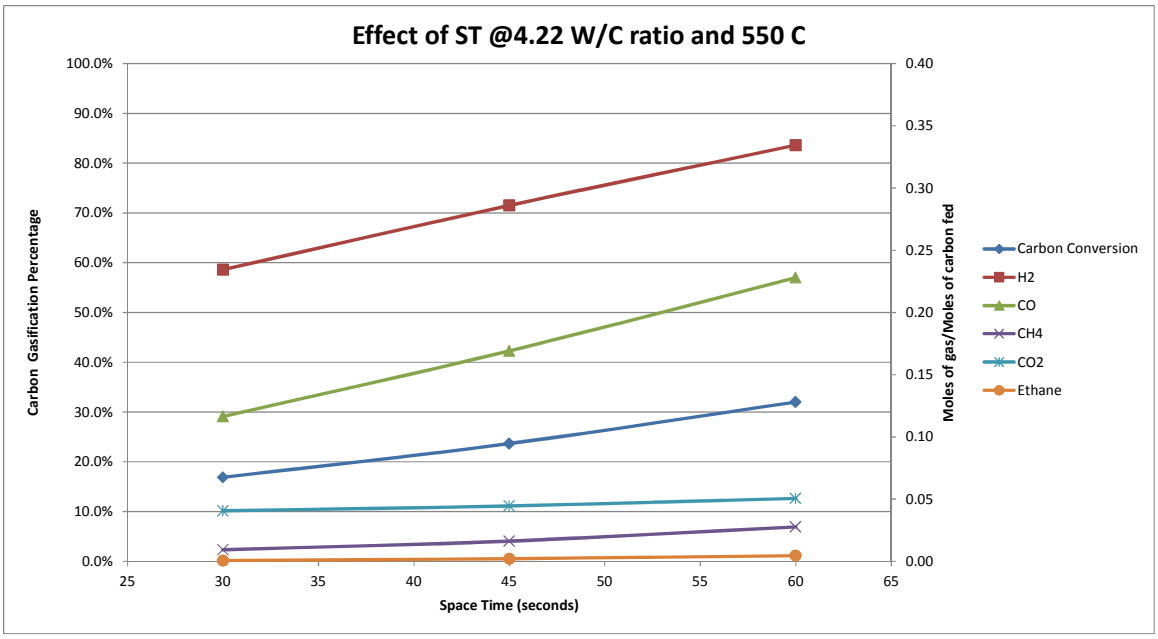

Figure 36. The effect of space time at a 4.22 water-to-carbon molar ratio and 550°C on carbon gasification and gas composition (moles/moles carbon fed).

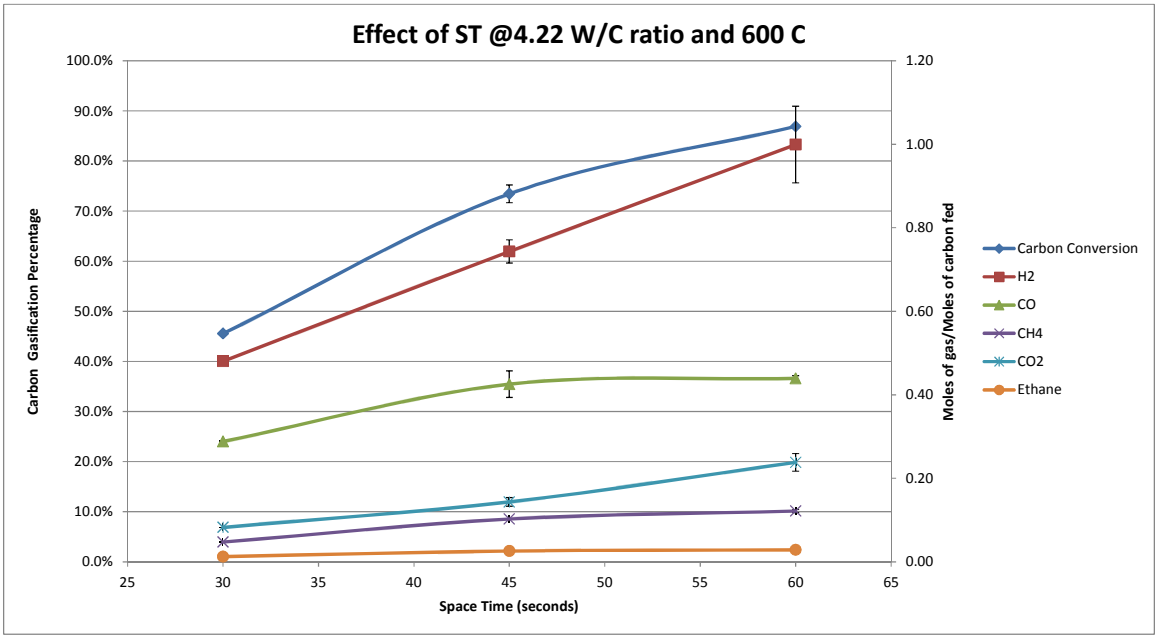

Figure 37. The effect of space time at a 4.22 water-to-carbon molar ratio and 600°C on carbon gasification and gas composition (moles/moles carbon fed).

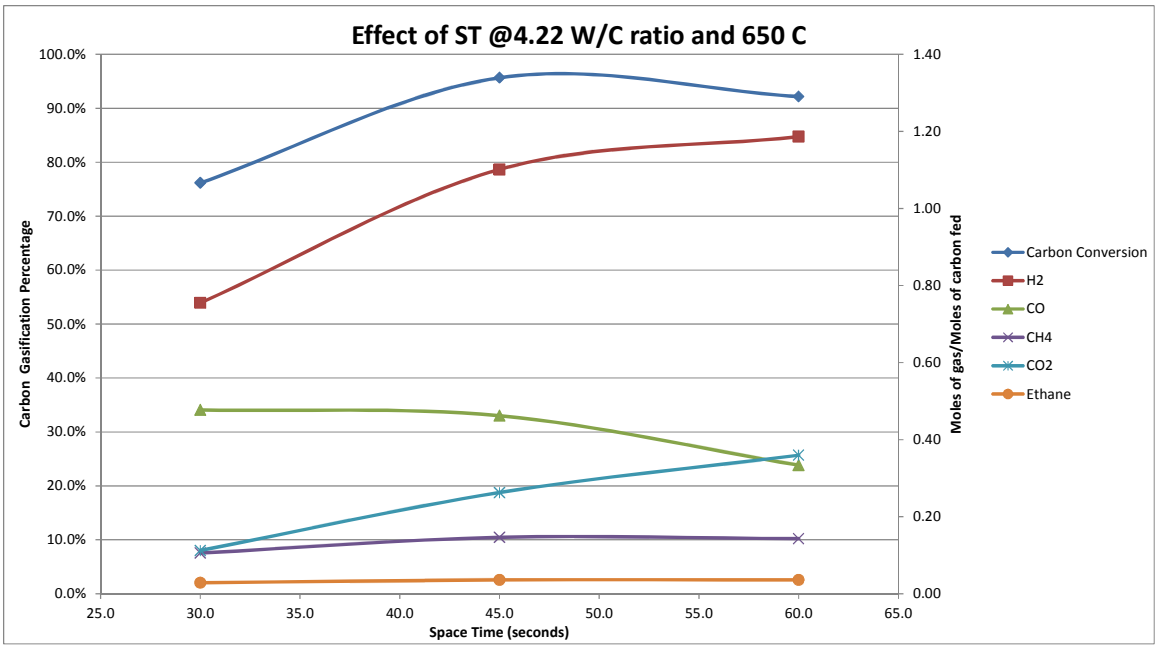

Figure 38. The effect of space time at a 4.22 water-to-carbon molar ratio and 650°C on carbon gasification and gas composition (moles/moles carbon fed).

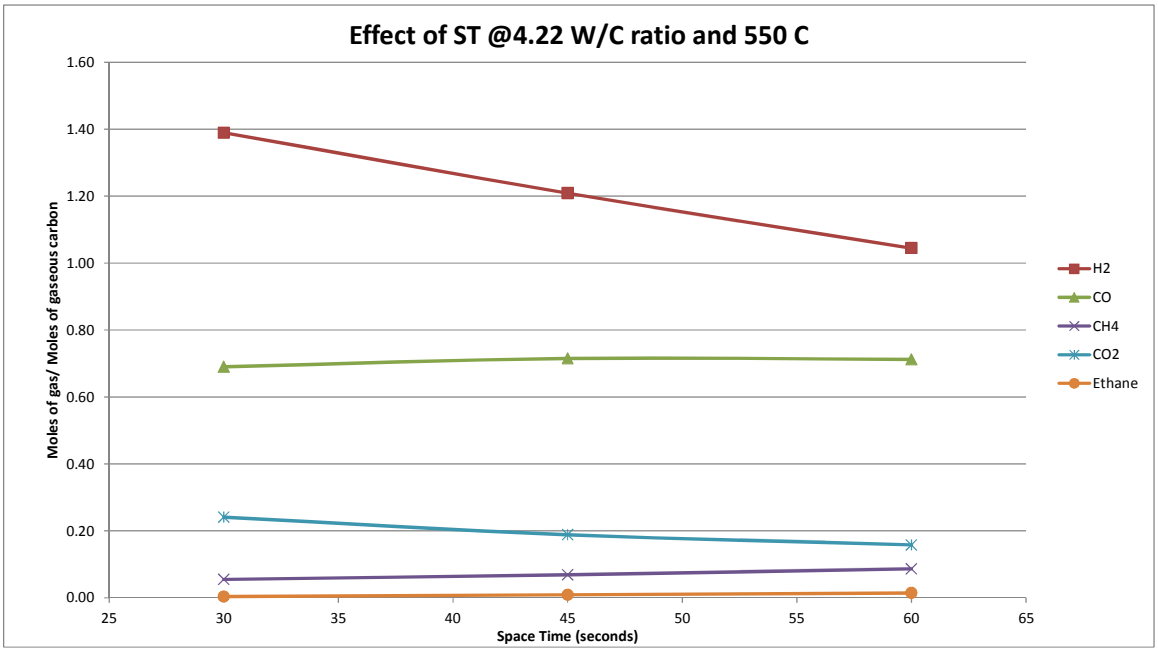

Figure 39. The effect of space time at a 4.22 water-to-carbon molar ratio and 550°C on gas composition (moles/moles gaseous carbon).

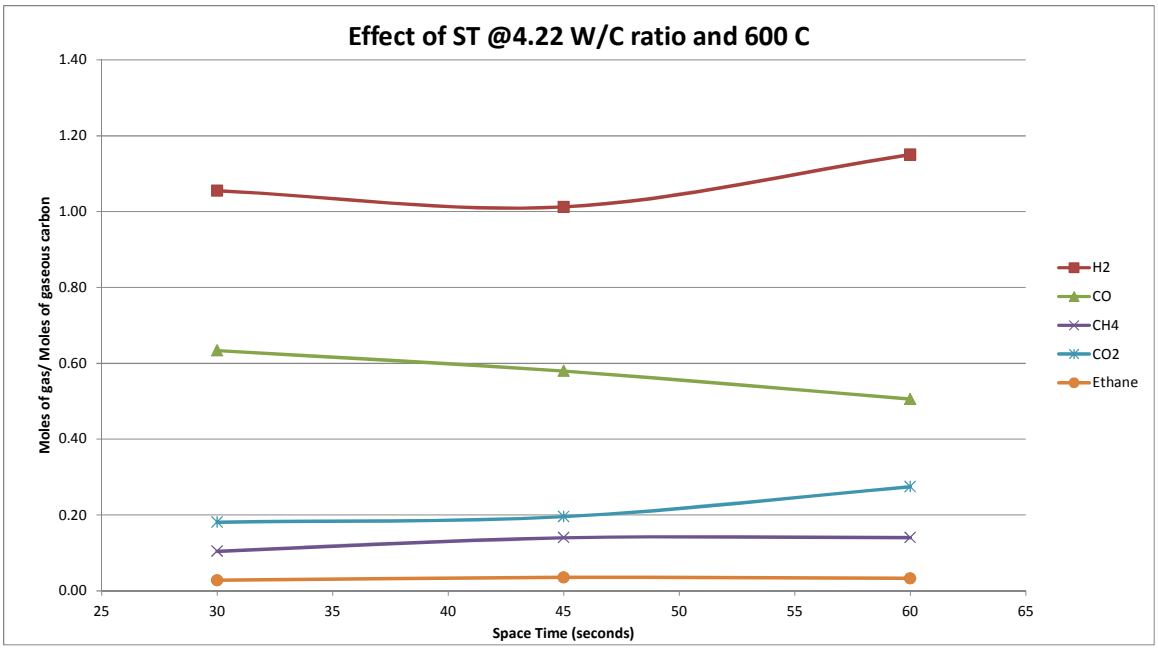

Figure 40. The effect of space time at a 4.22 water-to-carbon molar ratio and 600°C on gas composition (moles/moles gaseous carbon).

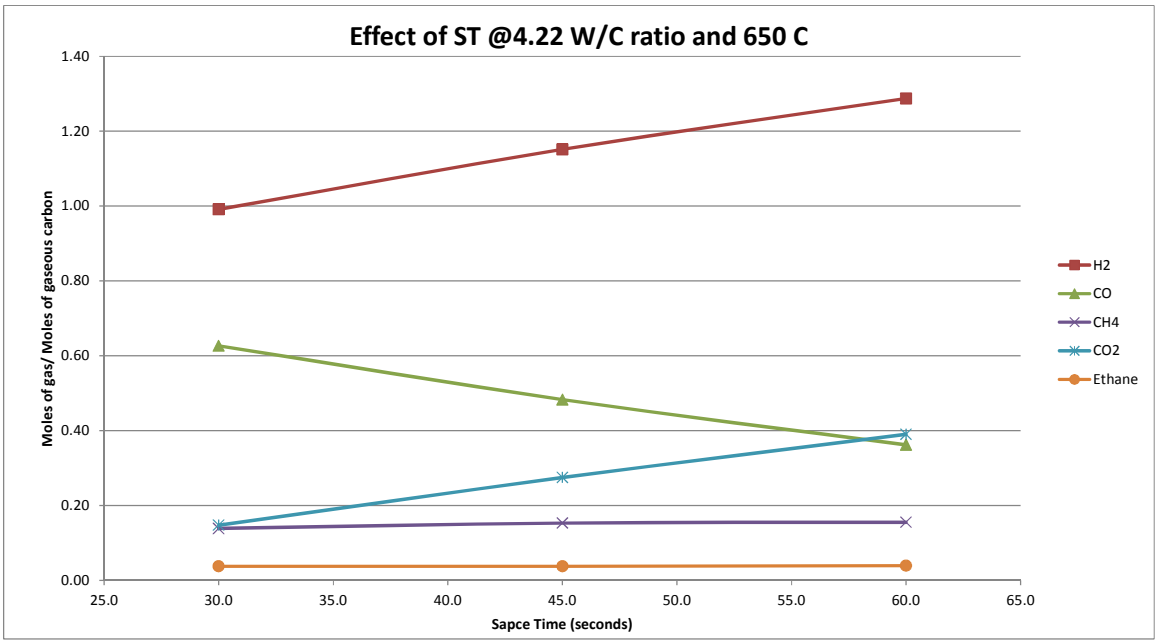

Figure 41. The effect of space time at a 4.22 water-to-carbon molar ratio and 650°C on gas composition (moles/moles gaseous carbon).

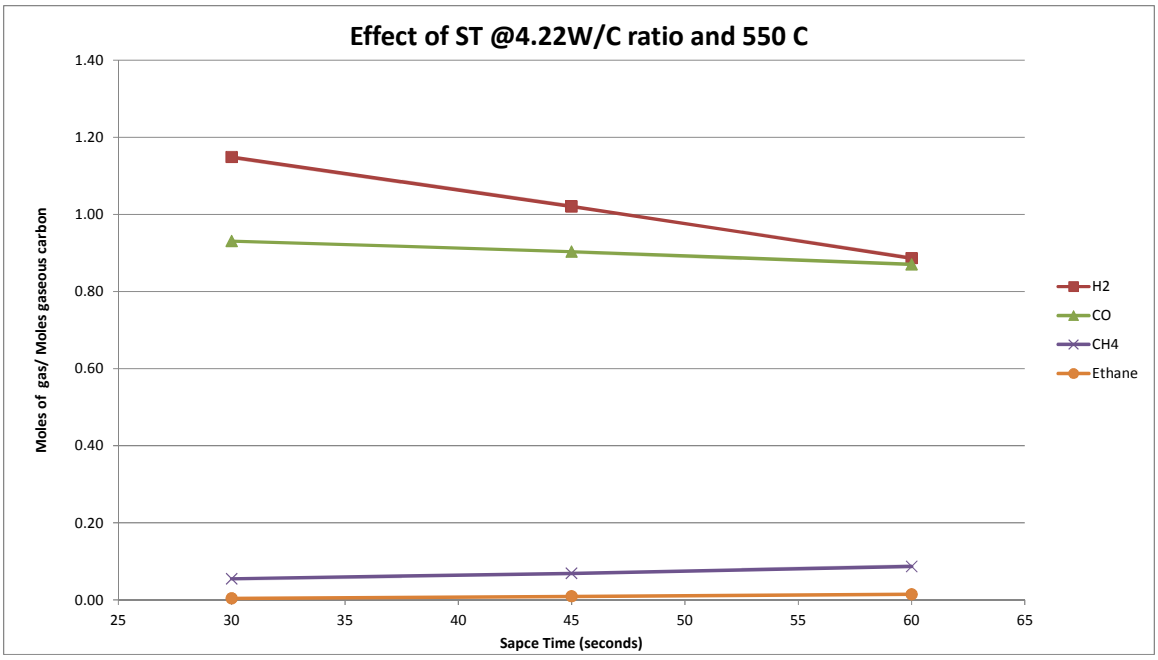

Figure 42. The effect of space time at a 4.22 water-to-carbon molar ratio and 550°C on gas composition (moles/moles gaseous carbon) with the water gas shift reaction undone.

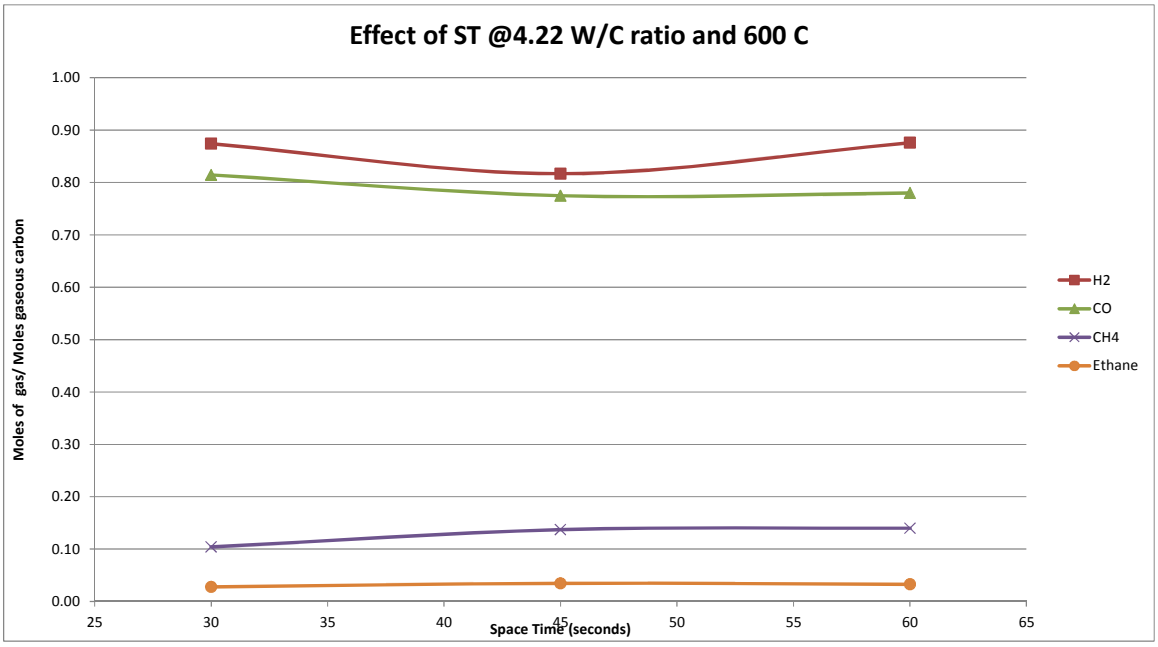

Figure 43. The effect of space time at a 4.22 water-to-carbon molar ratio and 600°C on gas composition (moles/moles gaseous carbon) with the water gas shift reaction undone.

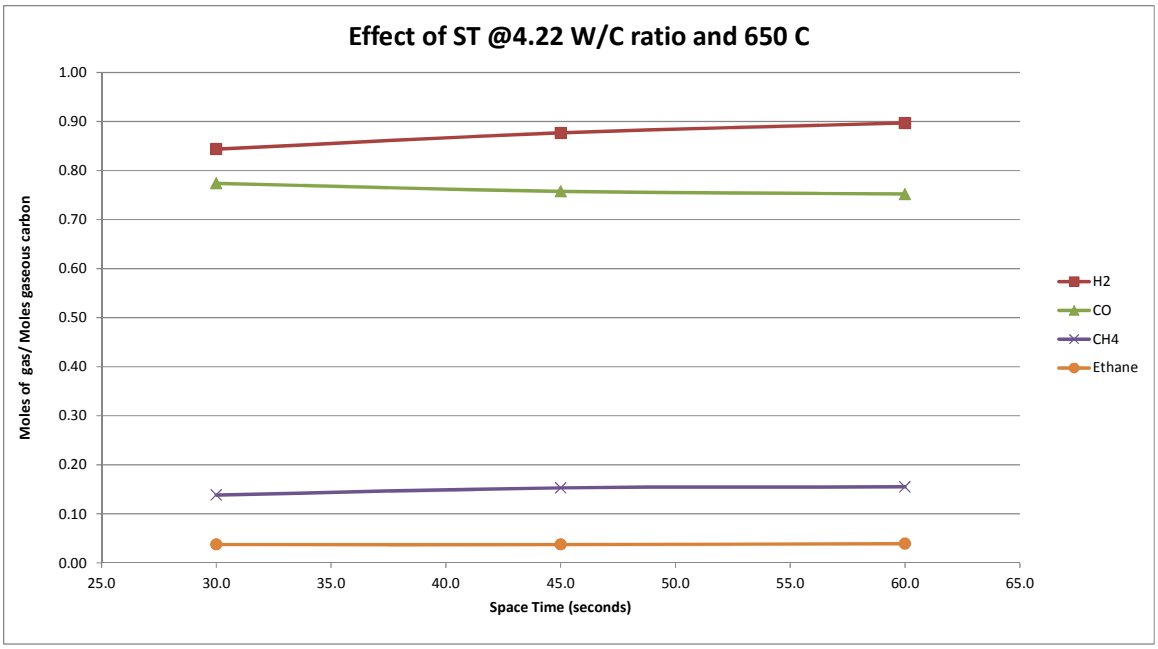

Figure 44. The effect of space time at a 4.22 water-to-carbon molar ratio and 650°C on gas composition (moles/moles gaseous carbon) with the water gas shift reaction undone.

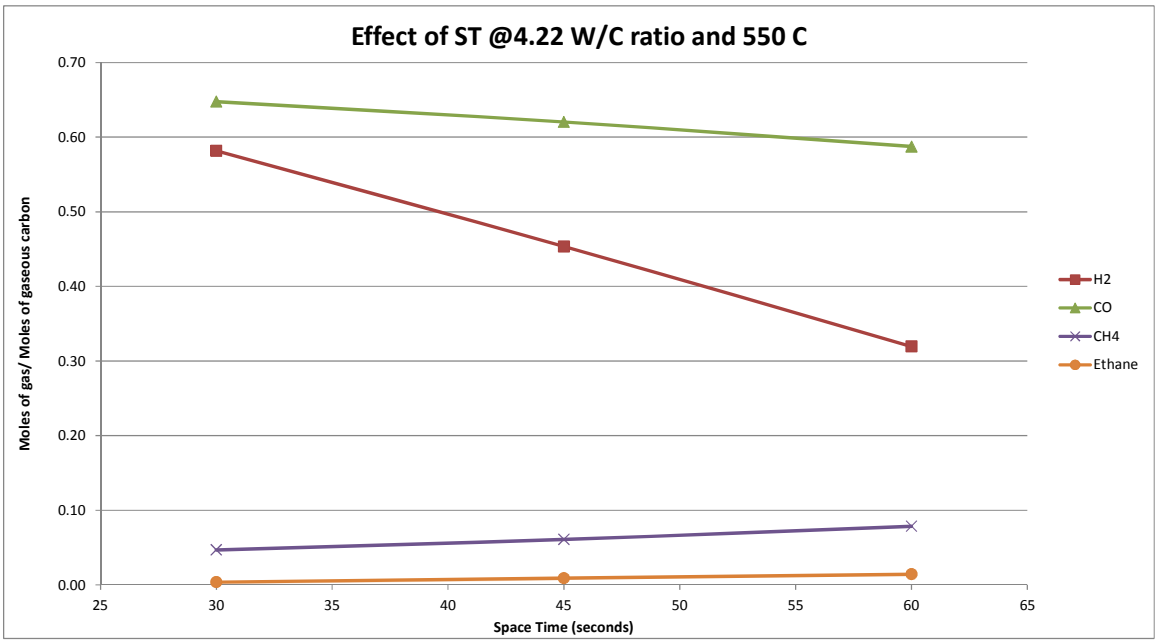

Figure 45. The effect of space time at a 4.22 water-to-carbon molar ratio and 550°C on gas composition (moles/moles gaseous carbon) with the water gas shift reaction undone and predicted methanol decomposition results removed.

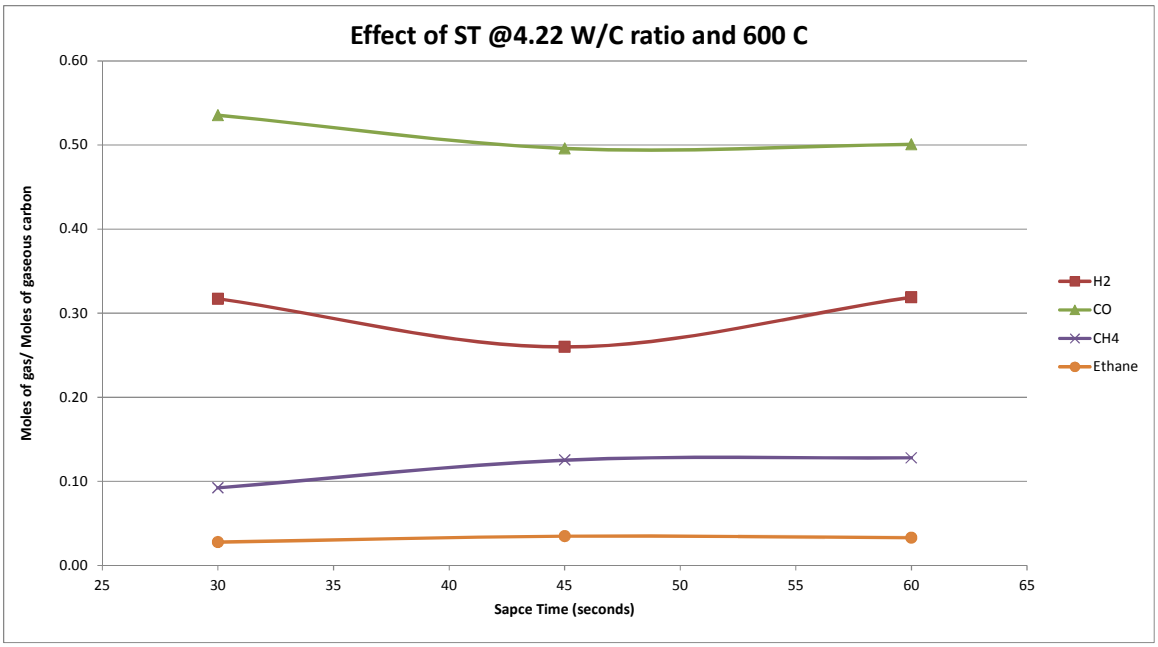

Figure 46. The effect of space time at a 4.22 water-to-carbon molar ratio and 600°C on gas composition (moles/moles gaseous carbon) with the water gas shift reaction undone and predicted methanol decomposition results removed.

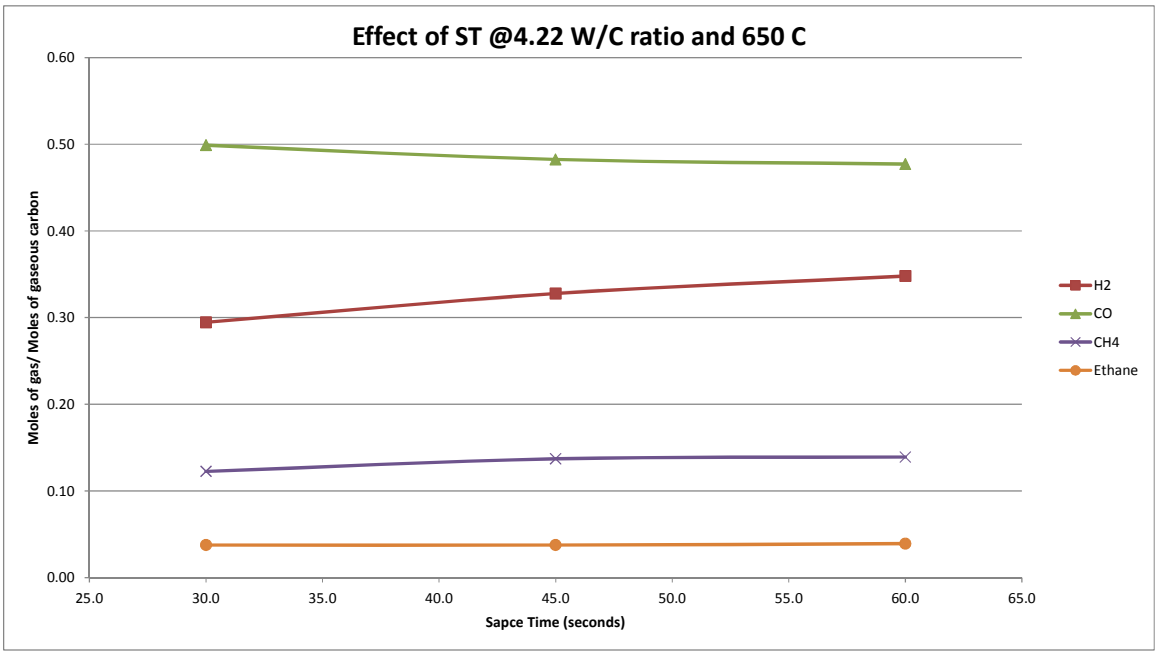

Figure 47. The effect of space time at a 4.22 water-to-carbon molar ratio and 650°C on gas composition (moles/moles gaseous carbon) with the water gas shift reaction undone and predicted methanol decomposition results removed.

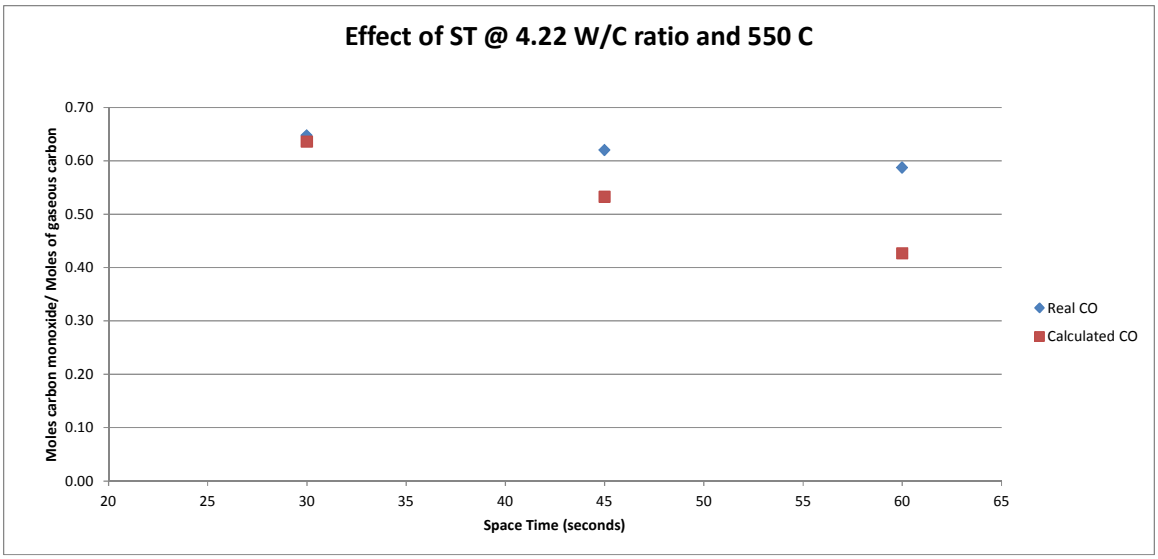

Figure 48. The effect of space time at a 4.22 water-to-carbon molar ratio and 550°C on the accuracy of the glycerin decomposition mechanism.

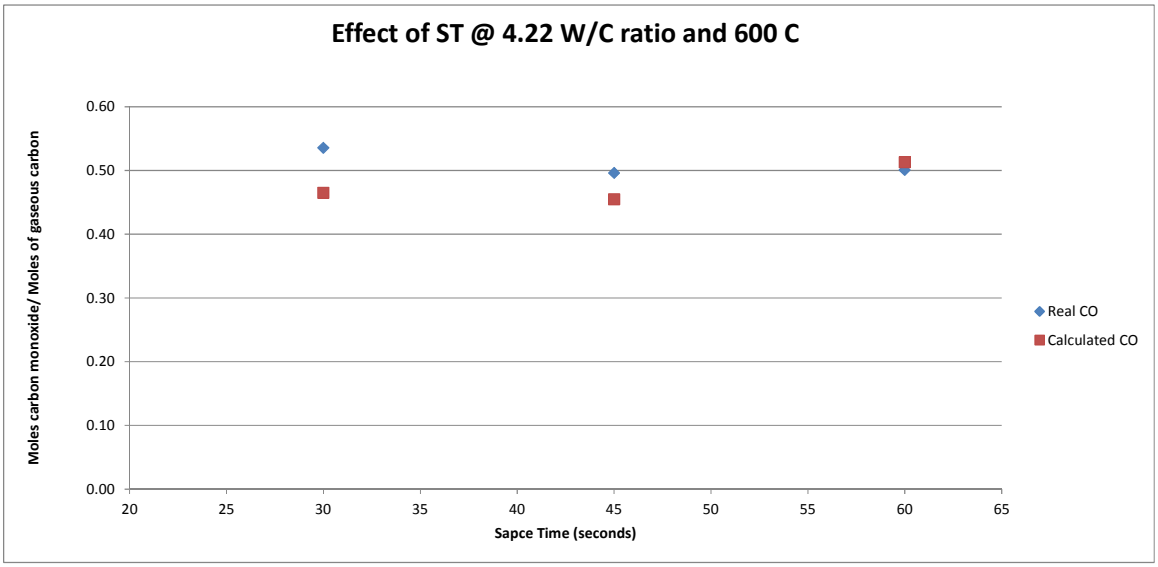

Figure 49. The effect of space time at a 4.22 water-to-carbon molar ratio and 600°C on the accuracy of the glycerin decomposition mechanism.

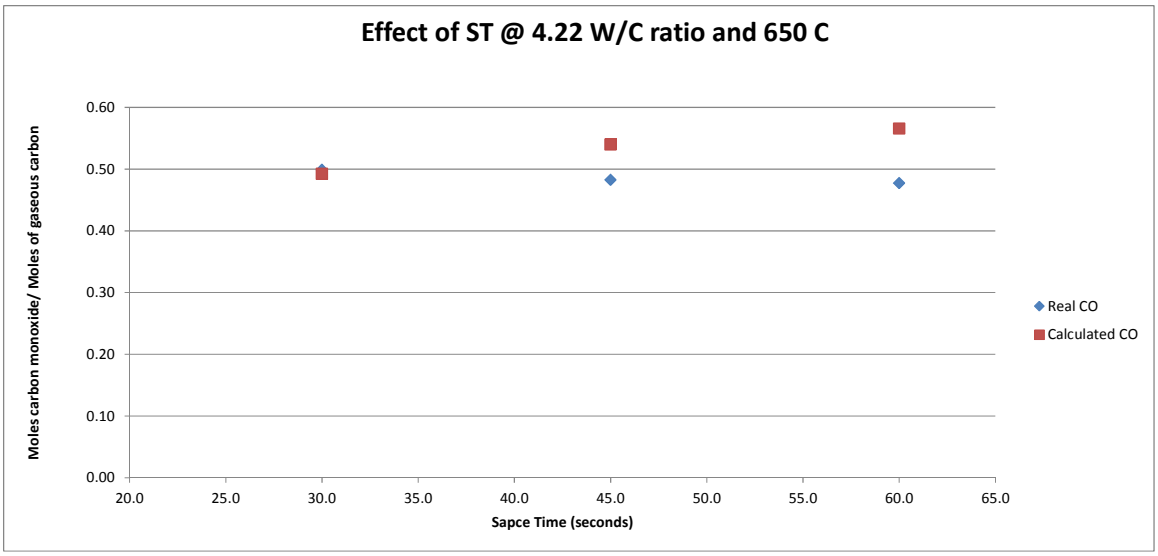

Figure 50. The effect of space time at a 4.22 water-to-carbon molar ratio and 650°C on the accuracy of the glycerin decomposition mechanism.

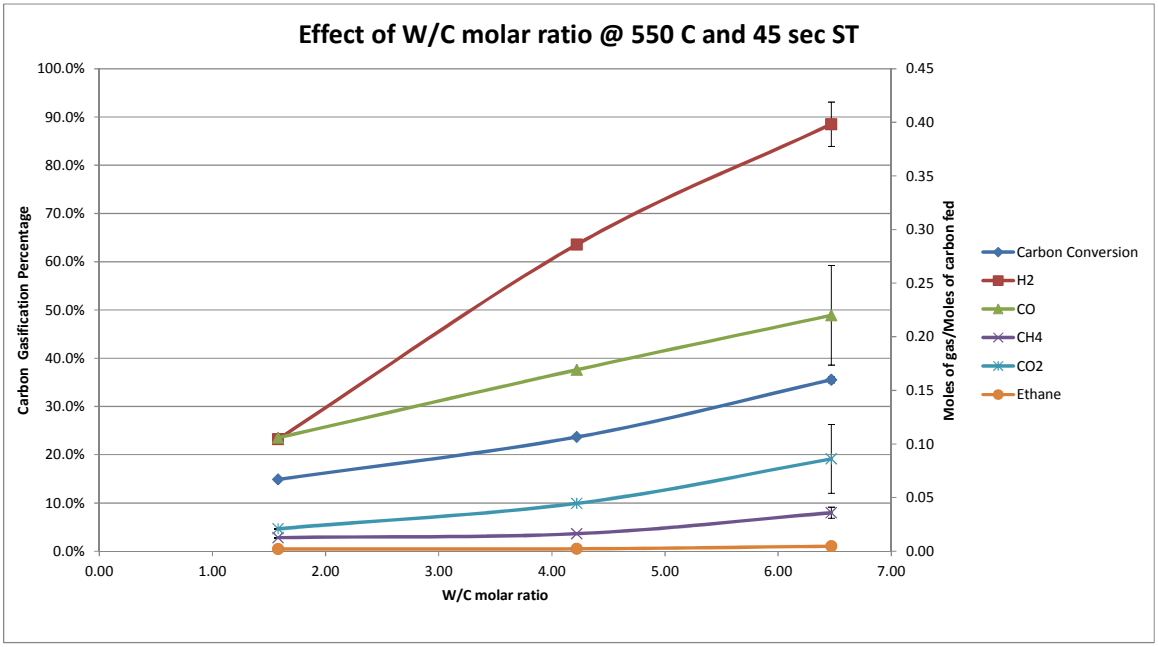

Figure 51. The effect of water-to-carbon molar ratio at 550°C and 45 second space time on carbon gasification and gas composition (moles/moles carbon fed).

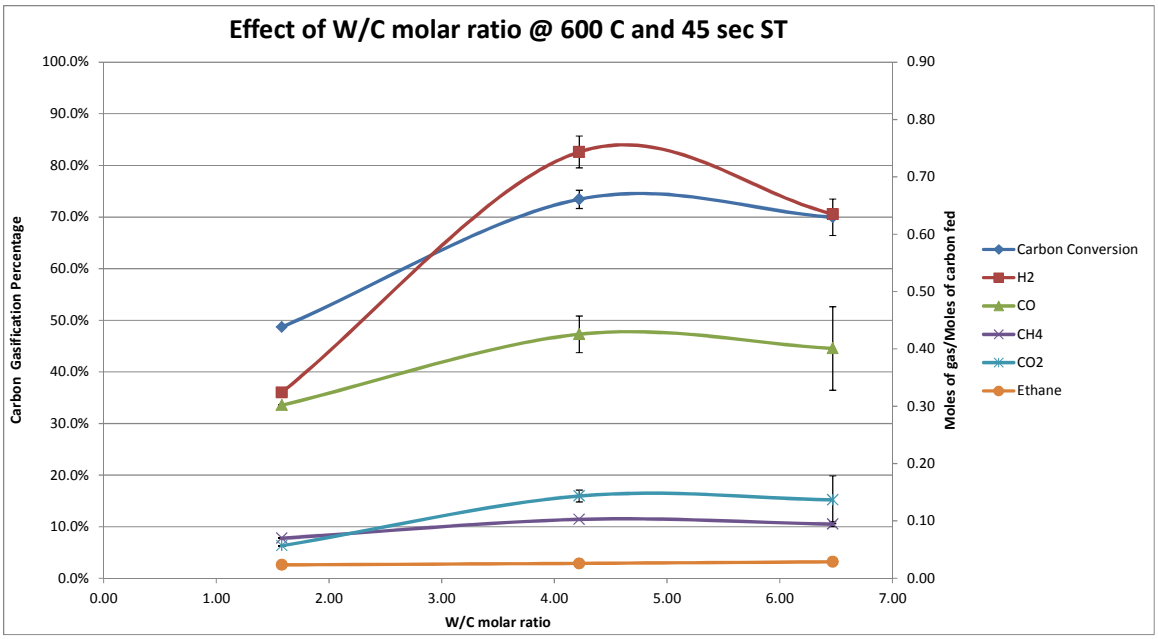

Figure 52. The effect of water-to-carbon molar ratio at 600°C and 45 second space time on carbon gasification and gas composition (moles/moles carbon fed).

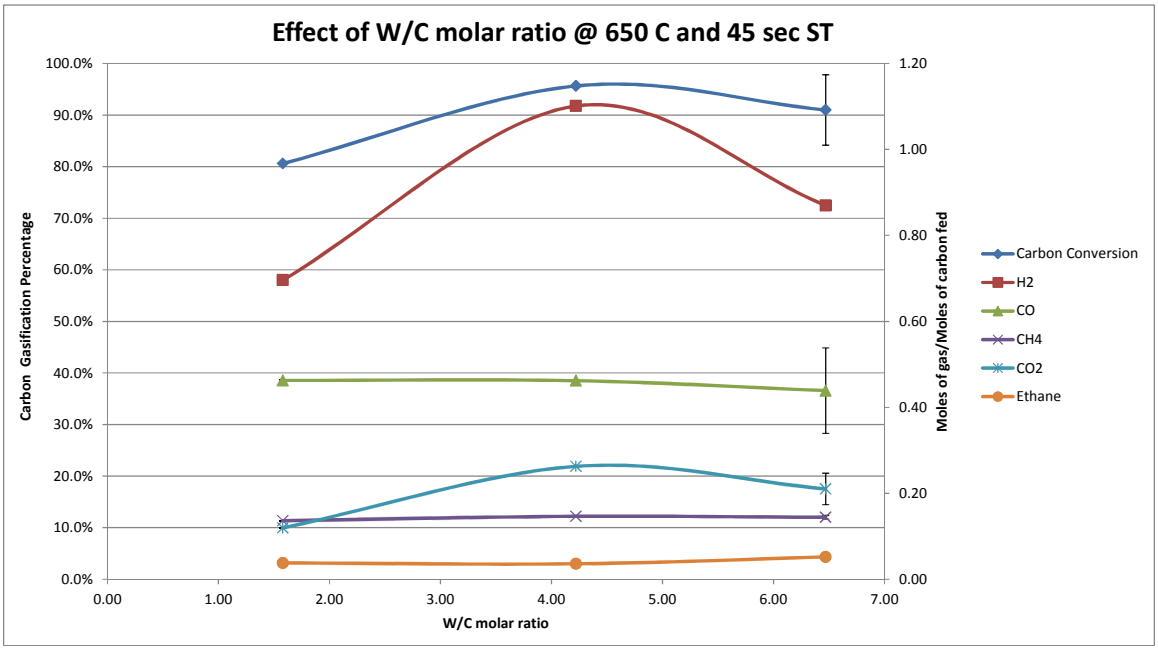

Figure 53. The effect of water-to-carbon molar ratio at 650°C and 45 second space time on carbon gasification and gas composition (moles/moles carbon fed).

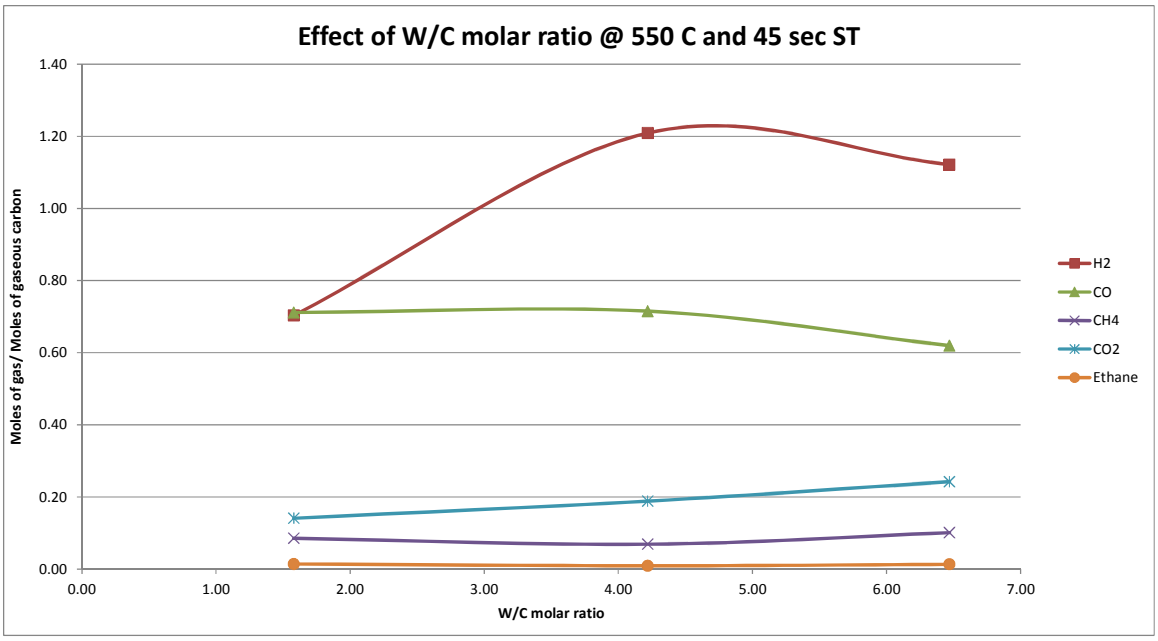

Figure 54. The effect of water-to-carbon molar ratio at 550°C and 45 second space time on gas composition (moles/moles gaseous carbon).

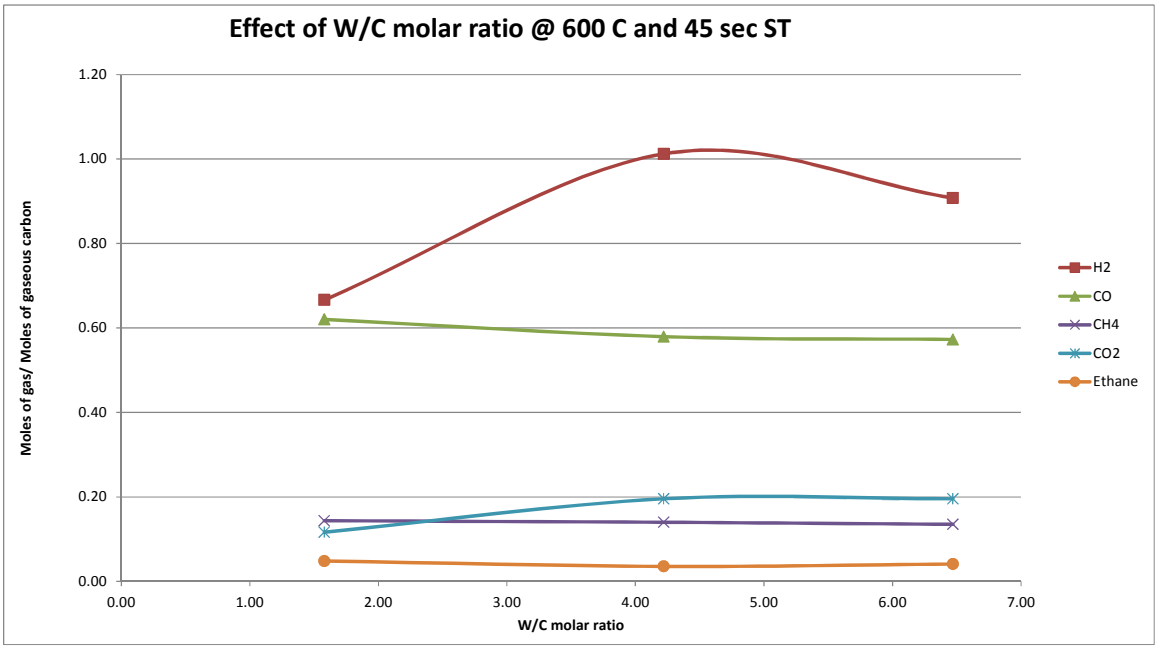

Figure 55. The effect of water-to-carbon molar ratio at 600°C and 45 second space time on gas composition (moles/moles gaseous carbon).

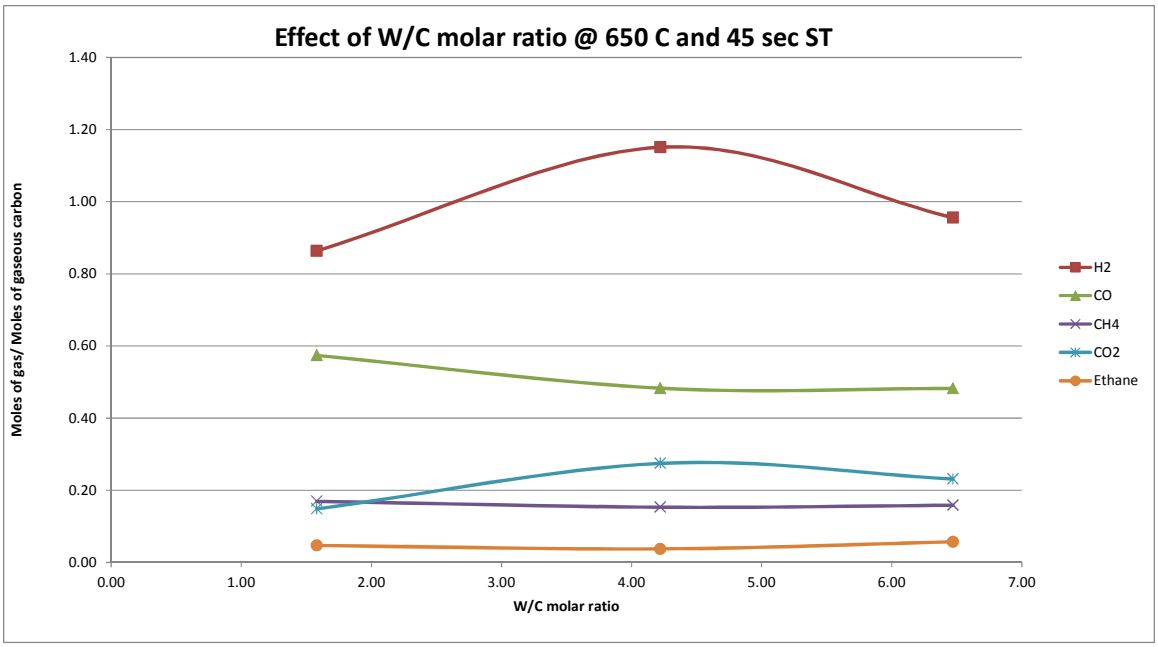

Figure 56. The effect of water-to-carbon molar ratio at 650°C and 45 second space time on gas composition (moles/moles gaseous carbon).

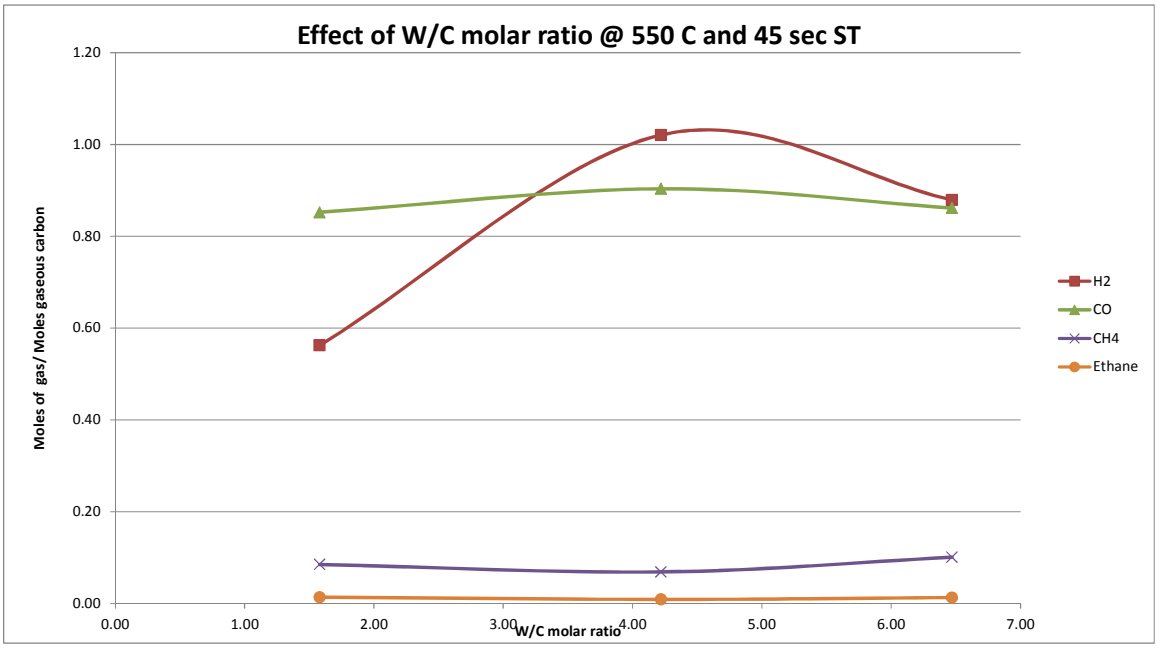

Figure 57. The effect of water-to-carbon molar ratio at 550°C and 45 second space time on gas composition (moles/moles gaseous carbon) with the water gas shift reaction undone.

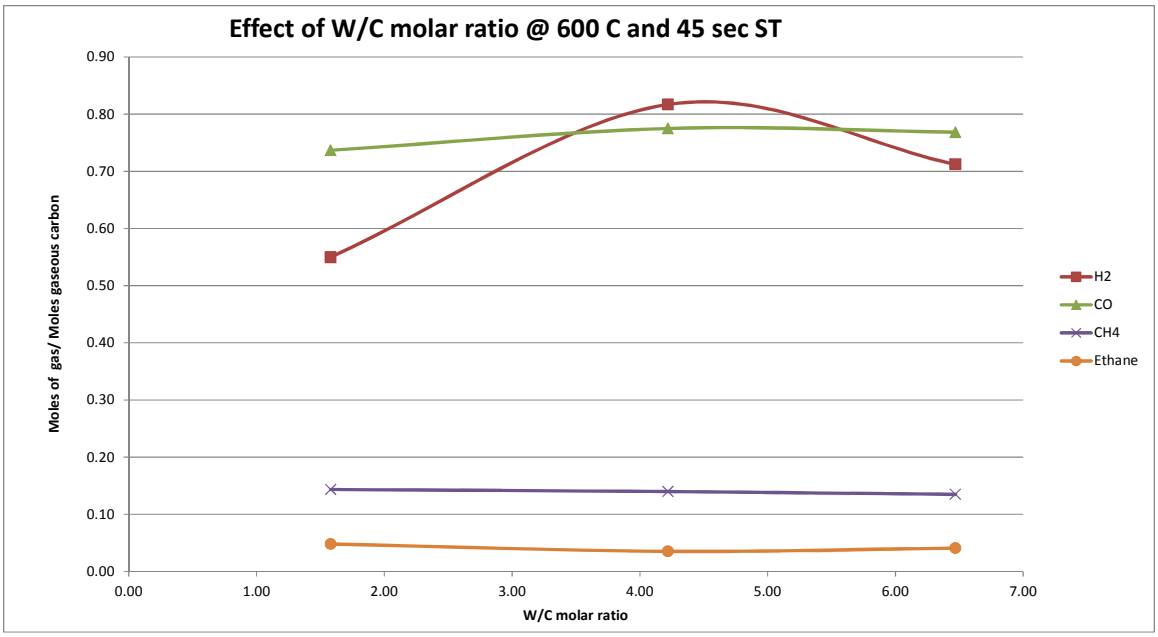

Figure 58. The effect of water-to-carbon molar ratio at 600°C and 45 second space time on gas composition (moles/moles gaseous carbon) with the water gas shift reaction undone.

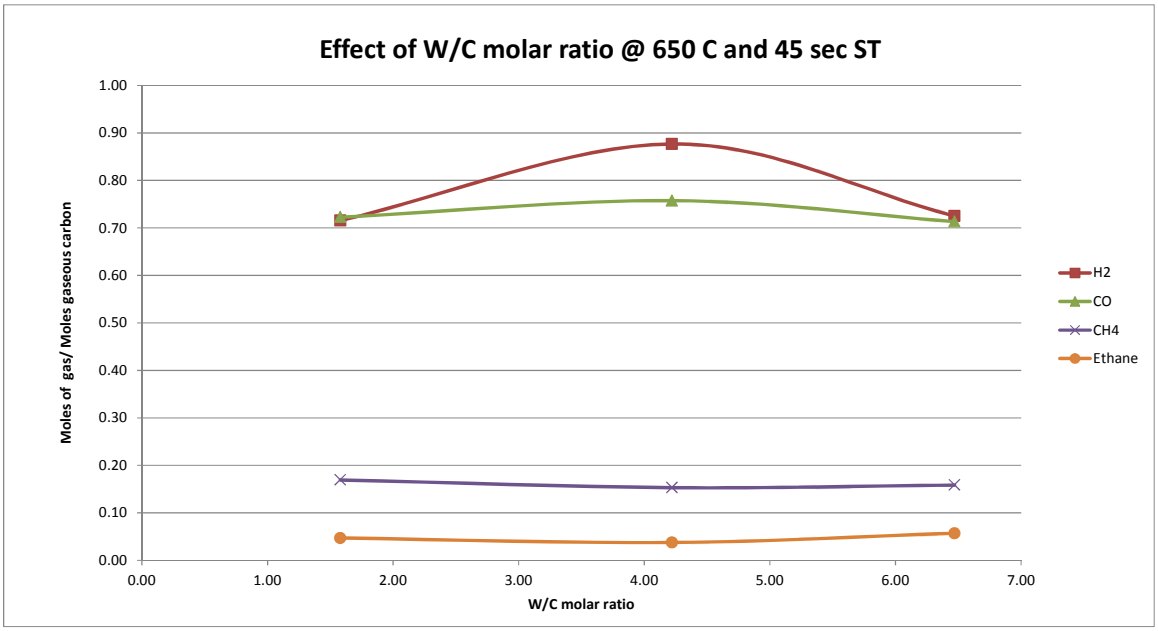

Figure 59. The effect of water-to-carbon molar ratio at 650°C and 45 second space time on gas composition (moles/moles gaseous carbon) with the water gas shift reaction undone.

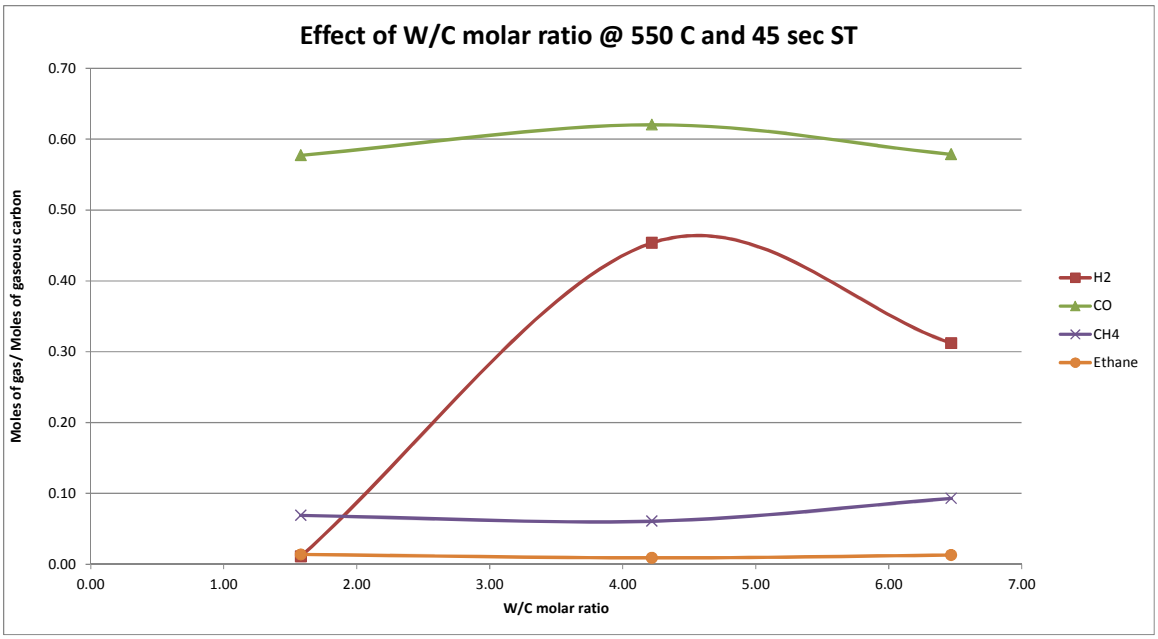

Figure 60. The effect of water-to-carbon molar ratio at 550°C and 45 second space time on gas composition (moles/moles gaseous carbon) with the water gas shift reaction undone and predicted methanol decomposition results removed.

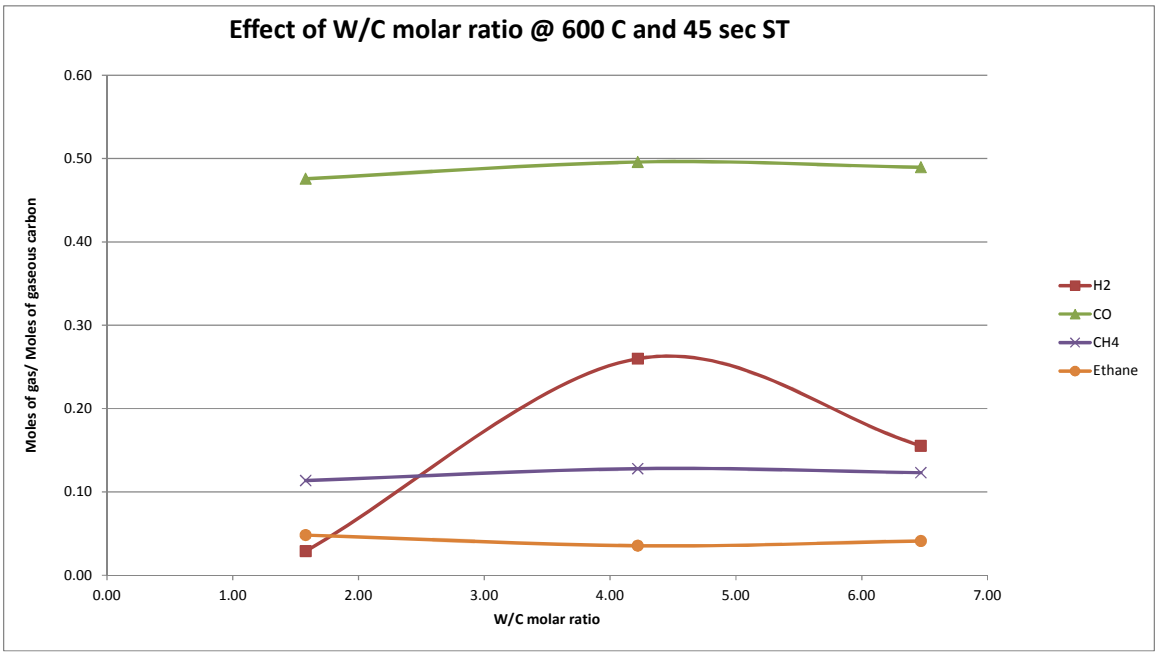

Figure 61. The effect of water-to-carbon molar ratio at 600°C and 45 second space time on gas composition (moles/moles gaseous carbon) with the water gas shift reaction undone and predicted methanol decomposition results removed.

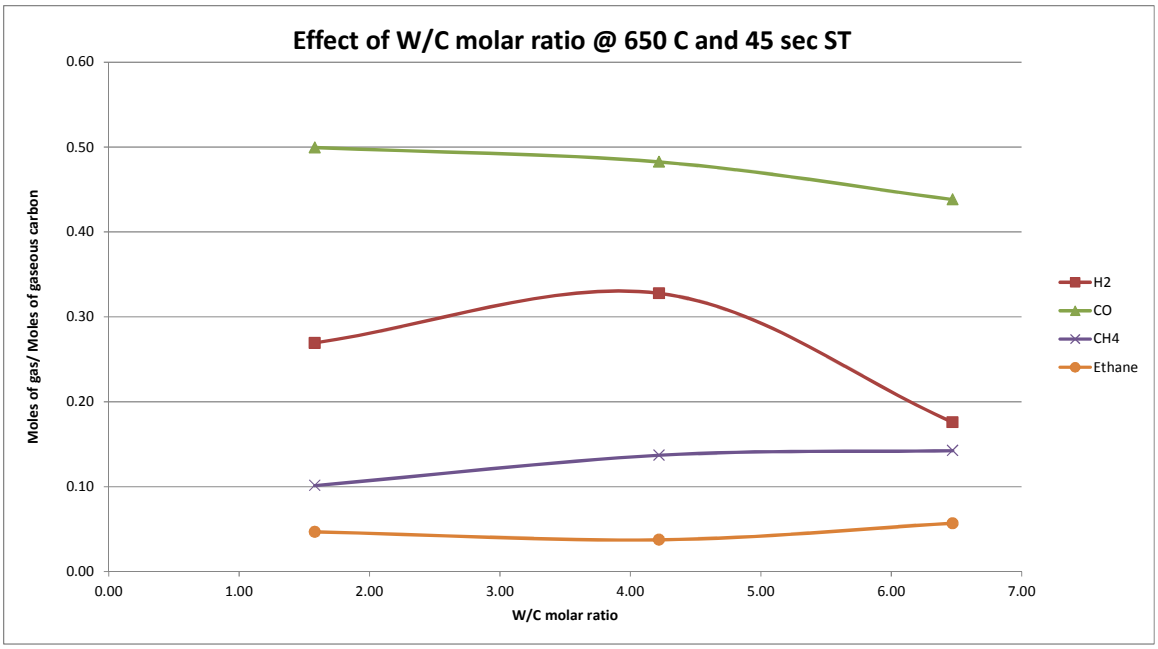

Figure 62. The effect of water-to-carbon molar ratio at 650°C and 45 second space time on gas composition (moles/moles gaseous carbon) with the water gas shift reaction undone and predicted methanol decomposition results removed.

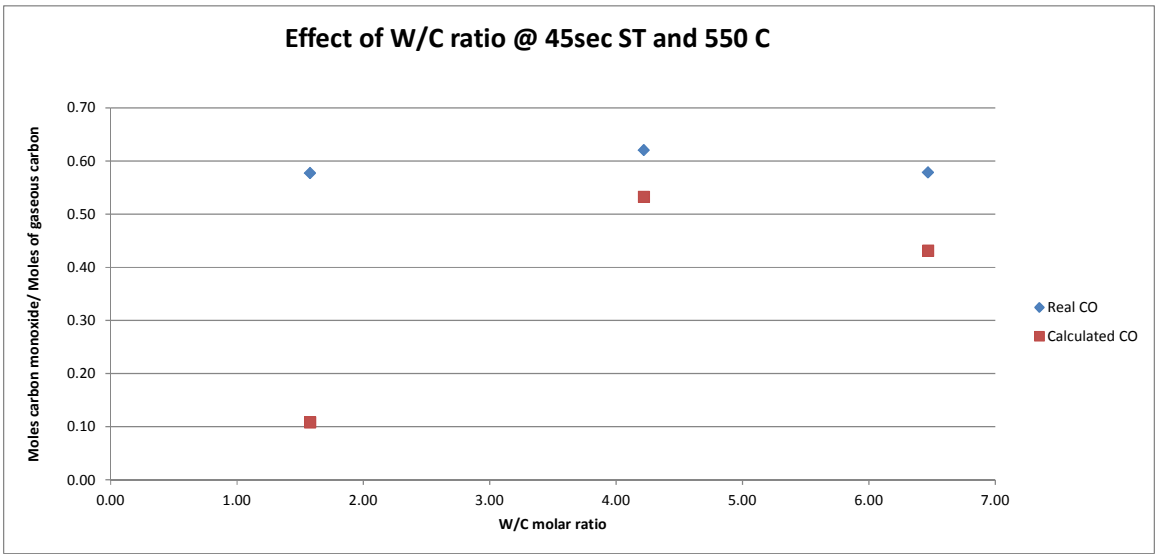

Figure 63. The effect of water-to-carbon molar ratio at 550°C and 45 second space time on the accuracy of the glycerin decomposition mechanism.

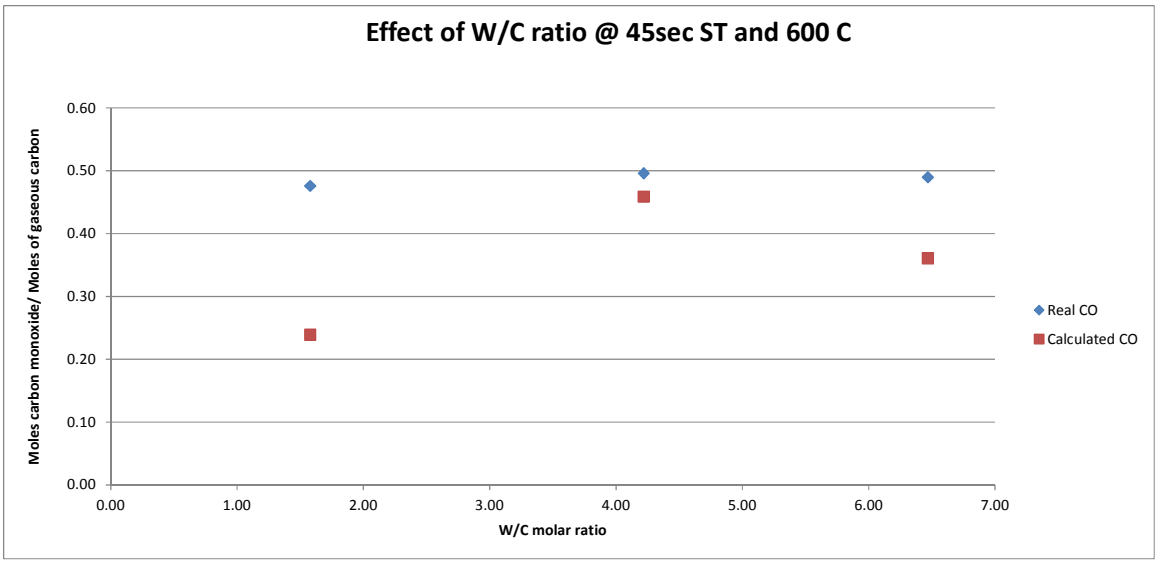

Figure 64. The effect of water-to-carbon molar ratio at 600°C and 45 second space time on the accuracy of the glycerin decomposition mechanism.

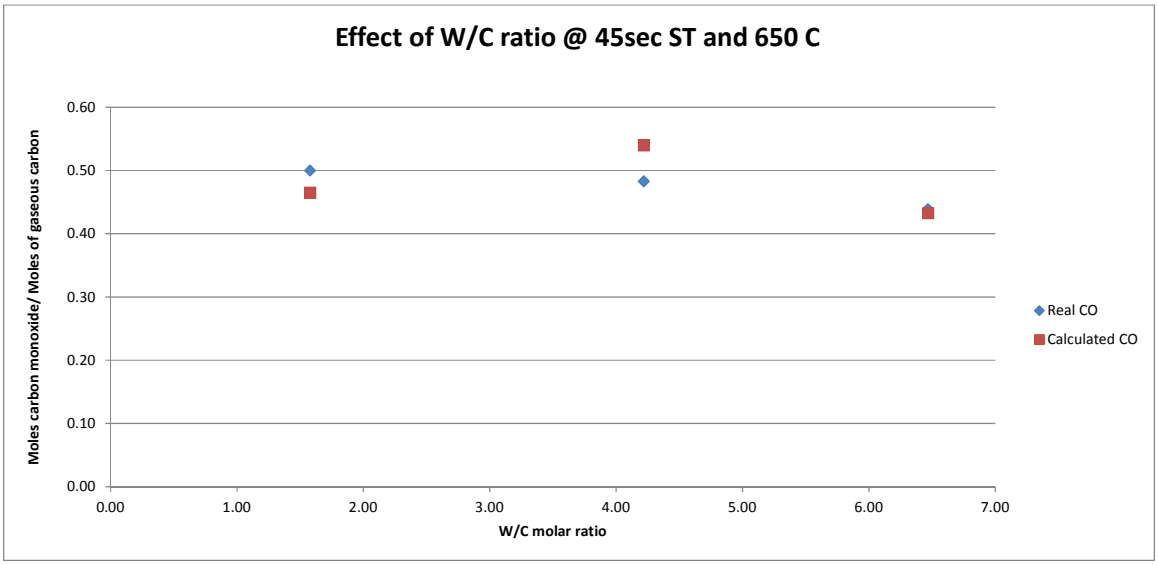

Figure 65. The effect of water-to-carbon molar ratio at 650°C and 45 second space time on the accuracy of the glycerin decomposition mechanism.

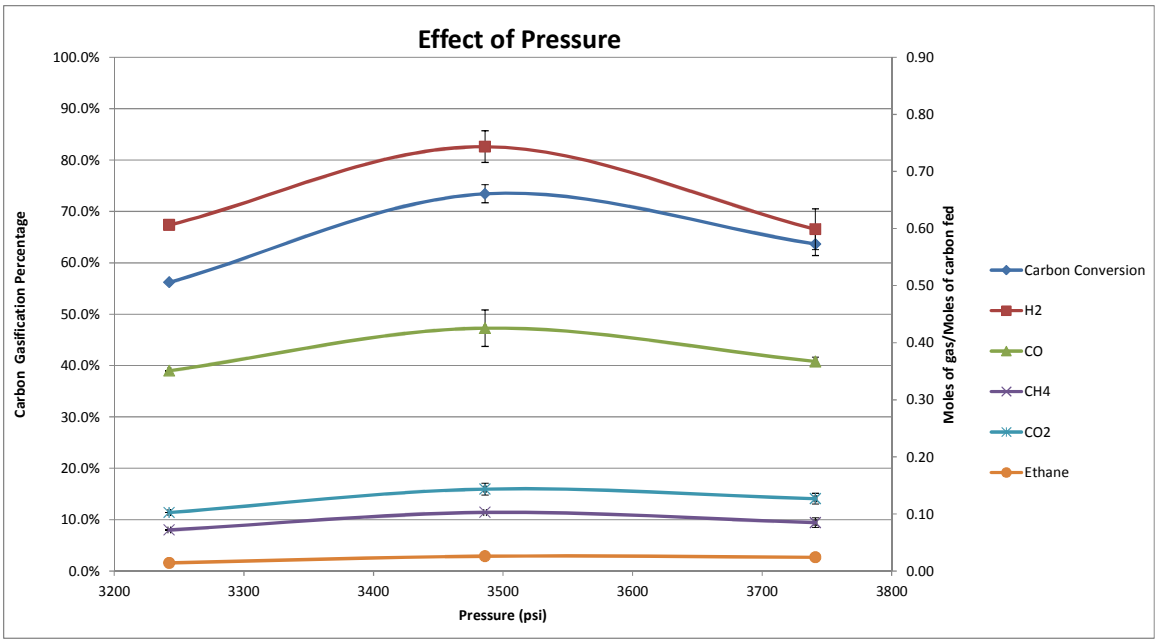

Figure 66. The effect of pressure on carbon gasification and gas composition (moles/moles carbon fed).

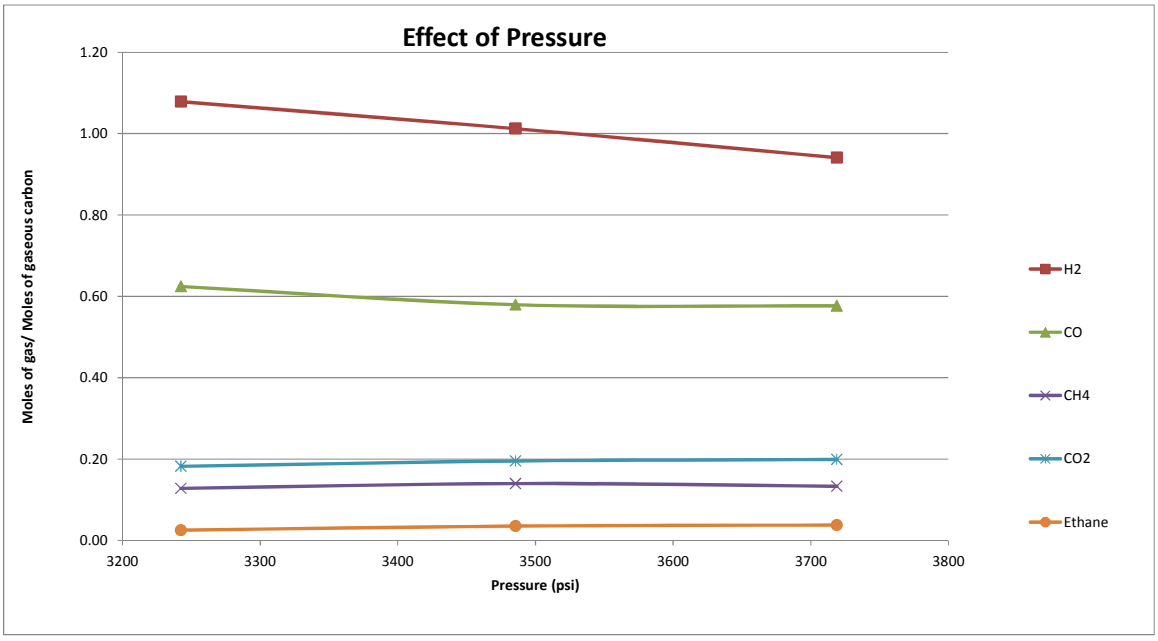

Figure 67. The effect of pressure on gas composition (moles/moles gaseous carbon).

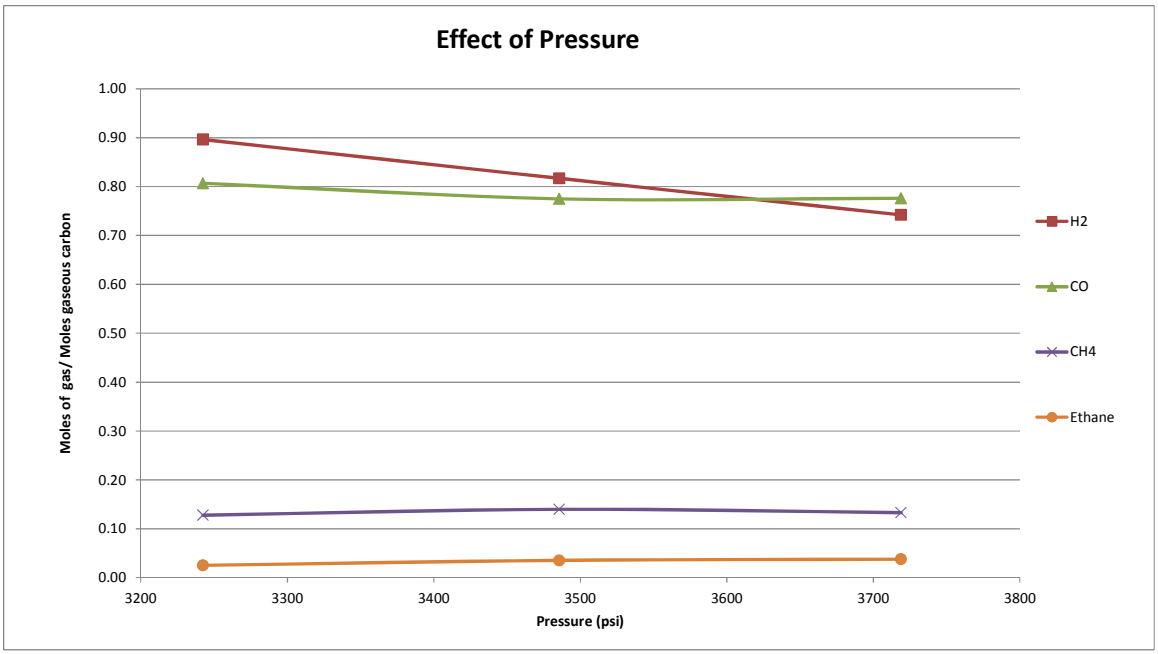

Figure 68. The effect of pressure on gas composition (moles/moles gaseous carbon) with the water gas shift reaction undone.

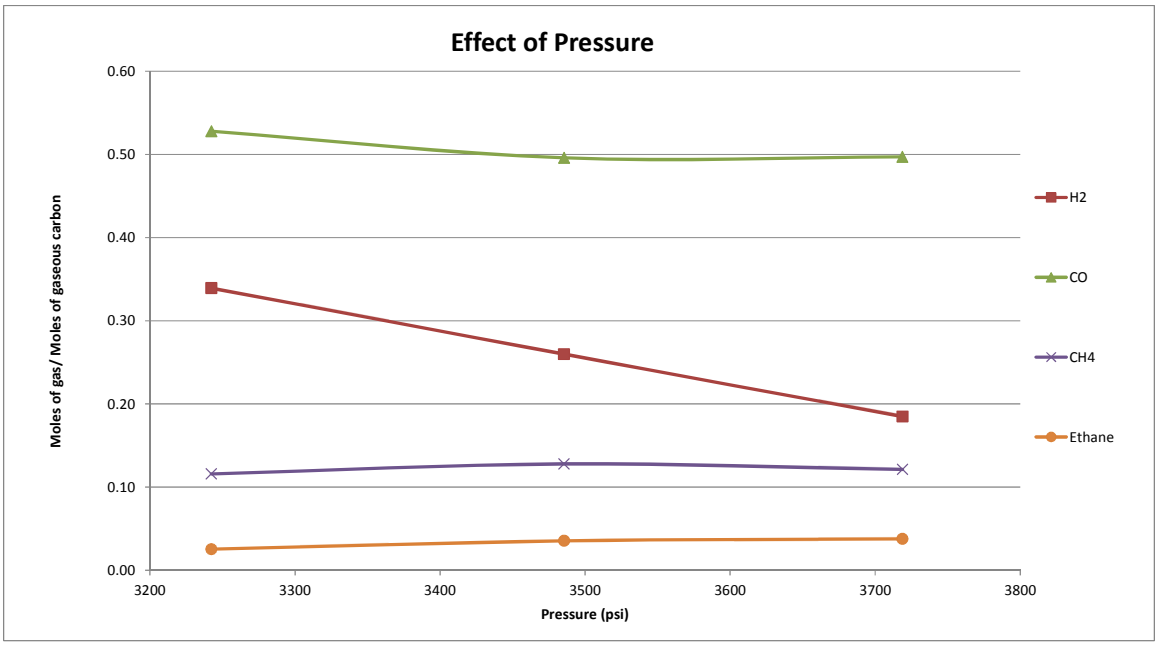

Figure 69. The effect of pressure on gas composition (moles/moles gaseous carbon) with the water gas shift reaction undone and predicted methanol decomposition results removed.

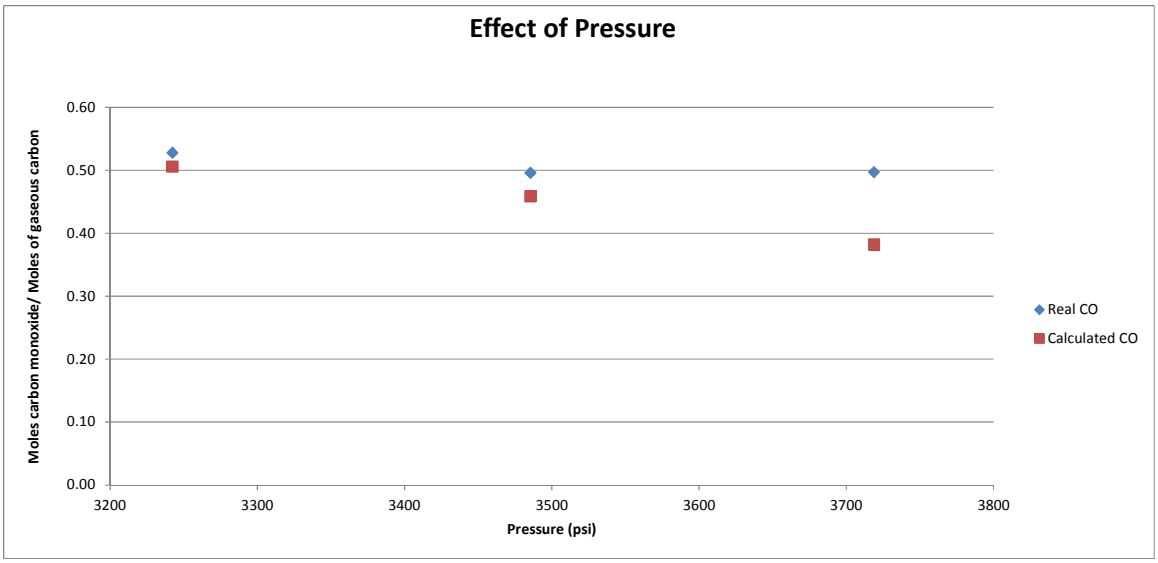

Figure 70. The effect of pressure on the accuracy of the glycerin decomposition mechanism.

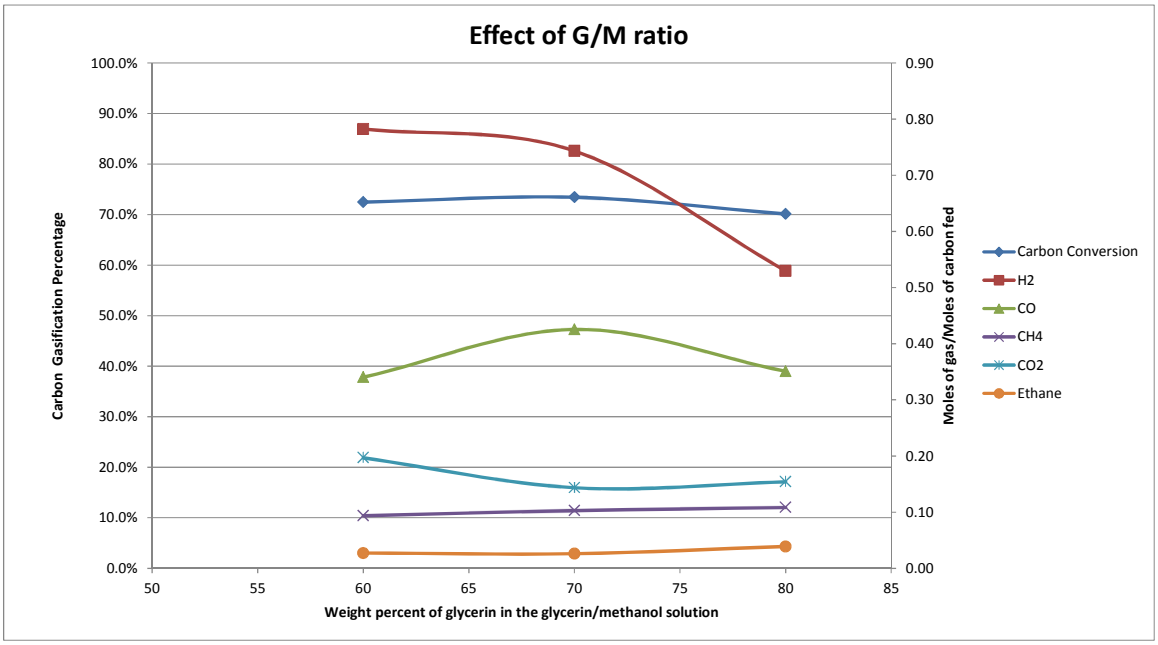

Figure 71. The effect of glycerin-to-methanol weight ratio on carbon gasification and gas composition (moles/moles carbon fed).

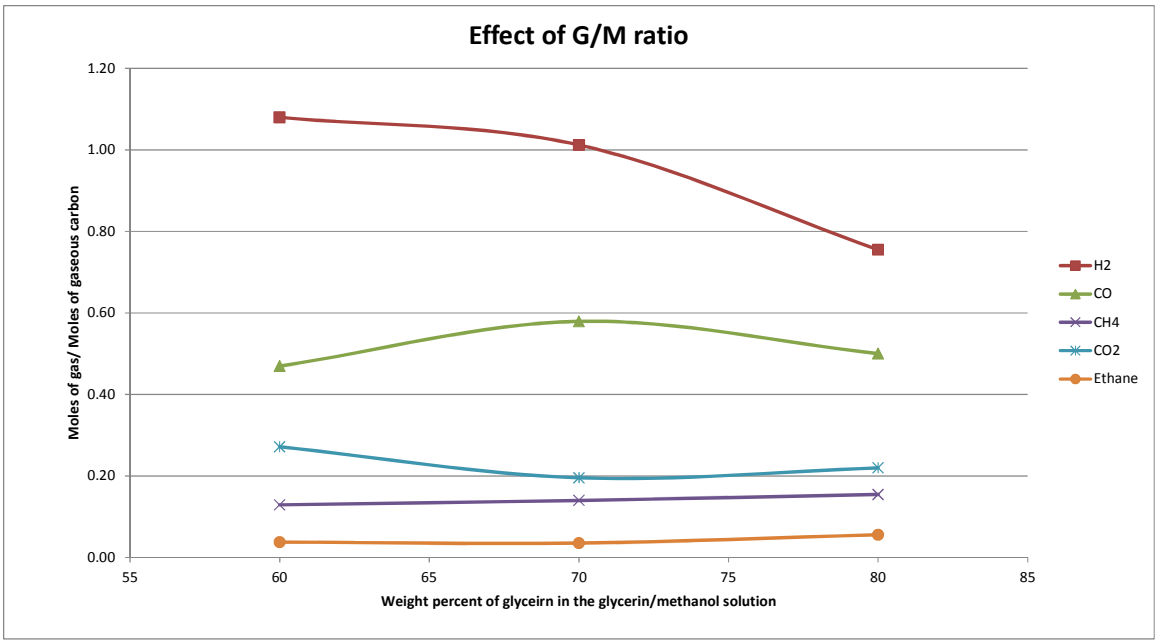

Figure 72. The effect of glycerin-to-methanol weight ratio on gas composition (moles/moles gaseous carbon).

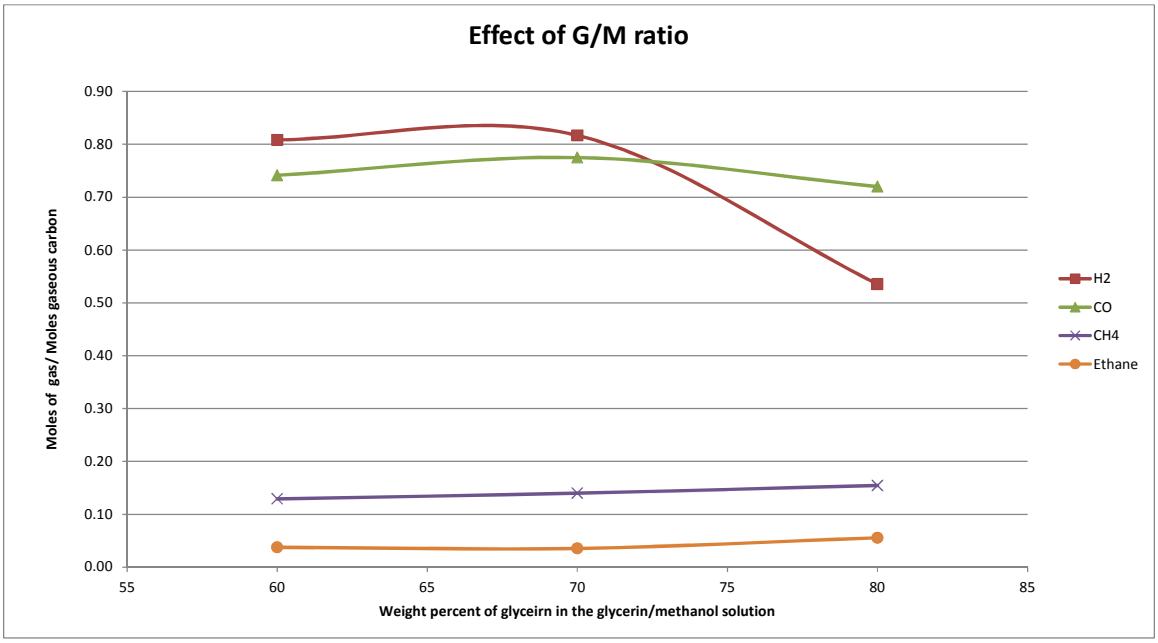

Figure 73. The effect of glycerin-to-methanol weight ratio on gas composition (moles/moles gaseous carbon) with the water gas shift reaction undone.

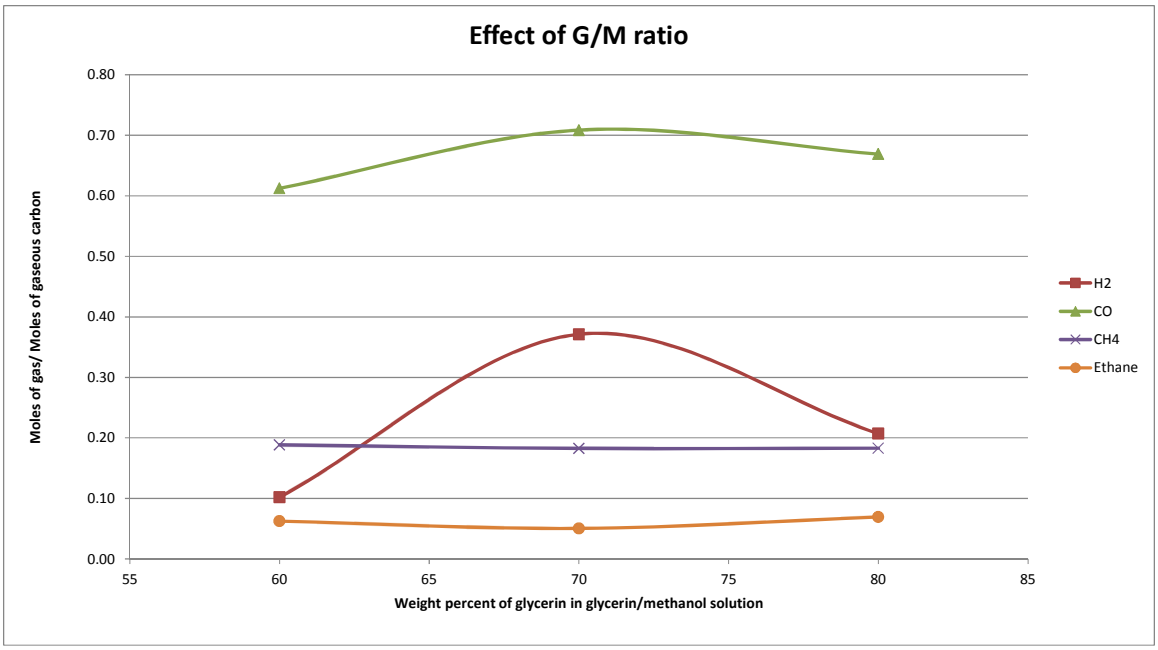

Figure 74. The effect of glycerin-to-methanol weight ratio on gas composition (moles/moles gaseous carbon) with the water gas shift reaction undone and predicted methanol decomposition results removed.

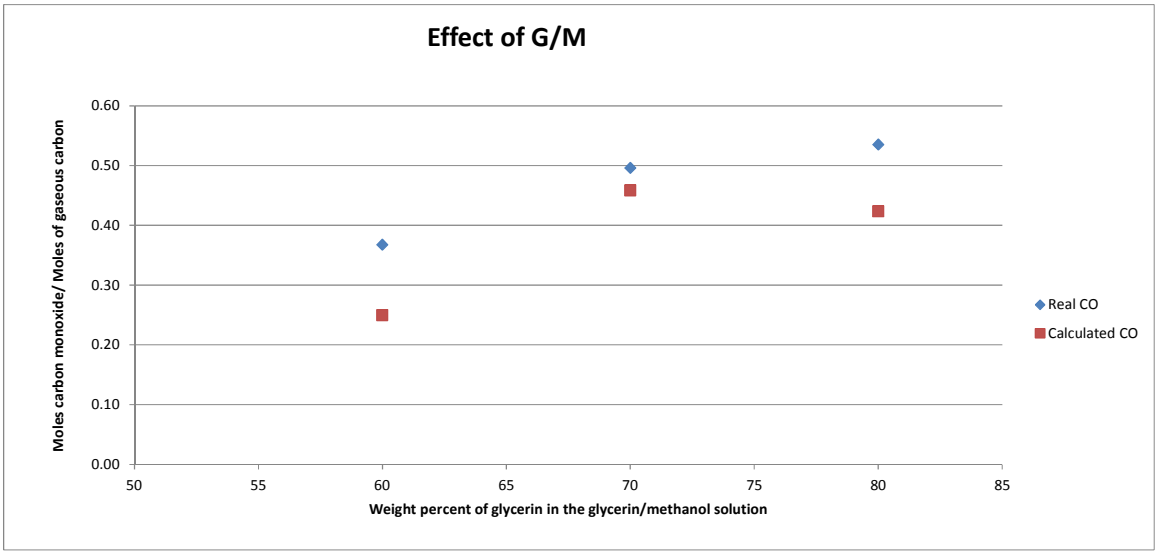

Figure 75. The effect of glycerin-to-methanol weight ratio on the accuracy of the glycerin decomposition mechanism.

Table 1. The weight, molar compositions, and critical points of solutions of crude glycerin and water.

Solution Type		Weight percent			Mole percent			Critical Point	
Water/Carbon molar ratio	Glycerin/Methanol weight ratio	Water%	Glycerin%	Methanol%	Water%	Glycerin%	Methanol%	Critical Temp (°C)	Critical Pressure (psi)
4.22	70:30	71.0	20.3	8.7	88.9	5.0	6.1	401	3116
4.22	60:40	70.9	17.5	11.6	87.7	4.2	8.1	397	3131
4.22	80:20	71.1	23.1	5.8	90.1	5.7	4.1	409	3116
1.58	70:30	47.9	36.5	15.6	75.1	11.2	13.7	416	2764
6.47	70:30	79.0	14.7	6.3	92.5	3.4	4.1	396	3234

Table 2. Experimental run conditions summary.

Run No.	Temp	Pressure	Water	Fuel	Glycerin wt%	MeOH wt%	W/C ratio
	(°C)	(psig)	(g/min)				
WCG-97M	598	3469	8.6	CG Soln 70/30	20.3	8.7	4.22
WCG-98M	598	3486	8.8	CG Soln 70/30	20.3	8.7	4.22
WCG-99M	648	3415	8.0	CG Soln 70/30	20.3	8.7	4.22
WCG-100M	499	3496	11.6	CG Soln 70/30	20.3	8.7	4.22
WCG-101M	549	3472	9.8	CG Soln 70/30	20.3	8.7	4.22
WCG-102M	599	3468	11.5	CG Soln 70/30	20.3	8.7	4.22
WCG-103M	648	3464	10.3	CG Soln 70/30	20.3	8.7	4.22
WCG-104M	498	3508	15.7	CG Soln 70/30	20.3	8.7	4.22
WCG-105M	549	3513	12.8	CG Soln 70/30	20.3	8.7	4.22
WCG-106M	598	3486	17.8	CG Soln 70/30	20.3	8.7	4.22
WCG-107M	599	3739	12.7	CG Soln 70/30	20.3	8.7	4.22
WCG-108M	548	3497	19.6	CG Soln 70/30	20.3	8.7	4.22
WCG-109M	599	3242	10.9	CG Soln 70/30	20.3	8.7	4.22
WCG-110M	698	3427	9.6	CG Soln 70/30	20.3	8.7	4.22
WCG-111M	698	3489	7.6	CG Soln 70/30	20.3	8.7	4.22
WCG-112M	598	3503	11.8	CG Soln 70/30	20.3	8.7	4.22
WCG-113M	648	3511	7.8	CG Soln 70/30	20.3	8.7	4.22
WCG-114M	599	3718	12.6	CG Soln 70/30	20.3	8.7	4.22
WCG-115M	648	3501	16.2	CG Soln 70/30	20.3	8.7	4.22
WCG-116M	599	3499	14.5	CG Soln 70/30	36.5	15.6	1.58
WCG-117M	648	3494	13.3	CG Soln 70/30	36.5	15.6	1.58
WCG-118M	500	3507	20.4	CG Soln 70/30	36.5	15.6	1.58
WCG-119M	548	3503	17.6	CG Soln 70/30	36.5	15.6	1.58
WCG-120M	698	3488	12.4	CG Soln 70/30	36.5	15.6	1.58
WCG-121M	549	3474	11.8	CG Soln 70/30	14.7	6.3	6.47
WCG-122M	599	3489	10.6	CG Soln 70/30	14.7	6.3	6.47
WCG-123M	648	3468	10.2	CG Soln 70/30	14.7	6.3	6.47
WCG-124M	599	3497	12.2	CG Soln 80/20	25.4	6.3	4.22
WCG-125M	599	3493	11.4	CG Soln 60/40	16	10.7	4.22
WCG-138M	599	3483	11.8	CG Soln 80/20	23.1	5.8	4.22
WCG-139M	598	3463	11.6	CG Soln 60/40	17.5	11.6	4.22
WCG-140M	598	3487	11.5	CG Soln 70/30	20.3	8.7	4.22
WCG-141M	598	3743	12.7	CG Soln 70/30	20.3	8.7	4.22
WCG-142M	549	3455	12.7	CG Soln 70/30	14.7	6.3	6.47
WCG-143M	599	3462	11.0	CG Soln 70/30	14.7	6.3	6.47
WCG-144M	648	3477	10.0	CG Soln 70/30	14.7	6.3	6.47

Table 3. Experimental run results summary.

Run No.	Product Gas Flow	Gas Yield (mol gas/mol carbon fed)					
	(L/min)	H2	CO	CH4	CO2	C2H4	C2H6
WCG-97M	3.40	0.91	0.45	0.13	0.22	0.00	0.03
WCG-98M	3.85	1.09	0.43	0.12	0.26	0.00	0.02
WCG-99M	4.20	1.34	0.21	0.18	0.53	0.00	0.03
WCG-100M	0.71	0.15	0.09	0.01	0.02	0.00	0.00
WCG-101M	1.44	0.33	0.23	0.03	0.05	0.00	0.00
WCG-102M	3.76	0.74	0.43	0.10	0.14	0.00	0.02
WCG-103M	4.71	1.10	0.46	0.15	0.26	0.00	0.04
WCG-104M	0.73	0.12	0.07	0.00	0.01	0.00	0.00
WCG-105M	1.52	0.29	0.17	0.02	0.04	0.00	0.00
WCG-106M	3.70	0.48	0.29	0.05	0.08	0.00	0.01
WCG-107M	3.53	0.63	0.37	0.08	0.12	0.00	0.02
WCG-108M	1.80	0.23	0.12	0.01	0.04	0.00	0.00
WCG-109M	2.85	0.61	0.35	0.07	0.10	0.00	0.01
WCG-110M	4.75	1.25	0.11	0.24	0.56	0.00	0.02
WCG-111M	3.61	1.12	0.09	0.31	0.55	0.00	0.02
WCG-112M	4.12	0.79	0.48	0.10	0.13	0.00	0.02
WCG-113M	3.66	1.19	0.33	0.14	0.36	0.00	0.04
WCG-114M	2.91	0.48	0.35	0.08	0.08	0.00	0.02
WCG-115M	5.48	0.75	0.48	0.11	0.11	0.00	0.03
WCG-116M	4.63	0.32	0.30	0.07	0.06	0.00	0.02
WCG-117M	7.91	0.70	0.46	0.14	0.12	0.00	0.04
WCG-118M	0.86	0.05	0.03	0.00	0.01	0.00	0.00
WCG-119M	1.78	0.10	0.11	0.01	0.02	0.00	0.00
WCG-120M	9.62	0.96	0.36	0.20	0.32	0.00	0.05
WCG-121M	1.43	0.38	0.27	0.03	0.05	0.00	0.00
WCG-122M	2.33	0.64	0.47	0.10	0.10	0.00	0.03
WCG-123M	3.02	0.88	0.54	0.15	0.17	0.00	0.05
WCG-124M	3.36	0.51	0.40	0.08	0.08	0.00	0.02
WCG-125M	2.87	0.64	0.39	0.07	0.09	0.00	0.02
WCG-138M	3.20	0.53	0.35	0.11	0.15	0.00	0.04
WCG-139M	3.80	0.78	0.34	0.09	0.20	0.00	0.03
WCG-140M	3.58	0.70	0.37	0.10	0.16	0.00	0.03
WCG-141M	3.43	0.56	0.36	0.09	0.14	0.00	0.03
WCG-142M	1.59	0.42	0.17	0.04	0.12	0.00	0.01
WCG-143M	2.28	0.63	0.33	0.09	0.18	0.00	0.03
WCG-144M	2.71	0.86	0.34	0.14	0.25	0.00	0.05

Table 4. Reactions of glycerin decomposition in supercritical water.

1. Glycerin → Hydroxyacetone + Water	12. Propionaldehyde → Ethane + Carbon Monoxide
$C_3H_5(OH)_3 \rightarrow CH_3COCH_2OH + H_2O$	**$COHCH_2CH_3 \rightarrow C_2H_6 + CO$**
2. Glycerin → 3-Hydroxypropanal +Water	13. Propylene Glycol → Acetone + Water
$C_3H_5(OH)_3 \rightarrow COHCH_2CH_2OH + H_2O$	**$COHCH_2CH_3 \rightarrow CH_3COCH_3 + H_2O$**
3. 3-Hydroxypropanal → Acrolein + Water	14. Propionaldehyde + Hydrogen → 1-Propanol
$COHCH_2CH_2OH \rightarrow COHCH=CH_2 + H_2O$	**$COHCH_2CH_3 + H_2 \rightarrow CH_3CH_2CH_2OH$**
4. Acrolein → Ethylene + Carbon Monoxide	15. Acetone → Methane + Ethanone
$COHCH=CH_2 \rightarrow C_2H_4 + CO$	**$CH_3COCH_3 \rightarrow CH_4 + CH_2=C=O$**
5. Acrolein + Hydrogen → Propionaldehyde	16. 2 Ethanone → Ethylene +2 Carbon Monoxide
$COHCH=CH_2 + H_2 \rightarrow COHCH_2CH_3$	**2. $CH_2=C=O \rightarrow C_2H_4 + 2\ CO$**
6. Hydroxyacetone → Acetaldehyde + Formaldehyde	17. Acetone + Hydrogen → Isopropanol
$CH_3COCH_2OH \rightarrow COHCH_3 + COH_2$	**$CH_3COCH_3 + H_2 \rightarrow CH_3CHOHCH_3$**
7. 3-Hydroxypropanal → Acetaldehyde + Formaldehyde	18. 1-Propanol → Acetaldehyde + Methane
$CH_3COCH_2OH \rightarrow COHCH_3 + COH_2$	**$CH_3CH_2CH_2OH \rightarrow COHCH_3 + CH_4$**
8. Acetaldehyde → Methane + Carbon Monoxide	19. 1-Propanol → Propylene + Water
$COHCH_3 \rightarrow CH_4 + CO$	**$CH_3CH_2CH_2OH \rightarrow CH_3CH=CH_2 + H_2O$**
9. Formaldehyde → Hydrogen + Carbon Monoxide	20. Isopropanol → Propylene + Water
$COH_2 \rightarrow H_2 + CO$	**$CH_3CHOHCH_3 \rightarrow CH_3CH=CH_2 + H_2O$**
10. Hydroxyacetone + Hydrogen → Propylene Glycol	21. Propylene + Hydrogen → Propane
$CH_3COCH_2OH + H_2 \rightarrow CH_3CHOHCH_2OH$	**$CH_3CH=CH_2 + H_2 \rightarrow CH_3CH_2CH_3$**
11. Propylene Glycol → Propionaldehyde + Water	22. Propane → Ethylene + Methane
$CH_3CHOHCH_2OH \rightarrow COHCH_2CH_3 + H_2O$	**$CH_3CH_2CH_3 \rightarrow C_2H_4 + CH_4$**

Table 5. Glycerin-to-final products pathways.

		Net Final Products				
	Pathway	H2	CO	CH_4	C_2H_6	H_2O
1	Glycerin/hydroxyacetone/ acetaldehyde+formaldehyde	1	2	1	0	1
2	Glycerin/3-hydroxypropanal/ acetaldehyde+formaldehyde	1	2	1	0	1
3	Glycerin/3-hydroxypropanal/acrolein	-1	1	0	1	2
4	Glycerin/3-hydroxypropanal/ acrolein/propionaldehyde	-1	1	0	1	2
5	Glycerin/hydroxyacetone/propylene glycol/propionaldehyde	-1	1	0	1	2
6	Glycerin/hydroxyacetone/propylene glycol/acetone/ethanone	-1.5	1	1	0.5	2
7	Glycerin/3-hydroxypropanal/propionaldehyde/ 1-propanol/acetaldehyde	-2	1	2	0	2
8	Glycerin/hydroxyacetone/propylene glycol/propionaldehyde/1-propanol/ acetaldehyde	-2	1	2	0	2
9	Glycerin/hydroxyacetone/propylene glycol/propionaldehyde/1-propanol/ propylene/propane	-4	0	1	1	3
10	Glycerin/hydroxyacetone/propylene glycol/ acetone/isopropanol/propylene/propane	-4	0	1	1	3
11	Glycerin/3-hydroxypropanal/propionaldehyde/ 1-propanol/propylene/propane	-4	0	1	1	3

Table 6. Enthalpies and Gibbs free energies of reaction.

		in atomic energy units		in kJ/mol	
Reaction #	Reaction	ΔH	ΔG	ΔH	ΔG
1	Glycerin → Hydroxyacetone + Water	-0.01251	-0.05027	-32.83	-131.99
2	Glycerin → 3-Hydroxypropanal +Water	-0.00603	-0.04304	-15.82	-112.99
3	3-Hydroxypropanal → Acrolein + Water	0.00916	-0.02330	24.06	-61.17
4	Acrolein → Ethylene + Carbon Monoxide	0.00433	-0.02440	11.36	-64.06
5	Acrolein + Hydrogen → Propionaldehyde	-0.05208	-0.02352	-136.75	-61.75
6	Hydroxyacetone → Acetaldehyde + Formaldehyde	0.01452	-0.01902	38.11	-49.93
7	3-Hydroxypropanal → Acetaldehyde + Formaldehyde	0.01452	-0.01902	38.11	-49.93
8	Acetaldehyde → Methane + Carbon Monoxide	-0.00190	-0.02663	-5.00	-69.93
9	Formaldehyde → Hydrogen + Carbon Monoxide	0.01031	-0.01618	27.06	-42.49
10	Hydroxyacetone + Hydrogen → Propylene Glycol	-0.02616	0.00387	-68.68	10.17
11	Propylene Glycol → Propionaldehyde + Water	-0.01028	-0.04345	-27.00	-114.09
12	Propionaldehyde → Ethane + Carbon Monoxide	0.00077	-0.02678	2.02	-70.31
13	Propylene Glycol → Acetone + Water	-0.02056	-0.05644	-53.98	-148.19
14	Propionaldehyde + Hydrogen → 1-Propanol	-0.02699	0.00156	-70.86	4.11
15	Acetone → Methane + Ethanone	0.03101	0.00199	81.41	5.22
16	2 Ethanone → Ethylene +2 Carbon Monoxide	-0.01379	-0.03531	-36.20	-92.70
17	Acetone + Hydrogen → Isopropanol	-0.02181	0.00979	-57.26	25.71
18	1-Propanol → Acetaldehyde + Methane	0.00016	-0.03136	0.41	-82.34
19	1-Propanol → Propylene + Water	0.01085	-0.02421	28.49	-63.56
20	Isopropanol → Propylene + Water	0.01085	-0.02421	28.49	-63.56
21	Propylene + Hydrogen → Propane	0.01595	-0.01944	41.87	-51.05
22	Propane → Ethylene + Methane	0.02847	-0.00073	74.74	-1.91

Table 7. Mean bond energies of bonds containing carbon, oxygen, and hydrogen.[62]

Bond	Energy (KJ/mol)
Carbon-Carbon	348
Carbon Oxygen	360
Carbon-Hydrogen	412
Oxygen-Hydrogen	463
Carbon-Carbon double bond	612
Carbon-Oxygen double bond	743

Table 8. Linear regression values of the effect of space time on gas composition (moles of gas/mole of gaseous carbon) with water gas shift undone and methanol results removed.

Temp	Carbon Monoxide			Methane			Ethane		
deg C	m	b	R^2	m	b	R^2	m	b	R^2
550	-0.00201	0.709	0.997	0.00105	0.015	0.995	0.000352	-0.007	1.000
600	-0.00116	0.563	0.645	0.00119	0.062	0.806	0.000172	0.024	0.506
650	-0.00073	0.519	0.921	0.00055	0.108	0.842	0.000054	0.036	0.737

Table 9. Linear regression values of the slopes and intercepts from the space time regression with respect to temperature.

CO=m(T)*tau+B(T)					
m(T)			b(T)		
m1	m2	R^2	b1	b2	R^2
1.284E-05	-0.00900	0.97	-0.00190	1.74	0.91

CH_4=m(T)*tau+B(T)					
m(T)			b(T)		
m1	m2	R^2	b1	b2	R^2
-5.028E-06	0.00395	0.56	0.00093	-0.50	1.00

C_2H_6=m(T)*tau+B(T)					
m(T)			b(T)		
m1	m2	R^2	b1	b2	R^2
-2.983E-06	0.00198	0.99	0.00042	-0.24	0.94

Table 10. Comparison of experimental and calculated values from equations.

Temp	Res Time	Experimental Values			Calculated Values		
°C	sec	CO	CH_4	C_2H_6	CO	CH_4	C_2H_6
598	30	0.54	0.09	0.03	0.56	0.09	0.02
598	45	0.50	0.13	0.03	0.54	0.10	0.03
598	60	0.50	0.13	0.03	0.52	0.12	0.03
548	30	0.65	0.05	0.00	0.64	0.05	0.01
548	45	0.62	0.06	0.01	0.61	0.07	0.01
549	60	0.59	0.08	0.01	0.58	0.09	0.02
648	30	0.50	0.12	0.04	0.48	0.13	0.04
648	45	0.48	0.14	0.04	0.47	0.14	0.04
648	60	0.48	0.14	0.04	0.46	0.15	0.04
499	60	0.64	0.05	0.01	0.63	0.05	0.00
698	60	0.36	0.29	0.02	0.41	0.18	0.05
498	45	0.62	0.04	0.01	0.67	0.03	0.00
698	45	0.43	0.23	0.02	0.41	0.17	0.05

2. ROLES OF HYDROXYL GROUP IN THE SUPERCRITICAL WATER REACTION OF POLYHDRIC ALCOHOLS

2.1 ABSTRACT

Supercritical water reformation is a novel process that can be used to produce hydrogen for transportation fuels. The process is non-catalytic and can be used on a wide variety of feedstocks, such as diesel, jet fuel, sucrose, ethanol, methanol, and glycerin. With such a wide variety of fuels that can be used with supercritical water, gaining a better understanding of the chemistry behind supercritical water reformation and decomposition is important. One aspect of the process chemistry that seems to have a large impact on the supercritical water reformation and decomposition of hydrocarbons is the amount of hydroxyl functional groups present in the molecular structure of the feed oxygenated hydrocarbon. To examine the discerning effect of hydroxyl groups, experiments were performed using hydrocarbons of the same length with differing numbers of hydroxyl groups. Those hydrocarbons were isopropanol, propylene glycol, and glycerin, i.e., monohydric, dihydric, and trihydric alcohols of C_3. The experiments used a custom-designed Haynes® Alloy 282 reactor system, and experiments were conducted at temperatures of 550, 600, and 650°C for each chemical feed. Other run conditions include a water-to-fuel molar ratio of 8, a pressure of 3500 psi, and a reactor space time of 45 seconds. A thorough the analysis of carbon gasification, gaseous effluent compositions, and liquid effluent compositions, the mechanisms for supercritical water reformation or decomposition, and the impact of hydroxyl groups on those reaction mechanisms was conducted.

2.2 INTRODUCTION

A supercritical fluid is any fluid above its critical point. The critical point of water is 374°C and 217.7 atm.[6] When water becomes supercritical, it dissolves nonpolar molecules more readily and becomes a highly energetic reaction medium. The critical points and other physical properties of isopropanol, propylene glycol, glycerin, and water are shown in Table 1. With the exception of glycerin's critical temperature, all critical values for the pure species of these chemicals are below that of water.

Supercritical water reformation and decomposition of hydrocarbons is a versatile and non-catalytic process to produce hydrogen. A variety of hydrocarbon feedstocks can be used as fuel, such as ethanol, jet fuel, ethanol, sucrose, methanol, and glycerin.[7-9, 12, 15, 19] Even with the wide variety of hydrocarbon fuels, the end products are always hydrogen, carbon monoxide, methane, carbon dioxide, ethylene, ethane, and trace propane and propylene for larger hydrocarbons.

While all hydrocarbon fuels break down to make hydrogen, each reacts differently with supercritical water. Some fuels undergo supercritical water reformation and react with the water and produce hydrogen and carbon monoxide. Other fuels do not react with the supercritical water, and instead use it as a medium for decomposition. Understanding the different mechanisms is important, and one factor that bears considerable significance is the presence and quantity of hydroxyl groups in the molecular structure.

In the presence of supercritical water, glycerin tends to undergo decomposition, as opposed to reacting with supercritical water for reformation.[14] In glycerin decomposition,

the first step is dehydration into either hydroxyacetone or 3-hydroxypropanal. Both of these intermediates can decompose into formaldehyde and acetaldehyde.[24, 27, 57] The formaldehyde decomposes readily into carbon monoxide and hydrogen, while acetaldehyde decomposes into methane and carbon monoxide.[14, 49] 3-hydroxypropanal can also undergo dehydration to make acrolein, and then acrolein decomposes into carbon monoxide and ethylene.[50, 51] Ethylene produced then reacts with hydrogen to produce ethane. Other liquid intermediates from hydroxyacetone and acrolein include propionaldehyde, acetone, propylene glycol, 1-propanol, allyl alcohol, 2-butanone, cyclopentanone, and phenol.[23, 24, 26]

Like glycerin, propylene glycol has multiple decomposition mechanisms in the presence of supercritical water. The first pathway for propylene glycol decomposition is dehydrogenation to hydroxyacetone.[45] This is followed by decomposition to formaldehyde and acetaldehyde, which can decompose further into carbon monoxide and hydrogen and carbon monoxide and methane, respectively.[14, 49] Another mechanism of propylene glycol decomposition is dehydration to propionaldehyde, which subsequently decomposes to ethane and carbon monoxide. [47, 48]

There are many decomposition pathways that isopropanol can go through before making all gaseous products. Isopropanol can first decompose by dehydrogenating and becoming acetone.[34, 35] From there, it decomposes further into methane and ethanone.[36] Two ethanone molecules can then react to produce ethylene and two carbon monoxide molecules.[36, 37] It is also possible that acetone may undergo free radical decomposition by dissociation to methyl and acetyl radicals.[40]

Another possible mechanism for isopropanol decomposition starts with dehydration to become propylene.[41, 42] Propylene can then undergo a series of free radical decomposition reactions which produce primarily methane, ethylene, and hydrogen, with small quantities of higher hydrocarbons.[43] Propylene can also be hydrogenated by the hydrogen produced from the other decomposition pathway to produce propane, which can then undergo its own series of decomposition reacitons.[44] Propylene may also under go supercritical water reformation.

Any carbon monoxide produced in these reactions may then undergo a forward water gas shift reaction to produce carbon dioxide and hydrogen, if the imposed condition is appropriate. While the reaction is of a reversible kind, the forward reaction is dominant at temperatures below 815°C.[16] As the water gas shift reaction is the only reaction to produce carbon dioxide, it is easy to determine the extent of water gas shift reaction taking place.

2.3 EXPERIMENTAL

2.3.1 Materials. The chemicals used for these experiments were deionized water, 99.7 percent pure glycerin from the chemistrystore.com, 99 percent extra pure propylene glycol from Acros Organics, and 70 percent isopropanol and 30 percent water solution from Fisher Scientific. Glycerin above 80 percent purity by weight is hygroscopic and will absorb atmospheric water. To prevent unknown quantities of water from diluting the glycerin and confounding the experimental results, freshly unsealed containers were pre-diluted with water to 75 percent purity. The solutions for these experiments were mixed

so there was a water-to-fuel molar ratio of 8. The molar and weight compositions of these solutions are shown in Table 2.

2.3.2 Reactor System. These experiments were performed on the Multi-Fuel Supercritical Water Reformer of Ohio University's Sustainable Energy and Advanced Materials Laboratory. The multi-fuel reformer is a custom-designed mini-pilot scale supercritical reforming system consisting of a solution feed system, a preheating system, a reactor with a zone heater, a liquid effluent collection/analysis system and a gas sampling/analysis system. The entire process system is controlled using Labview® data acquisition and control system. Figure 1 shows a schematic diagram of the entire reaction system.

The solution feed system includes an Eldex piston pump to continuously feed water and fuel solution and get the system up to pressure. The solution then enters the preheat system which consists of an integrated heat exchanger where hot reactor effluent warms the incoming solution. The preheat system also warms solution with heat tape and prevents heat loss with ceramic insulation.

The reactor system consists of a Haynes® Alloy 282 reactor with a zone heater. Haynes® Alloy 282 contains primarily nickel with of chromium, cobalt, molybdenum, titanium, aluminum, and iron.[53] Thermocouples in a thermowell running through the center of the reactor are used to monitor the temperature in the reactor. Inside the reactor is where the solution reaches the temperature specified for the experiment.

The solution then goes back through the integrated heat exchanger to heat incoming feed solution, followed by a water-cooled heat exchanger. The solution then

flows through a control valve where it is returned to ambient pressure and the liquid and gaseous effluents are separated. Samples of the liquid are collected for further analysis. The gaseous effluent flows through a wet-test meter where the volumetric flow rate can be determined, and then gas samples can be taken through a septum with a gas sample syringe.

2.3.3 Analysis. The analysis of the gas samples for these experiments was performed on a HP 5890 Series A gas chromatograph with a thermal conductivity detector. Argon was used as a carrier gas for the gas samples, and the column was calibrated with a standard from Praxair to detect hydrogen, air, carbon monoxide, methane, carbon dioxide, ethylene, ethane, propylene, and propane.

Samples of the liquid effluent were collected at ambient conditions and stored in screw-top bottles. The samples were then analyzed using a Thermo Scientific ISQ gas chromatograph/mass spectrometer system. Before analysis, each sample was diluted using methanol to a 1/5 sample-to-methanol solution to aid in separation and reduce noise peaks in the sample.

2.3.4 Procedure. The Multi-Fuel Reformer reactor system was regularly cleaned with supercritical and sub-critical water before and after each day that experimental runs were being conducted. Each experimental run would continue until steady state conditions were achieved. An experiment was considered to have reached steady state when two gas samples showed matching percentages of all of the effluent gases. During the same time period there also need to be no significant changes in the volumetric flow rate of the gas or any process variables, such as temperature or pressure. Table 3 shows a summary of the experimental runs conducted.

2.3.5 Definitions. The reactor space time given for each experimental run was calculated using the internal volume of the Haynes® Alloy 282 reactor and the estimated volumetric flow rate of the solution at the reactor conditions. The volumetric flow rate was calculated at the reactor temperature and pressure with Aspen®-Plus simulation software using Peng-Robinson equation of state with Wong-Sandler mixing rules. This ensures that a uniform volumetric flow rates enter the reactor regardless of temperatures and pressure changes that effect density.

The carbon gasification for each of the experiments is defined the moles of carbon exiting in the gaseous effluent divided by the moles of carbon entering. The amount of carbon exiting in the gaseous effluent is calculated using the volumetric flow rate of the gaseous effluent and the gaseous composition from the gas chromatograph results. The amount of moles of carbon entering the reactor system is based on the mass flow rate entering the reactor and the composition of the feed solution.

The hydrogen conversion is based on the amount of hydrogen gas coming out in the gaseous effluent divided by the theoretical maximum that could be produced from supercritical water reformation. The theoretical maximum assumes that all hydrocarbon breaks down into carbon monoxide and hydrogen through supercritical water reformation, and that all carbon monoxide then undergoes the water gas shift reaction to produce more hydrogen and carbon dioxide. The theoretical maximum moles of hydrogen that can be produced per mole of glycerin, propylene glycol, and isopropanol are seven, eight, and nine, respectively.

The preliminary gas composition results are based on moles of the gaseous species per mole of carbon entering the reaction system. These results show overall

amounts of each gaseous species being produced at the different conditions, but it is difficult to tell what is happening with regard to reaction selectivity since the amount of all gaseous species tends to increase with increasing carbon gasification.

The next set of gas results show the amount of gaseous species per mole of gaseous carbon exiting the reactor. These results are obtained by dividing the moles of gaseous species per moles of carbon fed by the carbon gasification. Normalizing all experiments this way better displays trends in the selectivity of gaseous products rather than actual amount being produced.

Another operation that can be done to the gaseous results is to mathematically undo the water gas shift reaction. To do this, the moles of carbon dioxide per moles of gaseous carbon in the results are taken out, and the same value is subtracted from the hydrogen results and added to the carbon monoxide results. Undoing the results of the water gas shift reaction gives a clearer view of what is happening with regards to decomposition by eliminating the reaction that consumes the products of the decomposition.

2.4 RESULTS AND DISCUSSION

The results of each hydrocarbon species with increasing temperature will be examined first, followed by the effect of increasing the amount of hydroxyl groups at a given temperature. The primary gases produced in these experiments were hydrogen, carbon monoxide, methane, carbon dioxide, ethane, and ethylene. No noticeable

quantities of propane or propylene were produced. Table 4 shows the results of the experimental runs.

2.4.1 Glycerin. With increasing temperature, the amount of gasification of carbon in a glycerin solution increases, starting at 22% at 550°C and reaching 91% at 650°C. Likewise, the amount of moles of each gaseous species being produced per mole of carbon fed increase with increasing temperature. This increase of all gaseous species corresponds more to the increasing gasification rather than any change in reaction selectivity. Figure 2 shows the effect of temperature on glycerin.

To determine what is happening to the reaction selectivity with temperature, a gas composition was determined using a basis of moles of gaseous carbon exiting the reactor rather than moles of carbon fed. The results are shown in Figure 3. Carbon dioxide stays approximately constant, indicating little increase in the water gas shift reaction with temperature at these conditions. Hydrogen also stays relatively constant, while carbon monoxide decreases and ethane and methane increase. Figure 4 shows the gas results with the water gas shift reaction undone, to better show the decomposition products of glycerin, and again carbon monoxide decreases while methane and ethane increase.

A liquid sample from experimental run WG-127M was analyzed to determine the liquid intermediates that are produced in the gasification of glycerin in supercritical water, and the results are shown in Figure 5. WG-127M was performed at 600°C, 3500 psi, 8/1 water-to-glycerin molar ratio, and 45 sec space time. Results from the liquid analysis show the primary liquid intermediates produced were hydroxyacetone, acetic acid, propanoic acid, and methyl propionate. Minor products include 2-butanone, 1-propanol, allyl alcohol, phenol, and 2-methyl phenol. Acetaldehyde and propionaldhyde

oxidize to acetic acid and propanoic acid, respectively, when exposed to atmospheric acid, which explains their absence in the liquid sample.[54]

Using the mechanism developed in Figure 19 in Paper 1: Determination of a Comprehensive Mechanistic Reaction Pathway and the Effects of Reaction Conditions on the Decomposition of a Crude Glycerin Solution in Supercritical Water, two primary reaction pathways for glycerin decomposition to gaseous products were determined. In the first pathway, glycerin was dehydrated to produce hydroxyacetone or 3-hydroxypropanal, both of which can decompose to formaldehyde and acetaldehyde.[14, 27, 55] Formaldehyde decomposes readily into carbon monoxide and hydrogen, while acetaldehyde gasifies to become methane and carbon monoxide.[14, 49] The second mechanistic pathway involves the decomposition of propionaldehyde into ethane and carbon monoxide.[48] Propionaldehyde can be produced from the hydrogenation of hydroxyacetone to propylene glycol which is then dehydrated, or it can be produced from the dehydration of 3-hydroxypropanal to acrolein which is then hydrogenated.[24, 27]

The favored mechanism for glycerin decomposition, as shown in Paper 1 Figure 20, was then analyzed. This was accomplished by comparing the amount of carbon monoxide actually produced to the amount calculated by the proposed mechanism and the amounts of other gaseous species present. The results are shown in Figure 6. At lower temperatures, the mechanism does not work well, while the values are approximately the same at 650°C when there is almost complete carbon gasification. The discrepancy at lower temperatures is believed to be the result of hydrogen produced reacting with liquid intermediates, and therefore being depleted from the gaseous effluent. When carbon

gasification is close to completion and there is very little liquid intermediates remaining, the favored glycerin decomposition mechanism's predictability improves.

2.4.2 Propylene Glycol. The amount of propylene glycol gasification increases with increasing temperature, with very little carbon gasifying at 550°C and almost 90 percent conversion at 650°C. The amounts of most gaseous species increased with increasing temperature, with only carbon dioxide and hydrogen staying about constant going from 600°C to 650°C. These trends are shown in Figure 7.

Looking at the gas composition in moles of gaseous species per mole of gaseous carbon exiting the reactor, as shown in Figure 8, increasing temperature led to decreased hydrogen and carbon monoxide. Carbon dioxide is only produced as a product of the water gas shift reaction, indicating a decrease in the relative amount of that reaction. The methane and ethane produced increase with increasing temperature. Figure 9 shows the gas composition of propylene glycol decomposition in supercritical water with the water gas shift reaction undone.

Figure 10 displays the results of the liquid analysis of run WPG-130M, which used propylene glycol as fuel. The experiment was carried out at 600°C, 3500 psi, 8/1 water-to-propylene glycol molar ratio, and 45 sec space time. The liquid species present appear to be very similar to those produced by glycerin, with hydroxyacetone being one of the primary products. Therefore, one of the primary pathways is the dehydrogenation of propylene glycol to hydroxyacetone, which is followed by the formation of acetaldehyde and formaldehyde and their respective gaseous products.[14, 45]

Another primary pathway involves the dehydration of propylene glycol to propionaldehyde, which is subsequently broken down into carbon monoxide and ethane.[48] Finally, because of the increased presence of 1-propanol compared to the liquid sample from the glycerin experiment, creation of 1-propanol from propionaldehyde hydrogenation must be occurring more readily. 1-propanol can decompose to produce acetaldehyde and methane.[58] The 2-ethyl-4-methyl-1,3 dioxolane and 2-methyl 1,3 dioxane are the likely condensation products of propylene glycol and propionaldehyde, and propylene glycol with acetaldehyde, respectively.[63] These larger molecules are not believed to contribute to the gaseous products, and are therefore not included in the analysis of a primary reaction pathway. Figure 11 shows the hypothesized propylene glycol decomposition pathway.

The proposed decomposition pathways were checked against the actual results. Figure 12 shows the calculated carbon monoxide produced using the mechanism plotted against the actual carbon monoxide. This decomposition mechanism appears to be consistent with the observed data at all temperatures, so gaseous species reacting with liquid intermediates is probably at a minimum. This is because the propylene glycol decomposition pathway only contains carbon-oxygen double bonds to hydrogenate and not the more thermodynamically favored carbon-carbon double bonds. This is different from glycerin decomposition which has a carbon-carbon double bond in acrolein.

2.4.3 Isopropanol. Figure 13 shows the carbon gasification and gas composition, in moles of gaseous species per mole of carbon fed, of isopropanol decomposition. With increasing temperature, carbon gasification increases reaching over 90 percent at 650°C. The amount of methane produced appears to increase at a similar

rate as carbon gasification, and the amounts of most other gaseous species produced increases with increasing temperature. The only gaseous species to show any decrease is hydrogen, which decreases substantially with increasing temperature. This is indicative of decomposition occurring instead of supercritical water reformation, since at higher temperatures more reformation would occur producing more hydrogen.

The gaseous composition for isopropanol based on moles of gas species per mole of gaseous carbon are shown in Figure 14. In Figure 14 the moles of hydrogen produced per moles of carbon coming out in the gaseous effluent is very high at low temperatures, with almost 3.5 hydrogen molecules coming out per carbon at 550°C. This is indicative of isopropanol dehydrogenation to produce acetone occurring substantially at lower temperatures, while the subsequent decomposition reactions of acetone not occurring as easily. This leads to a small amount of carbon-containing molecules being present in the gaseous effluent. At higher temperatures where more carbon is gasified, the amount of hydrogen per gaseous carbon is much smaller. The relative amount of carbon dioxide produced decreases with increasing temperature, meaning less water gas shift reaction is occurring per carbon atom. The amounts of ethane, ethylene, and carbon monoxide increase with increasing temperature, while methane decreases slightly.

The liquid effluent from experimental run WI-133M, which was conducted at 600˚C, 3500 psi, 8/1 water-to-isopropanol molar ratio, and 45 sec space time, was analyzed. The species with the highest relative abundance was isopropanol, which is the result of WI-133M only achieving only 22.9 percent carbon gasification. Other liquid species were 2-butanone, 2-pentanone, 2-hexanone, acetic acid, methyl isobutyl ketone, and 2,5-hexadione. Due to the amount of hydrogen produced from run WI-133M at such

low carbon gasification, one would expect to find acetone, which is suspiciously absent from this liquid sample. The lack of acetone in this liquid sample could be the result of acetone being a short-lived intermediate species in supercritical water, or it could be the result of poor liquid separation from the large isopropanol peak. The results of the liquid analysis are shown in Figure 15.

These liquid species are indicative of isopropanol dehydrogenating to acetone, and then undergoing a series of free radical reactions. The first step involves acetone dissociating to a methyl radical and acetyl radical.[40] The methyl radical can then react with other acetone molecules to produce 2-butanone and a hydrogen radical. Methyl radicals can continue to chain to produce 2-pentanone, methyl isobutyl ketone, and 2-hexanone. Methyl radicals may also react with hydrogen radicals to produce methane, which there is a significant amount in the gaseous effluent. If an acetone loses two methyl radicals then a carbon monoxide is produced, while two methyl radicals can react to produce ethane. The hydrogen radicals can react with the acetyl radicals to produce acetaldehyde. Two acetone molecule can also react to produce 2,5 hexadione and hydrogen gas.

Due to the wide variety of reactions that can occur with free radical isopropanol decomposition, a stoichiometric evaluation of the mechanistic pathway could not be performed. At 500°C there is very little carbon gasification occurring, but a great deal of hydrogen being produced, indicative of dehydrogenation to acetone. Based on the liquid intermediates found at 600°C, it seems the primary reaction pathway is free radical decomposition of acetone, and not decomposition of acetone to ethanone or dehydration to propylene. Because of the low hydrogen and carbon monoxide values at 650°C, it is

apparent that the supercritical water reformation of isopropanol does not become a prominent reaction until higher temperatures.

2.4.4 Effect of Increasing Number of Hydroxyl Groups. The effect of increasing hydroxyl groups on the different C_3 hydrocarbons was then analyzed. Figures 16-21 show the trends in carbon gasification as well as gas composition at 550, 600, and 650°C. Points with hydroxyl group to carbon ratios of 0.33, 0.66, and 1 correspond to isopropanol, propylene glycol, and glycerin, respectively.

In Figure 16, which shows the gasification and decomposition results at 550°C, increasing the number of hydroxyl functional groups increases carbon conversion as well as carbon monoxide produced, which makes sense since there are more oxygenated carbons present with more hydroxyl groups. In other words, more hydroxyl groups make the chemical species that much easier to reform or decompose. Carbon dioxide and ethane show little increase with more hydroxyl groups, and both hydrogen and methane appear be at a minimum with propylene glycol. This difference in hydrogen is likely due to differences in decomposition mechanisms between isopropanol and propylene glycol. Isopropanol produces a great deal of hydrogen from dehydrogenation to acetone, for the ranges of temperatures studied.

To see a clearer view of the selectivity of different gaseous products, Figure 17 shows the results of the gas composition per mole of gaseous carbon. With an increasing ratio of hydroxyl groups to carbons, the amount of carbon monoxide produced steadily rises while methane decreases. This result is expected as molecules with more oxygenated carbons will be more prone to producing carbon monoxide, while molecules

with fewer oxygenated carbons are more likely to produce methane. The amount of hydrogen being produced per gaseous carbon is very high for isopropanol and propylene glycol. This is due to dehydrogenation reactions occurring that produce gaseous hydrogen, but very little gaseous carbon. With increasing number of hydroxyl groups in a molecule there is also a decrease in carbon dioxide, likely due to a decrease in the water gas shift reaction, and ethane production reaches a maximum with propylene glycol decomposition. This is the result of propylene glycol producing ethane directly through propionaldehyde decomposition.

Figure 18 shows the gas results for increasing hydroxyl groups at 600°C. Carbon gasification increases substantially going from isopropanol to propylene glycol, but then seems to level off going to glycerin meaning the addition of a third hydroxyl group has little effect on additional carbon conversion at 600°C. With increasing hydroxyl groups the amount of carbon monoxide increases and methane decreases, as expected. Hydrogen production is decreasing with increasing hydroxyl group-to-carbon-ratio, though not as drastically as it was at 550°C. Finally carbon dioxide and ethane appear to reach a maximum at propylene glycol, though with the large change in carbon gasification it is difficult to tell if it is due to a change in the selectivity of reactions.

To find out how reaction selectivity is changing with the number of hydroxyl groups on the fuel, Figure 19 shows the gas composition per gaseous carbon. The trends appear identical to Figure 17, with increasing carbon monoxide, and decreasing hydrogen and methane. Carbon dioxide is again decreasing, meaning less of the water gas shift reaction, and ethane has it maximum value with propylene glycol due to propionaldehyde decomposition.

At 650°C, Figure 20 shows that all of the hydrocarbon starting materials have a uniform carbon conversion of around 90 percent, meaning that at 650°C the ratio of number of hydroxyl groups to carbon in the molecule has little effect in gasification. Other trends with increasing the number of hydroxyl groups are similar to the previous temperatures, with increasing carbon monoxide, decreasing methane, decreasing carbon dioxide, and ethane having a maximum with propylene glycol. The only difference is that hydrogen is increasing with increasing number of hydroxyl groups. This is likely due to an increase in isopropanol decomposing via dehydration to propylene rather than dehydrogenation, and increased hydrogen production from glycerin. Increased hydrogen production in glycerin is due to very little hydrogen reacting with liquid intermediates because gasification is almost complete. Also because propylene glycol has a larger ethane peak than glycerin, propylene glycol favors the propionaldehyde decomposition pathway more than glycerin. This supports the fact that propylene glycol produces less hydrogen than glycerin, since the propionaldehyde decomposition pathway produces no hydrogen. Figure 21 shows the results per gaseous carbon, which are basically the same as Figure 20 due to almost uniform carbon gasification.

2.5 CONCLUSION

There are a number of meaningful conclusions that can be drawn from the experimental results. By increasing the number of hydroxyl functional groups on the molecule, an increase in gasification was found at each temperature, except at 650°C were the carbon conversion was approximately 90 percent for each fuel. The reason more oxygenated hydrocarbons decompose and gasify more readily is due to the presence of

more carbon-oxygen bonds, which break much more readily than carbon-hydrogen bonds.

Also with an increasing amount of hydroxyl groups, the relative amount of carbon monoxide produced increased, while the amount of carbon dioxide and methane decreased. Hydrogen produced decreased with increasing hydroxyl-to-carbon ratio at lower temperatures, but hydrogen production increased at 650°C. This was due to the isopropanol decomposition favoring dehydration to produce propylene at higher temperatures rather than the dehydrogenation to produce acetone which occurs at lower temperatures. At 650°C, very little carbon monoxide and hydrogen are produced from isopropanol, indicating that little to no direct reformation is occurring at those temperatures, and will likely occur at higher temperatures. Also more hydrogen is produced from glycerin decomposition at higher temperatures due to fewer liquid intermediates the hydrogen can react with.

Also mechanisms for glycerin and propylene glycol decomposition were evaluated. The proposed glycerin decomposition mechanism was had good predictability with more carbon gasification, but at lower temperatures the carbon monoxide values that were calculated based on the proposed mechanism were much lower than the actual experimental values. This is likely due to some of the hydrogen produced at lower temperatures reacting with liquid intermediates and not coming out in the gaseous effluent. The proposed propylene glycol mechanism was found to correlate well for all temperatures. A mechanism was proposed for isopropanol decomposition as well, but due to the complexity of the free radical reactions involved, it could not be evaluated like the glycerin and propylene glycol mechanism.

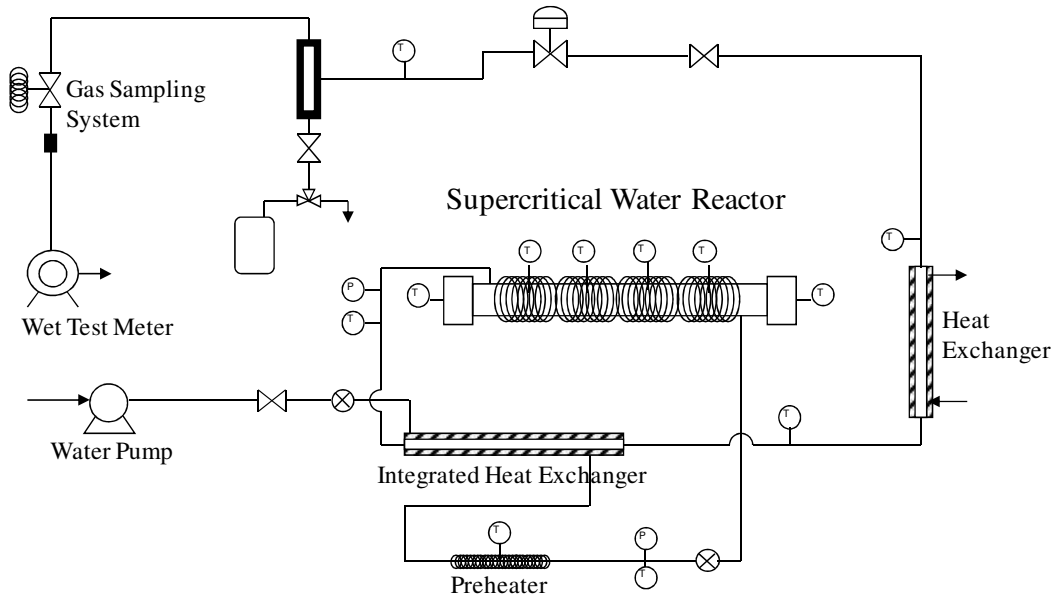

Figure 1. The multi-fuel reformation reaction system at Ohio University.

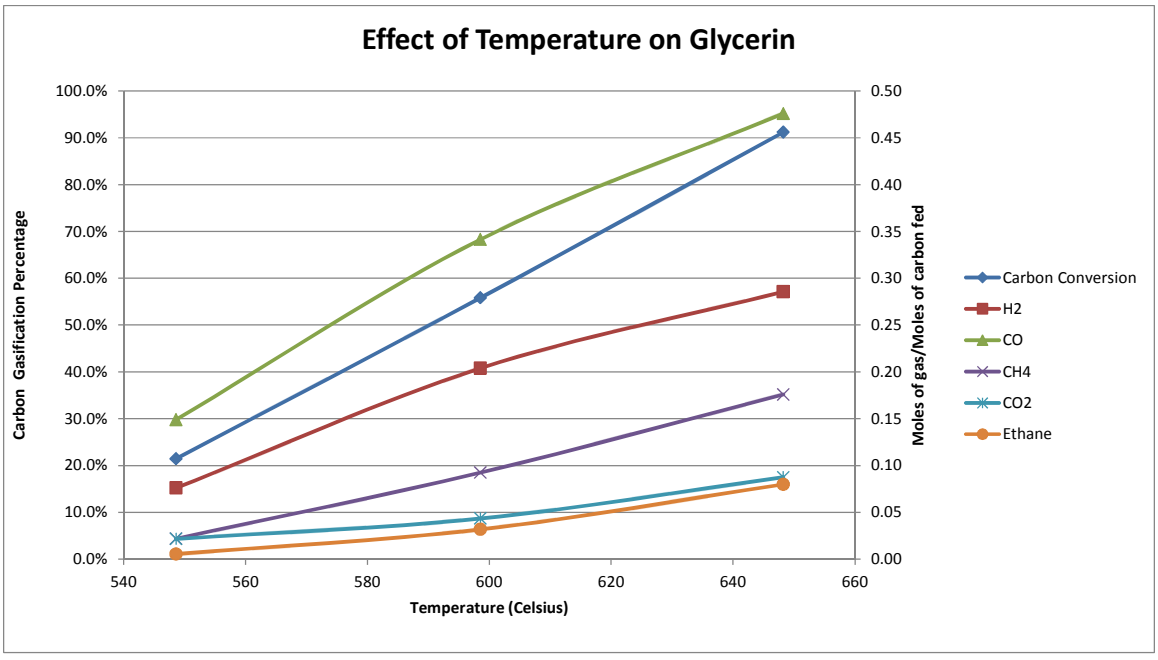

Figure 2. The effect of temperature on the carbon gasification and gas composition (moles/moles carbon fed) of glycerin decomposition.

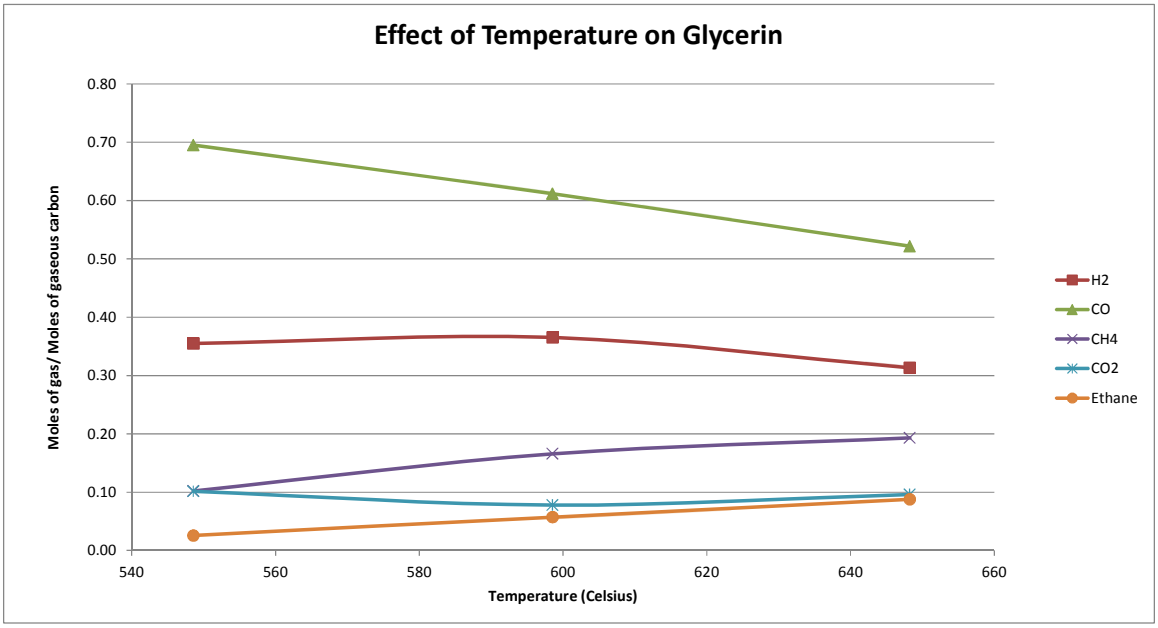

Figure 3. The effect of temperature on the gas composition (moles/moles gaseous carbon) of glycerin decomposition.

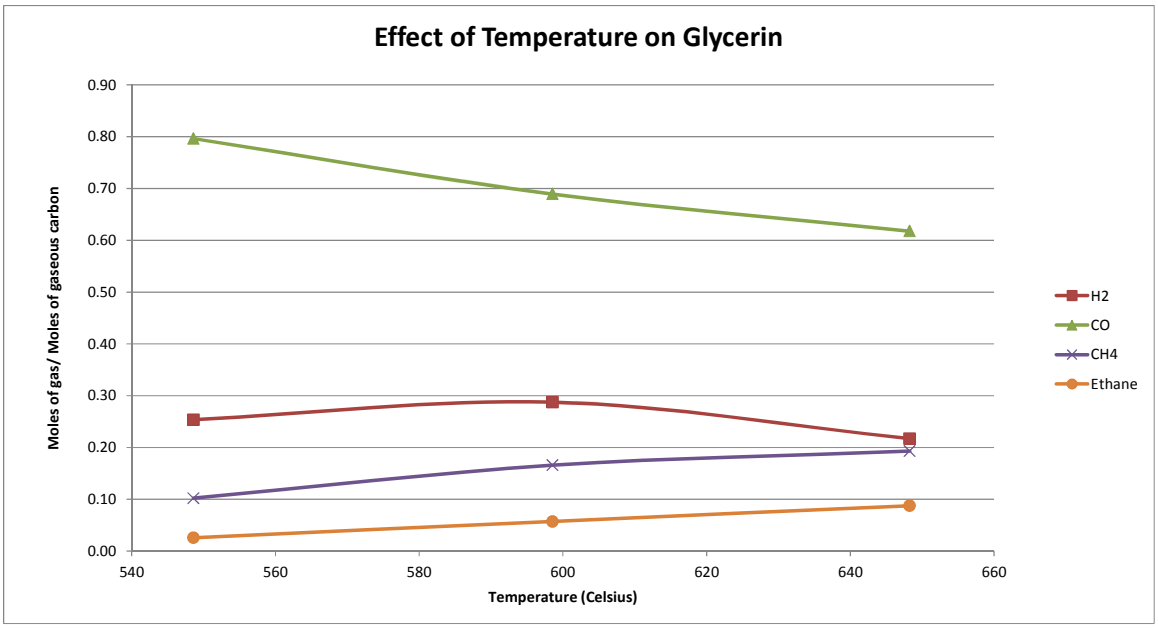

Figure 4. The effect of temperature on the gas composition (moles/moles gaseous carbon) of glycerin decomposition with the water gas shift reaction undone.

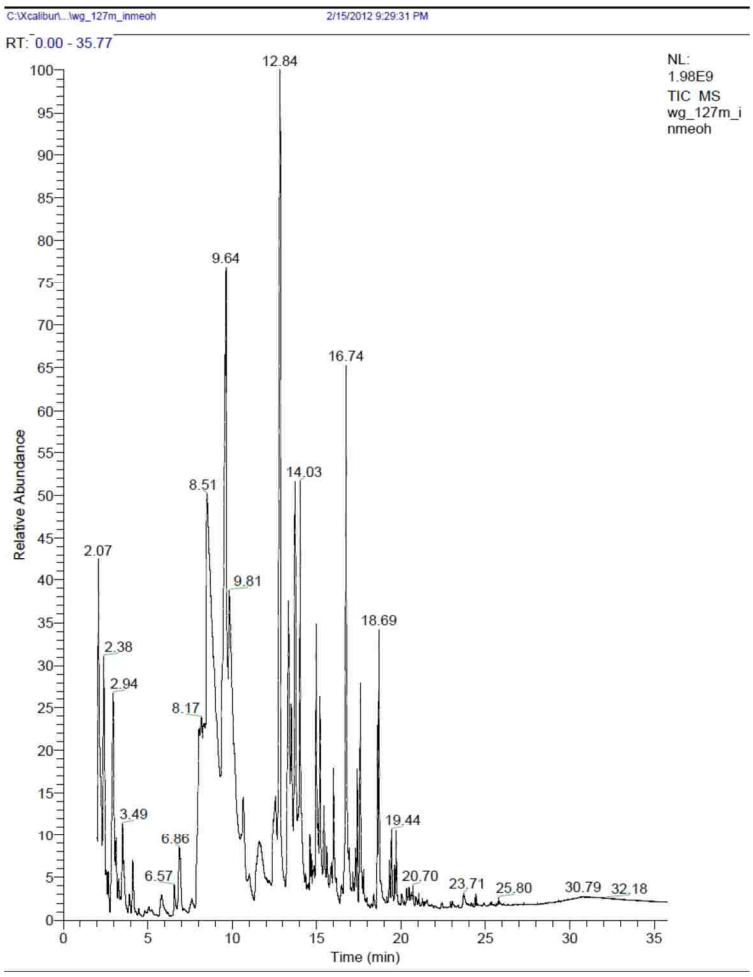

WG-127M	
Residence time	Species
2.07	Methyl Propionate
2.38	2-Buntanone
2.94	1-Propanol
3.49	Allyl Alcohol
6.86	Cyclopentanone
8.51	Acetic Acid
9.64	Hydroxyacetone
9.81	Propionic Acid
13.13	Propylene Glycol
18.69-19.44	Phenols
23.71	Glycerin
12.84,14.03,16.74	Silicon Based Column Bleed

Figure 5. Gas chromatography/mass spectrometry results of liquid sample from experiment WG-127M.

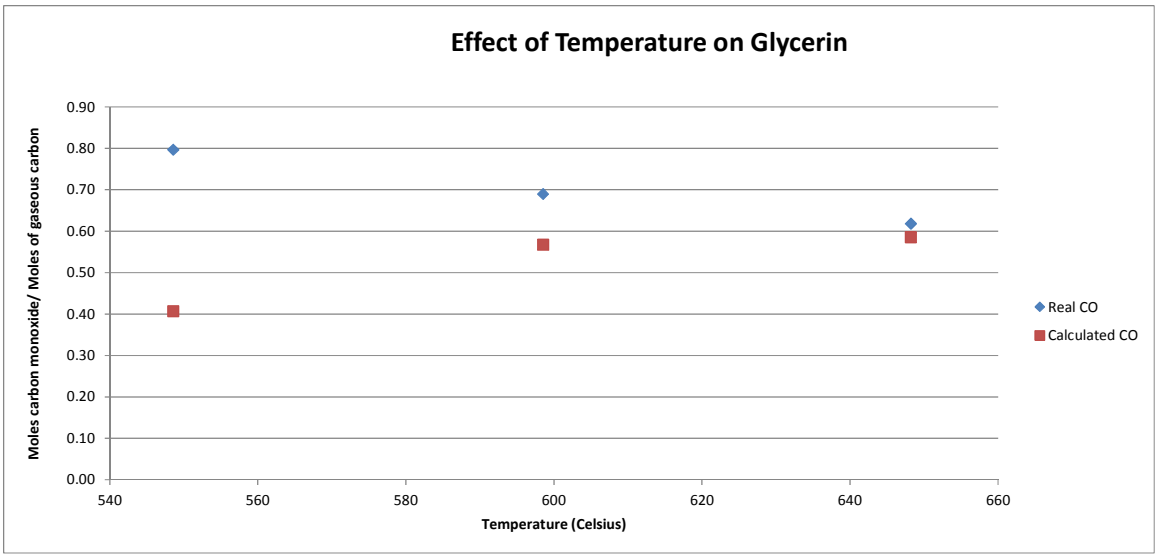

Figure 6. The effect of temperature on the accuracy of the glycerin decomposition mechanism.

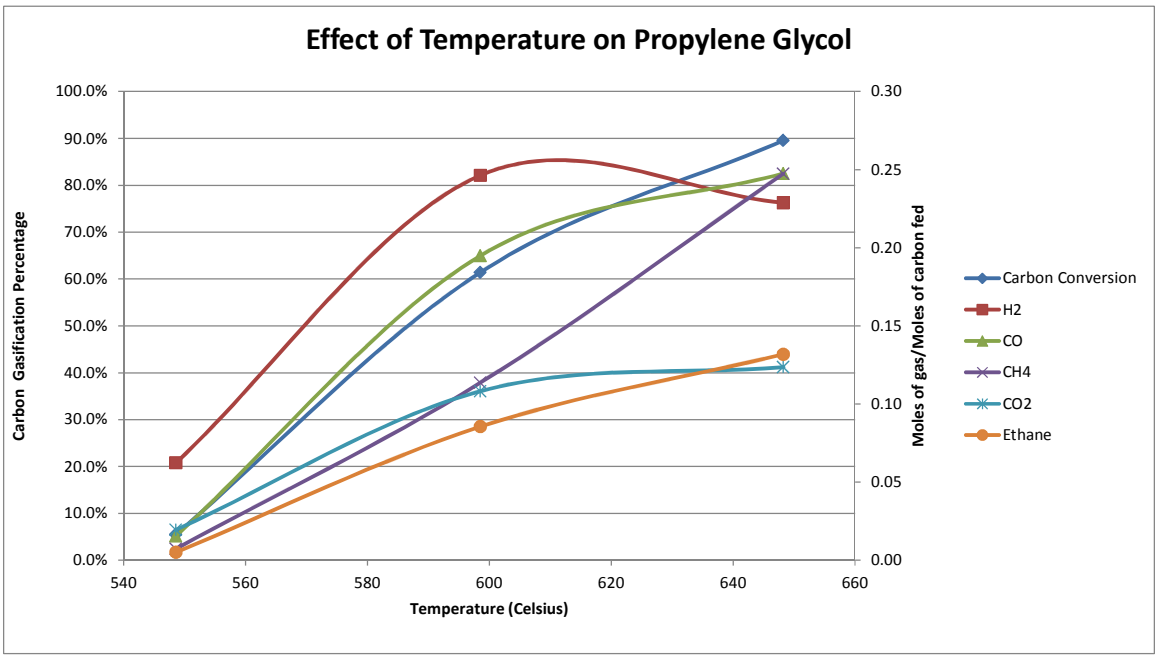

Figure 7. The effect of temperature on the carbon gasification and gas composition (moles/moles carbon fed) of propylene glycol decomposition.

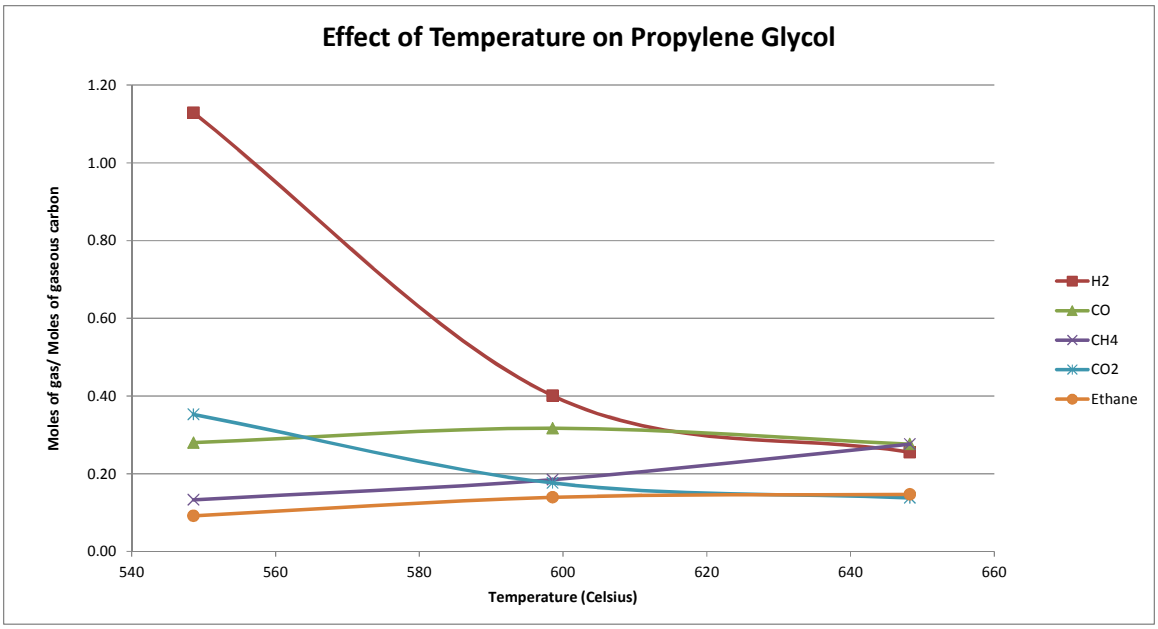

Figure 8. The effect of temperature on the gas composition (moles/moles gaseous carbon) of propylene glycol decomposition.

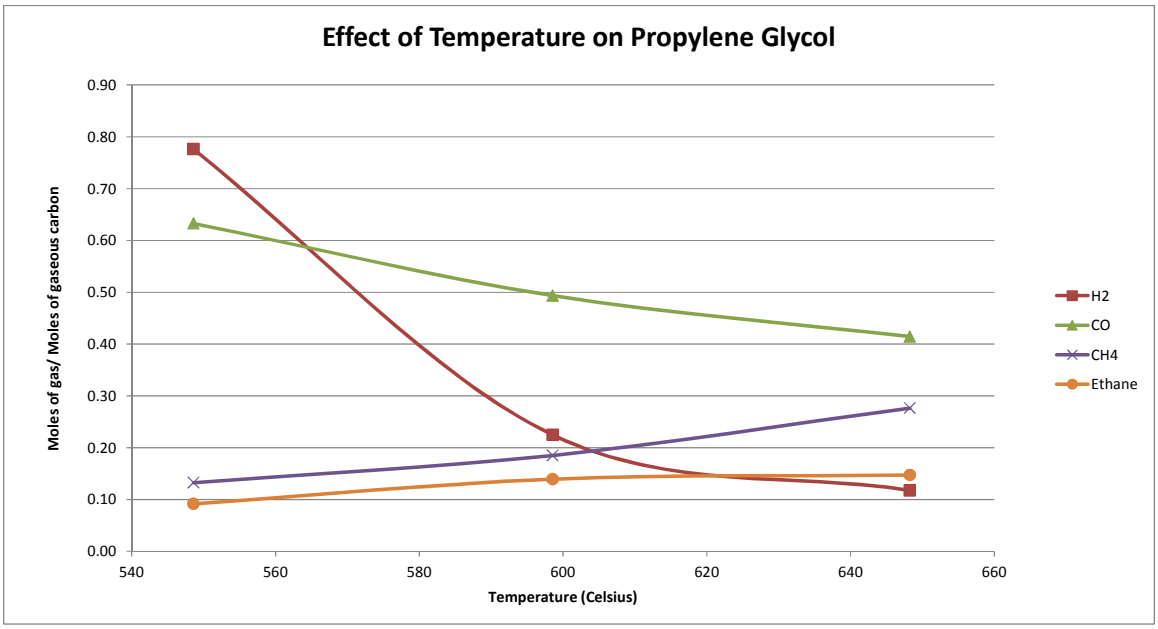

Figure 9. The effect of temperature on the gas composition (moles/moles gaseous carbon) of propylene glycol decomposition with the water gas shift reaction undone.

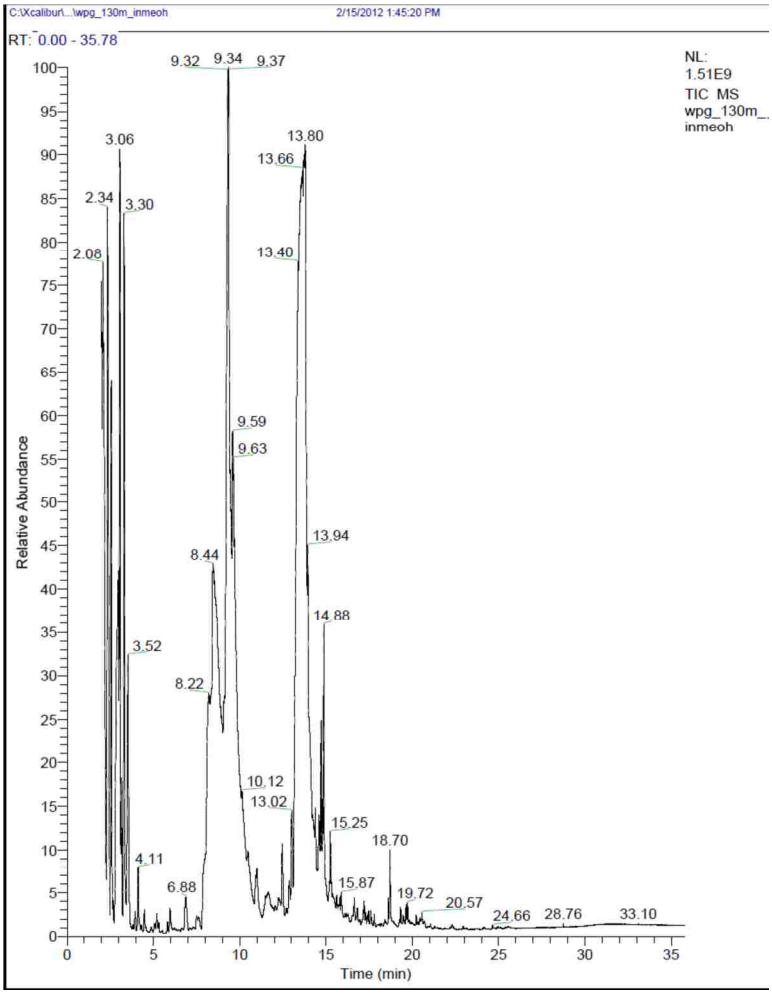

WPG-130M	
Residence time	Species
2.08	Methyl Propionate
2.34	1,3 Dioxane, 2-Methyl
3.06	1,3 Dioxolane, 2-Ethyl-4methyl
3.30	1-Propanol
6.88	Cyclopentanone
8.44	Acetic Acid
9.32	Hydroxyacetone
9.59	Propionic Acid
13.8	Propylene Glycol
18.7-19.72	Phenols
13.02,14.88	Silicon Based Column Bleed

Figure 10. Gas chromatography/mass spectrometry results of liquid sample from experiment WPG-130M.

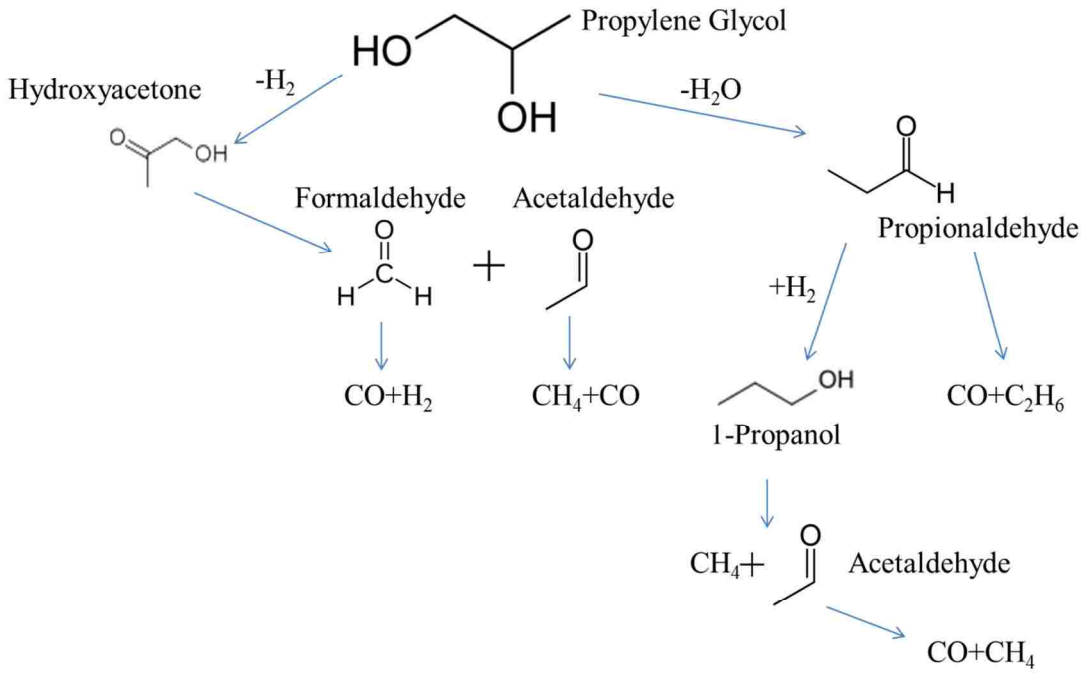

Figure 11. Preferred propylene glycol decomposition pathway.

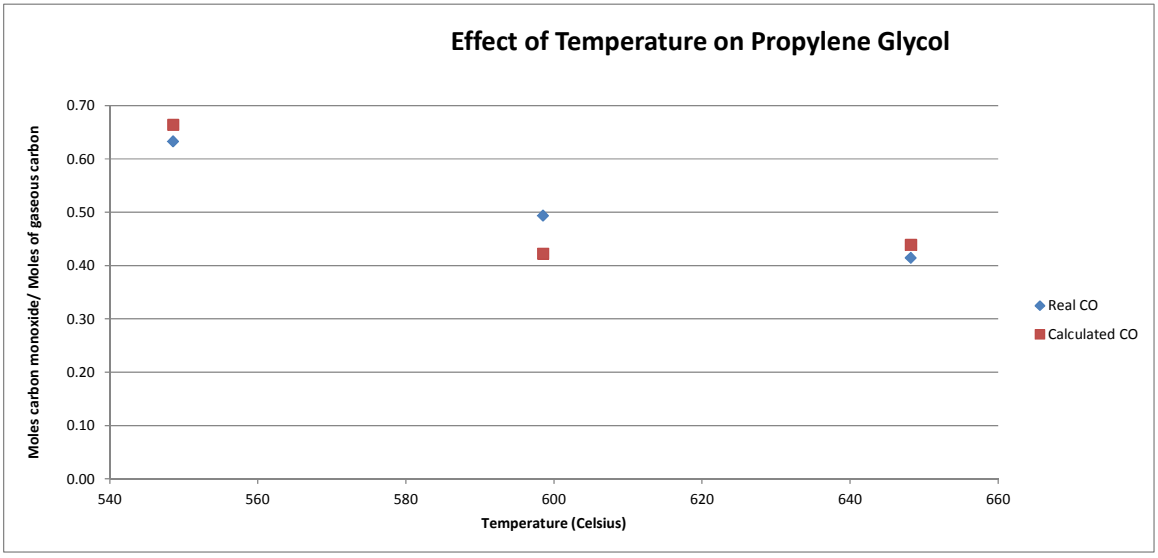

Figure 12. The effect of temperature on the accuracy of the propylene glycol decomposition mechanism.

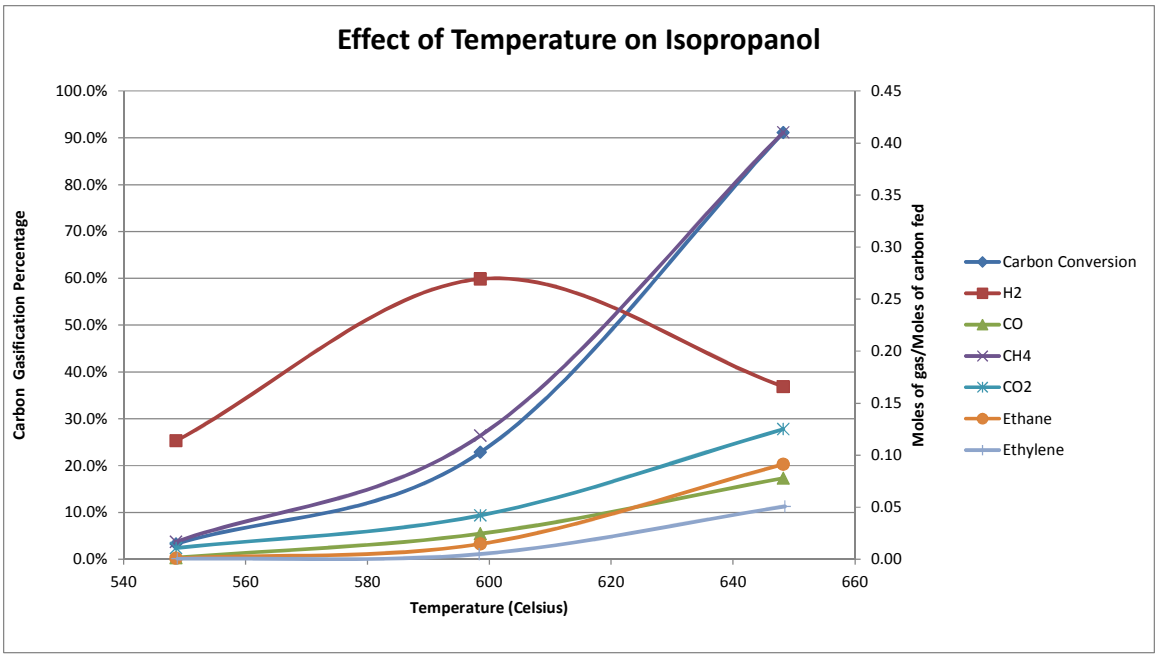

Figure 13. The effect of temperature on the carbon gasification and gas composition (moles/moles carbon fed) of isopropanol decomposition.

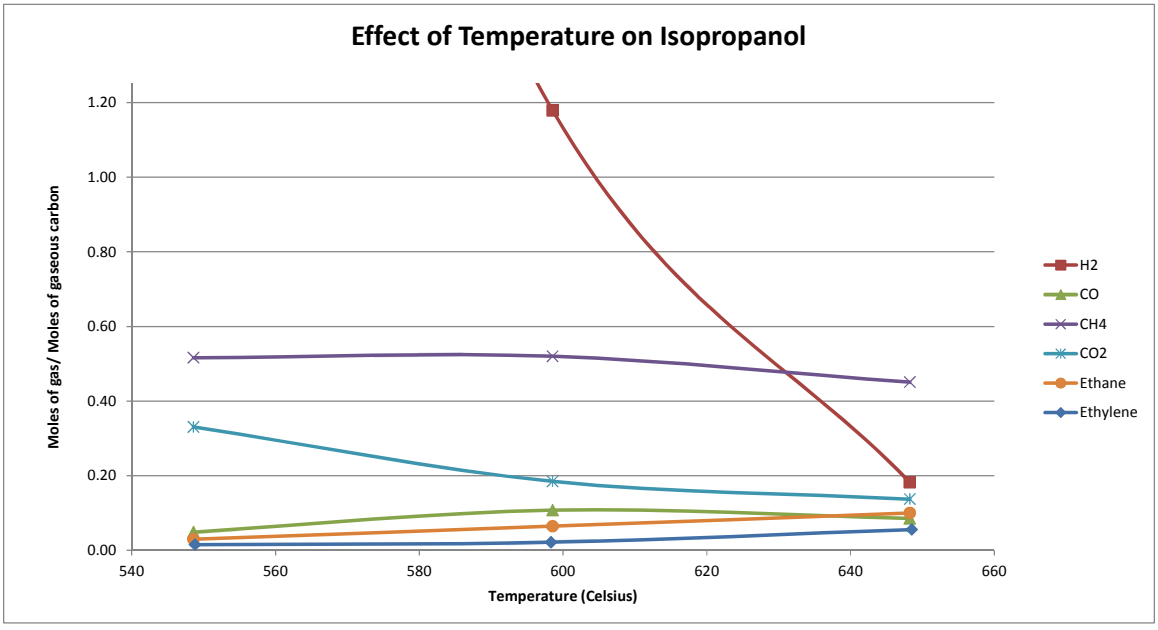

Figure 14.* The effect of temperature on the gas composition (moles/moles gaseous carbon) of isopropanol decomposition.

* The hydrogen produced at 550°C was 3.48 moles/moles gaseous carbon. The data point was omitted so that the trends in other gaseous species are more visible.

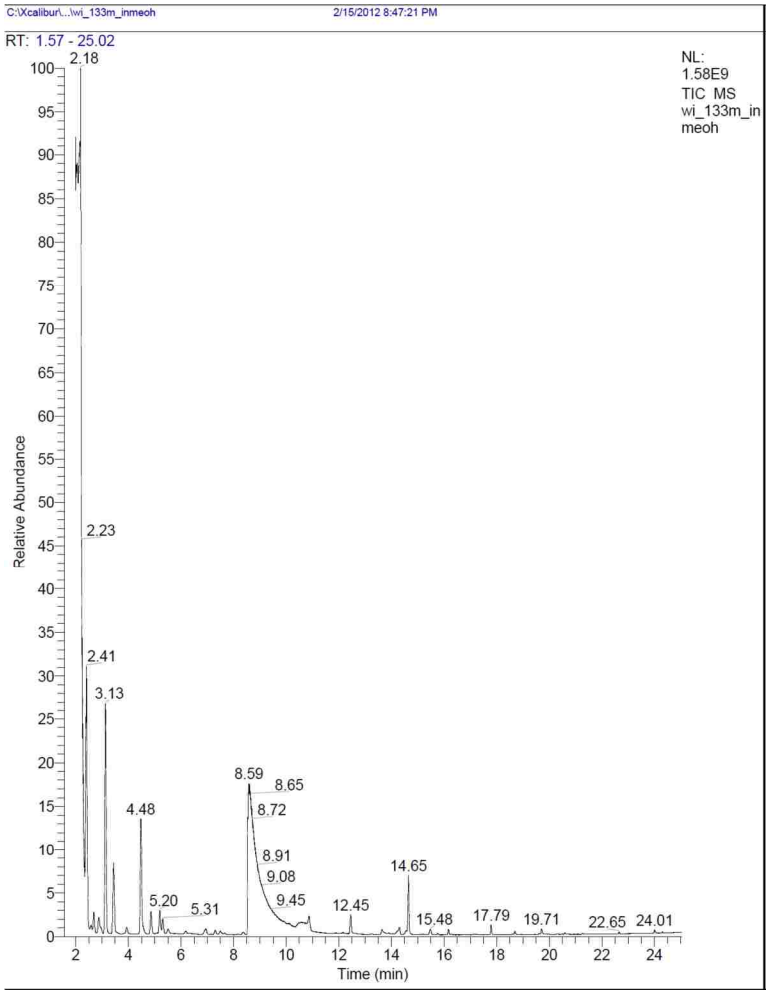

WI-133M	
Residence time	Species
2.18	Isopropanol
2.41	2-Butanone
3.13	2-Pentanone
3.44	Methyl Isobutyl Ketone
4.48	2-Hexanone
8.59	Acetic Acid
14.65	2,5-Hexadione
12.45	Silicon Based Column Bleed

Figure 15. Gas chromatography/mass spectrometry results of liquid sample from experiment WI-133M.

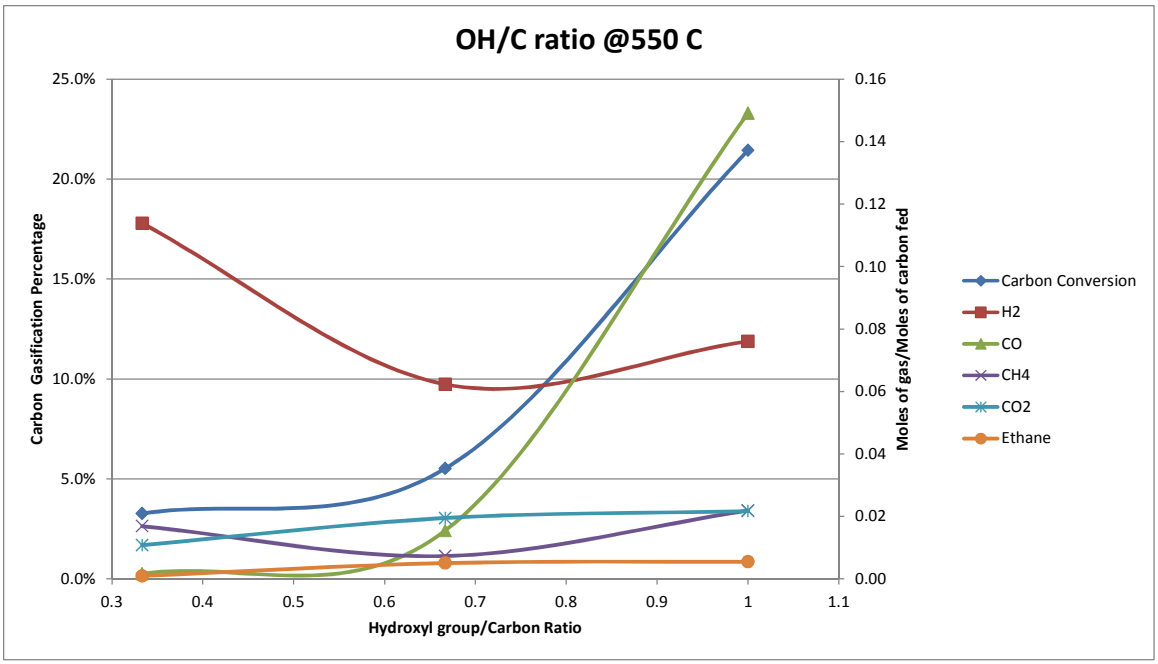

Figure 16. The effect of increasing hydroxyl-to-carbon ratio at 550°C on the carbon gasification and gas composition (moles/moles carbon fed) of hydrocarbons.

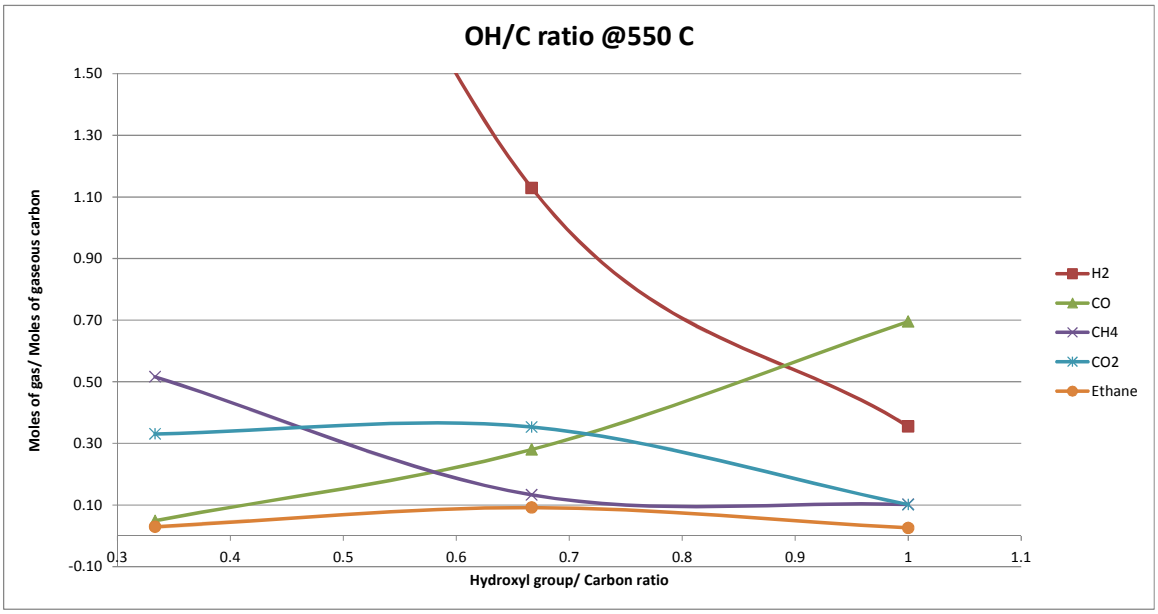

Figure 17.* The effect of increasing hydroxyl-to-carbon ratio at 550°C on the gas composition (moles/moles gaseous carbon) of hydrocarbons.

* The hydrogen produced at from isopropanol (OH/C=.333) was 3.48 moles/moles gaseous carbon. The point was omitted so that the trends in other gaseous species are more visible.

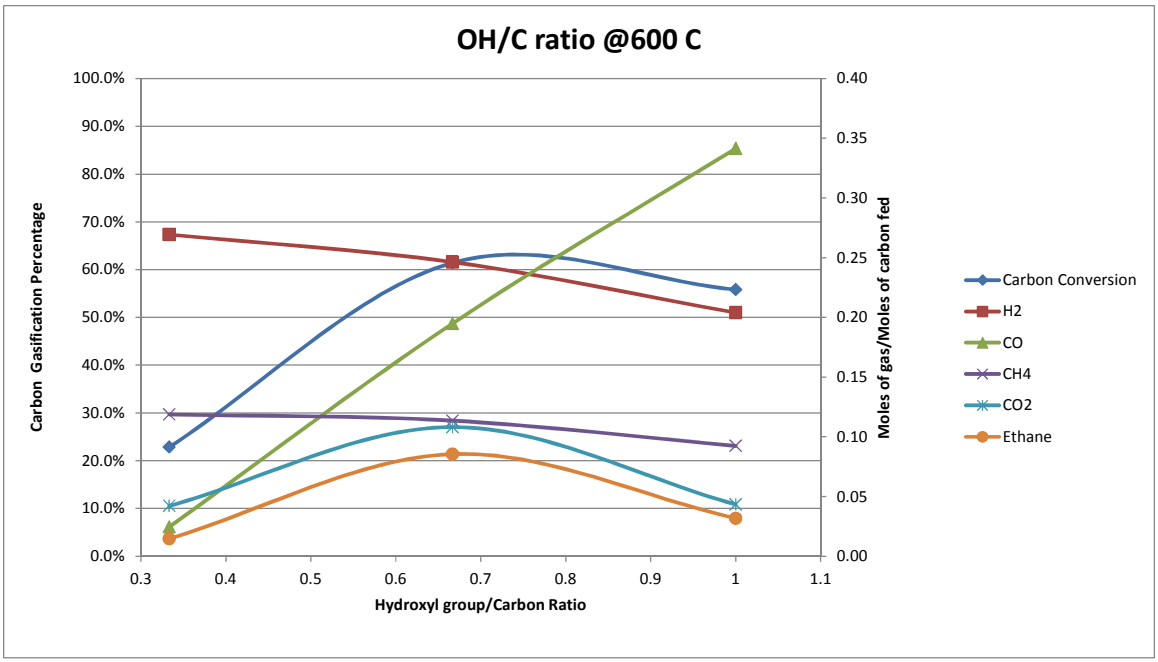

Figure 18. The effect of increasing hydroxyl-to-carbon ratio at 600°C on the carbon gasification and gas composition (moles/moles carbon fed) of hydrocarbons.

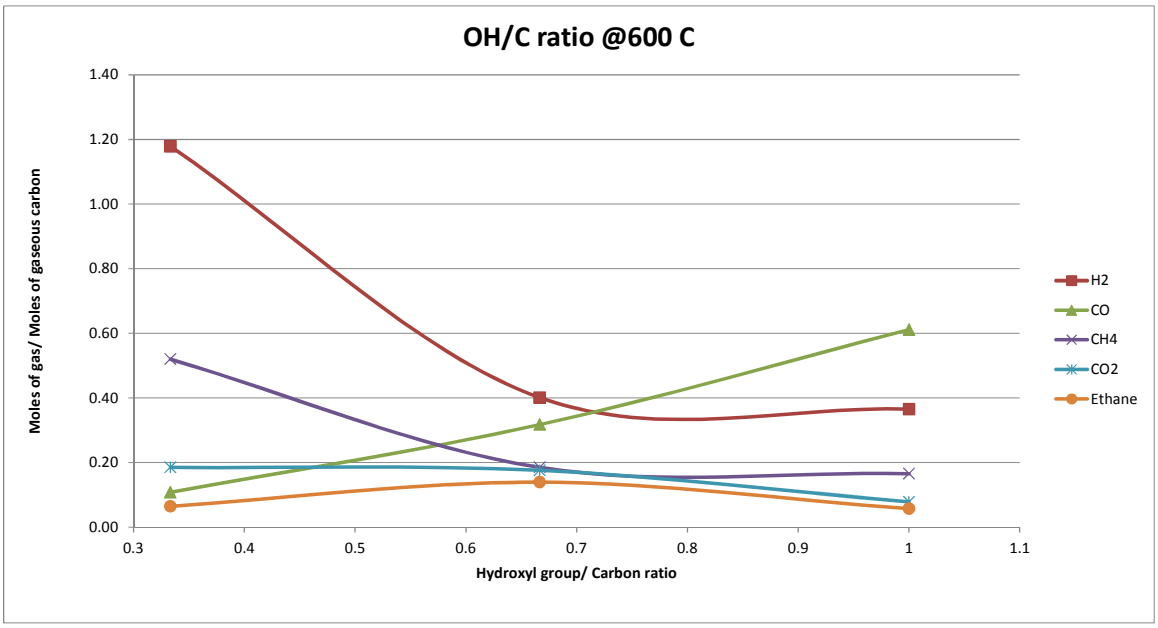

Figure 19. The effect of increasing hydroxyl-to-carbon ratio at 600°C on the gas composition (moles/moles gaseous carbon) of hydrocarbons.

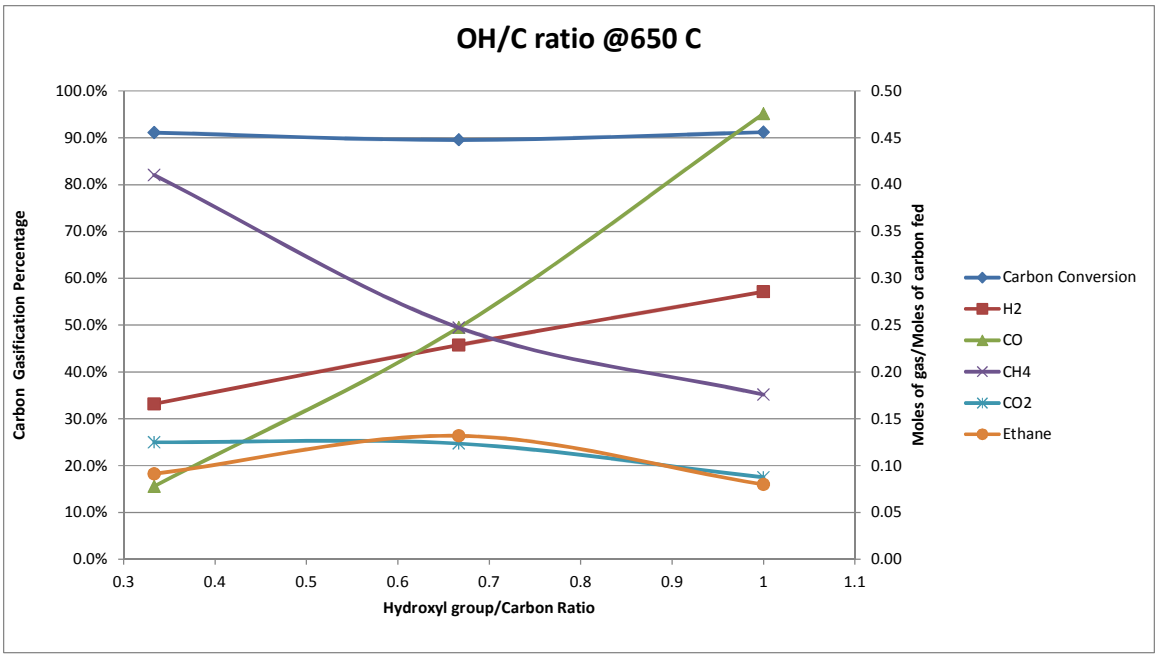

Figure 20. The effect of increasing hydroxyl-to-carbon ratio at 650°C on the carbon gasification and gas composition (moles/moles carbon fed) of hydrocarbons.

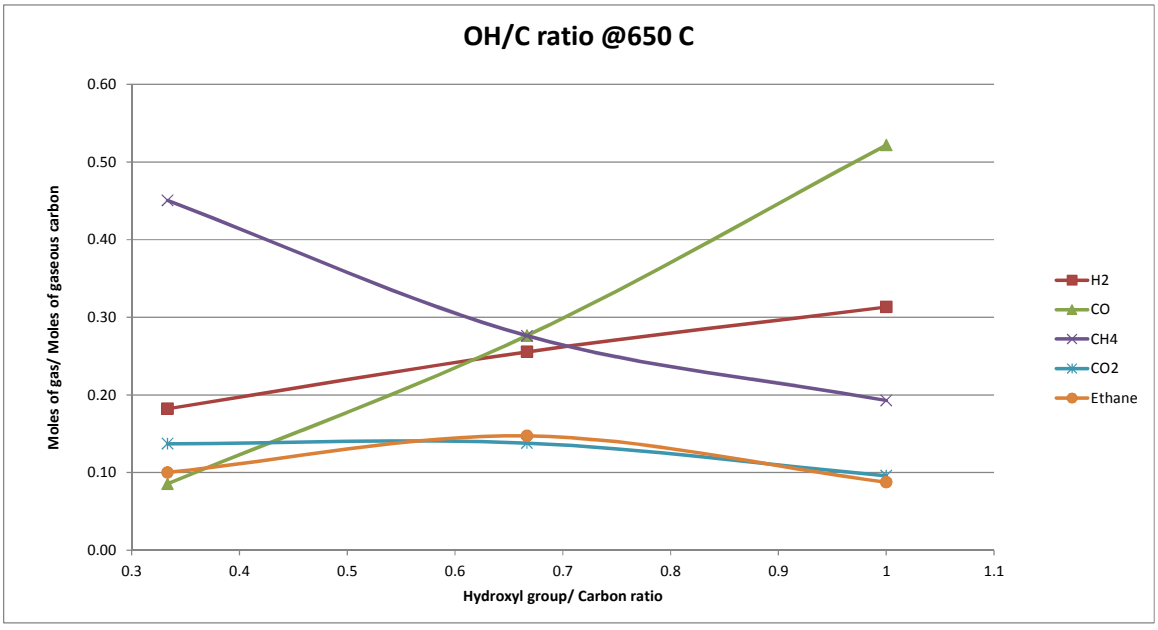

Figure 21. The effect of increasing hydroxyl-to-carbon ratio at 650°C on the gas composition (moles/moles gaseous carbon) of hydrocarbons.

Table 1. Physical properties of glycerin, propylene glycol, isopropanol, and water.

Property	Glycerin	Prop. Glycol	Isopropanol	Water
Molecular Weight (g/mol)	92.09	76.09	60.09	18.02
Density at 25 ˚C and 1 bar (g/cm^3)	1.26	1.032	0.786	0.99
Melting Point (˚C)	17	-60	-88	0
Boiling Point (˚C)	287	189	82	100
Critical Temperature (˚C)	577	353	236	375
Critical Pressure (atm)	74.02	60.2	48.35	217.7

Table 2. Weight and mole percent of the water/fuel solutions.

Solution Type		Weight percent		Mole percent	
Fuel	Water/fuel molar r	Water%	Fuel%	Water%	Fuel%
Glycerin	8.00	61.03	38.97	88.89	11.11
Propylene Glycol	8.00	65.45	34.55	88.89	11.11
Isopropanol	8.00	70.58	29.42	88.89	11.11

Table 3. Summary of experimental run conditions.

Run No.	Temp	Pressure	Water	Fuel	Fuel wt%	Water/Fuel ratio
	(^{o}C)	(psig)	(g/min)			
WG-126M	549	3498	17.1	Glycerin	38.97	8
WG-127M	599	3485	14.4	Glycerin	38.97	8
WG-128M	648	3452	13.0	Glycerin	38.97	8
WPG-129M	549	3510	13.5	Prop. Gly.	34.55	8
WPG-130M	599	3480	12.2	Prop. Gly.	34.55	8
WPG-131M	648	3456	11.2	Prop. Gly.	34.55	8
WI-132M	549	3501	12.3	Isopropanol	29.42	8
WI-133M	598	3485	11.1	Isopropanol	29.42	8
WI-134M	649	3499	10.6	Isopropanol	29.42	8

Table 4. Summary of experimental run results.

Run No.	Product Gas Flow	Gas Yield (mol gas/mol carbon fed)					
	(L/min)	H_2	CO	CH_4	CO_2	C_2H_4	C_2H_6
WG-126M	1.48	0.08	0.15	0.02	0.02	0.00	0.01
WG-127M	3.21	0.20	0.34	0.09	0.04	0.00	0.03
WG-128M	4.46	0.29	0.48	0.18	0.09	0.00	0.08
WPG-129M	0.50	0.06	0.02	0.01	0.02	0.00	0.01
WPG-130M	3.09	0.25	0.19	0.11	0.11	0.01	0.09
WPG-131M	3.65	0.23	0.25	0.25	0.12	0.00	0.13
WI-132M	0.64	0.11	0.00	0.02	0.01	0.00	0.00
WI-133M	1.89	0.27	0.02	0.12	0.04	0.00	0.01
WI-134M	3.52	0.17	0.08	0.41	0.12	0.05	0.09

CONCLUSIONS

In summary, the effect supercritical water on a crude glycerin solution and other polyols was thoroughly analyzed. Through evaluation of the liquid and gas compositions of the experiments conducted, and comprehensive decomposition mechanism of glycerin in supercritical water was elucidated. Using Gaussian modeling software to evaluate the thermodynamic properties of the reactions that were occurring, it was determined that the primary reactions pathways were those that produced acetaldehyde, formaldehyde, and propionaldehyde. This preferred decomposition pathway was evaluated by comparing the gas composition of carbon monoxide determined experimentally to the value of carbon monoxide calculated using the proposed decomposition pathway. For experiments with high carbon gasification the preferred model matches with the experimental data, while the model deviates from the experimental values for experiments with low carbon gasification due to hydrogen reacting with acrolein and other intermediate liquid species.

The effect of temperature, space time, water-to-carbon molar ratio, pressure, and glycerin-to-methanol weight ratio on the gas composition and carbon gasification was determined as well. Overall, increasing temperature, space time, and water-to carbon molar ratio increased the amount of carbon gasification. Increased methane and ethane with decreasing hydrogen and carbon monoxide selectivity was observed with increasing temperatures and space times. Changing the glycerin-to-methanol weight ratio had no effect on the amount of carbon gasification, showing that glycerin and methanol decompose at the same rate. Additionally, a set of empirical equations for carbon monoxide, methane, and ethane were elucidated to show the linear trend in the selectivity of the gases with temperature and space time.

Finally the role of the hydroxyl group in supercritical water was determined by conducting experiments using glycerin, propylene glycol, and isopropanol. Decomposition mechanisms for all three hydrocarbons were determined, and the mechanisms for glycerin and propylene glycol were evaluated by comparing them to gas compositions found experimentally. In addition, it was shown that increasing the hydroxyl group-to-carbon ratio increased the amount of carbon gasification as well as the amount of carbon monoxide produced. Species with fewer hydroxyl groups were shown to produce more methane.

REFERENCES

(1) Renewable Energy Policy Network for the 21st Century Renewables 2010 Global Status Report. 2010.

(2) US Energy Information Administration Annual Energy Review 2009. (accessed 09/02, 2011).

(3) Bunyakiat, K.; Makmee, S.; Sawangkeaw, R.; Ngamprasertsith, S. Continuous Production of Biodiesel via Transesterification from Vegetable Oils in Supercritical Methanol. *Energy Fuels* 2006*, 20*, 812-817.

(4) Jungermann, E.; Sonntag, N. O. V. In *Glycerine, a Key Cosmetic Ingredient;* Marcel Dekker Inc.: New York, 1991.

(5) Nilles, D. A Glycerin Factor. *Biodiesel Magazine* 2005.

(6) National Insititute of Standards and Technology Water Phase Change Properties.

(7) Picou, J.; Lanterman, B.; Wenzel, J.; Lee, S. In *In Autothermal Non-Catalytic Reformation of Jet Fuel in Supercritical Water Medium;* American Institute of Chemical Engineers: 2007.

(8) Picou, J.; Wenzel, J.; Lanterman, B.; Lee, S. Hydrogen Production by Noncatalytic Autothermal Reformation of Aviation Fuel Using Supercritical Water. *Energy Fuels* 2009*, 23*.

(9) Picou, J.; Wenzel, J.; Stever, M.; Bouquet, J.; Lee, S. In *In Noncatalytic Reformation of Sucrose in Supercritcal Water;* American Institute of Chemical Engineers: 2008.

(10) Stever, M.; Picou, J.; Bouquet, J.; Lee, S. In *In Effect of Water to Sucrose Ratio and Pressure on Hydrogen Production During Supercritical Water Reformation of Sucrose;* American Institute of Chemical Engineers: 2008.

(11) Stever, M.; Picou, J.; Wenzel, J.; Putta, S.; Lanterman, B.; Lee, S. In *In Effects of Supercritical and Subcritical Pressuresof Water on Coke Formation During Jet-A Reformation to Hydrogen;* American Institute of Chemical Engineers: 2008.

(12) Wenzel, J.; Niemoeller, A.; Stever, M.; Lee, S. In *In Kinetics of Reforming Ethanol into Hydrogen in a Supercritical Water Medium;* American Institute of Chemical Engineers: 2007.

(13) Wenzel, J.; Picou, J.; Lee, S. In *In Control of Ethanol Dehydration in the Supercritical Water Refromation of Ethanol into Hydrogen;* American Institute of Chemical Engineers: 2008.

(14) Bühler, W.; Dinjus, E.; Ederer, H. J.; Kruse, A.; Mas, C. Ionic reactions and pyrolysis of glycerol as competing reaction pathways in near- and supercritical water. *The Journal of Supercritical Fluids* 2002*, 22*, 37-53.

(15) Boukis, N.; Diem, V.; Habicht, W.; Dinjus, E. Methanol Reforming in Supercritical Water. *Ind Eng Chem Res* 2003*, 42*, 728-735.

(16) Lee, S. In *Alternative Fuels;* Taylor & Francis: Philadelphia, 1996; Vol. 1, pp 140-151.

(17) J.C. Thompson, B. B. H. Characterization of Crude Glycerol from Biodiesel Production from Multiple Feedstocks. *Applied Engineering in Agriculture* 2006*, 22*, 261-265.

(18) Van Gerpen, J.; Shanks, B.; Pruszko, R. Biodiesel Production Technology. 2004.

(19) van Bennekom, J. G.; Venderbosch, R. H.; Assink, D.; Heeres, H. J. Reforming of methanol and glycerol in supercritical water. *The Journal of Supercritical Fluids* 2011*, 58*, 99-113.

(20) Bouquet, J.; Picou, J.; Stever, M.; Wenzel, J.; Tschannen, R.; Lee, S. In *In The Effects of Temperature Upon the Supercritical Water Reformation of Alcohols for Hydrogen Production*.

(21) Gadhe, J. B.; Gupta, R. B. Hydrogen Production by Methanol Reforming in Supercritical Water: Suppression of Methane Formation. *Ind Eng Chem Res* 2005*, 44*, 4577-4585.

(22) Watanabe, M.; Iida, T.; Aizawa, Y.; Aida, T. M.; Inomata, H. Acrolein synthesis from glycerol in hot-compressed water. *Bioresour. Technol.* 2007*, 98*, 1285-1290.

(23) Lauriol-Garbey, P.; Postole, G.; Loridant, S.; Auroux, A.; Belliere-Baca, V.; Rey, P.; Millet, J. M. M. Acid–base properties of niobium-zirconium mixed oxide catalysts for glycerol dehydration by calorimetric and catalytic investigation. *Applied Catalysis B: Environmental* 2011*, 106*, 94-102.

(24) Corma, A.; Huber, G. W.; Sauvanaud, L.; O'Connor, P. Biomass to chemicals: Catalytic conversion of glycerol/water mixtures into acrolein, reaction network. *Journal of Catalysis* 2008*, 257*, 163-171.

(25) Sato, S.; Akiyama, M.; Takahashi, R.; Hara, T.; Inui, K.; Yokota, M. Vapor-phase reaction of polyols over copper catalysts. *Applied Catalysis A: General* 2008*, 347*, 186-191.

(26) Wawrzetz, A.; Peng, B.; Hrabar, A.; Jentys, A.; Lemonidou, A. A.; Lercher, J. A. Towards understanding the bifunctional hydrodeoxygenation and aqueous phase reforming of glycerol. *Journal of Catalysis* 2010*, 269*, 411-420.

(27) Suprun, W.; Lutecki, M.; Haber, T.; Papp, H. Acidic catalysts for the dehydration of glycerol: Activity and deactivation. *Journal of Molecular Catalysis A: Chemical* 2009*, 309*, 71-78.

(28) Antal Jr., M. J.; Mok, W. S. L.; Roy, J. C.; -Raissi, A. T.; Anderson, D. G. M. Pyrolytic sources of hydrocarbons from biomass. *J. Anal. Appl. Pyrolysis* 1985*, 8*, 291-303.

(29) Ramayya, S.; Brittain, A.; DeAlmeida, C.; Mok, W.; Antal Jr, M. J. Acid-catalysed dehydration of alcohols in supercritical water. *Fuel* 1987*, 66*, 1364-1371.

(30) Valliyappan, T. Hydrogen or Syn Gas Production from Glycerol Using Pyrolysis and Steam Gasification Processes, University of Saskatchewan, 2004.

(31) Chaudhari, S. T.; Bej, S. K.; Bakhshi, N. N.; Dalai, A. K. Steam Gasification of Biomass-Derived Char for the Production of Carbon Monoxide-Rich Synthesis Gas. *Energy Fuels* 2001*, 15*, 736-742.

(32) May, A.; Salvadó, J.; Torras, C.; Montané, D. Catalytic gasification of glycerol in supercritical water. *Chem. Eng. J.* 2010*, 160*, 751-759.

(33) Schmidt, L. D. In *The Engineering of Chemical Reactions;* Oxford University Press: 1998.

(34) Trenwith, A. B. Thermal decomposition of isopropanol. *J. Chem. Soc. , Faraday Trans. 1* , 2405.

(35) Zhang, J. H.; Zhou, X. L.; Wang, J. A. Water promotion or inhibition effect on isopropanol decomposition catalyzed with a sol–gel MgO-Al2O3 catalyst. *Journal of Molecular Catalysis A: Chemical* 2006*, 247*, 222-226.

(36) Hinshelwood, C. N.; Hutchison, W. K. In *In A Homogeneous Unimolecular Reactions-The Thermal Decomposition of Acetone in the Gaseous State;* 1926; Vol. 111, pp 245-257.

(37) Guenther, W. B.; Walters, W. D. The Thermal Decomposition of Ketene1. *J. Am. Chem. Soc.* 1959*, 81*, 1310-1315.

(38) Andraos, J.; Kresge, A. J. Correlation of rates of uncatalyzed and hydroxide-ion catalyzed ketene hydration. A mechanistic application and solvent isotope effects on the uncatalyzed reaction. *Can. J. Chem.* 2000*, 78*, 508-515.

(39) Nguyen, M. T.; Sengupta, D.; Raspoet, G.; Vanquickenborne, L. G. Theoretical Study of the Thermal Decomposition of Acetic Acid: Decarboxylation Versus Dehydration. *J. Phys. Chem.* 1995*, 99*, 11883-11888.

(40) Feldman, M. H.; Burton, M.; Ricci, J. E.; Davis, T. W. Determination of Free Radicals in Acetone Photolysis. *J. Chem. Phys.* 1945*, 13*, 440-447.

(41) Gottifredi, J. C.; Yeramian, A. A.; Cunningham, R. E. Vapor-phase reactions catalyzed by ion exchange resins: I. Isopropanol dehydration. *Journal of Catalysis* 1968*, 12*, 245-256.

(42) de Miguel, S. R.; Caballero Martinez, A.; Castro, A. A.; Scelza, O. A. Effect of lithium addition upon ?-Al2O3 for isopropanol dehydration. *Journal of Chemical Technology & Biotechnology* 1996*, 65*, 131-136.

(43) Laidler, K. J.; Wojciechowski, B. W. Kinetics of the Thermal Decomposition of Propylene, and of Propylene-Inhibited Hydrocarbon Decompositions. *Proceedings of the Royal Society of London. Series A. Mathematical and Physical Sciences* 1960*, 259*, 257-266.

(44) Laidler, K. J.; Sagert, N. H.; Wojciechowski, B. W. Kinetics and Mechanisms of the Thermal Decomposition of Propane. I. The Uninhibited Reaction. *Proceedings of the Royal Society of London. Series A. Mathematical and Physical Sciences* 1962*, 270*, 242-253.

(45) Dai, Z.; Hatano, B.; Tagaya, H. Decomposition of a polyol in supercritical water. *Polym. Degrad. Stab.* 2003*, 80*, 353-356.

(46) Ramos, M. C.; NavascuÃ©s, A. I.; GarcÃa, L.; Bilbao, R. Hydrogen Production by Catalytic Steam Reforming of Acetol, a Model Compound of Bio-Oil. *Ind Eng Chem Res* 2007*, 46*, 2399-2406.

(47) Dai, Z.; Hatano, B.; Tagaya, H. Catalytic dehydration of propylene glycol with salts in near-critical water. *Applied Catalysis A: General* 2004*, 258*, 189-193.

(48) Brown, N. F.; Barteau, M. A. Reactions of 1-propanol and propionaldehyde on rhodium(111). *Langmuir* 1992*, 8*, 862-869.

(49) Smith, R. E. The decomposition of acetaldehyde and deutero-acetaldehyde. *Transactions of the Faraday Society* 1939*, 35*, 1328-1336.

(50) Thompson, H. W.; Frewing, J. J. Homogeneous catalysis: the decomposition of acrolein catalysed by iodine. *Trans. Faraday Soc.*, 1660.

(51) Shekhar, R.; Barteau, M. A. Decarbonylation and hydrogenation reactions of allyl alcohol and acrolein on Pd(110). *Surf. Sci.* 1994*, 319*, 298-314.

(52) Pagliaro, M.; Rossi, M. In *The Future of Glycerol: New Uses of a Versatile Raw Material;* RSC Green Chemistry Book Series; RSC Publishing: Cambridge, 2008.

(53) Anonymous Haynes 282 Alloy. 2008.

(54) Smith, J. G. In *Organic Chemistry;* McGraw Hill: New York, 2007; pp 435.

(55) Laino, T.; Tuma, C.; Curioni, A.; Jochnowitz, E.; Stolz, S. A Revisited Picture of the Mechanism of Glycerol Dehydration. *J Phys Chem A* 2011*, 115*, 3592-3595.

(56) Mäki-Arvela, P.; Hájek, J.; Salmi, T.; Murzin, D. Y. Chemoselective hydrogenation of carbonyl compounds over heterogeneous catalysts. *Applied Catalysis A: General* 2005*, 292*, 1-49.

(57) Warneck, P. In *Chemistry of the Natural Atmosphere;* International Geophysics Series; Academic Press: San Diego, California, 1988; Vol. 41.

(58) Barnard, J. A.; Hughes, H. W. D. The pyrolysis of n-propanol. *Trans. Faraday Soc.* 1960*, 56*.

(59) Cortright, R. D.; Davda, R. R.; Dumesic, J. A. Hydrogen from Catalytic Refroming of Biomass-Derived Hydrocarbon in Liquid Water. *Nature* 2002*, 418*, 964-967.

(60) Honma, T.; Hakamada, M.; Sato, Y.; Tajima, K.; Hattori, H.; Inomata, H. In *In Density Functional Theory Study of Glyceraldehyde Hydrolysis in Supercritical Water;* American Institute of Chemical Engineers 2006 Annual Meeting; American Institute of Chemical Engineers: San Francisco, 2006.

(61) Byrd, A. Hydrogen production in supercritical water, Auburn University, 2011.

(62) Atkins, P.; Paula, J. In *Physical Chemistry;* W.H. Freeman and Company: New York, 2002; Vol. 1, pp 1139.

(63) Broekhuis, R. R.; Lynn, S.; King, C. J. Recovery of Propylene Glycol from Dilute Aqueous Solutions via Reversible Reaction with Aldehydes. *Ind Eng Chem Res* 1994*, 33*, 3230-3237.

VITA

Jared Bouquet was born in Saint Louis, Missouri, USA on June 24, 1987. In May of 2008 he received his B.S. in Chemical Engineering from Missouri University of Science and Technology in Rolla, Missouri, USA. In 2008, he joined Dr. Sunggyu Lee's laboratory at Missouri University of Science and Technology as a research assistant. In 2010 he was awarded a Graduate Assistance in Areas of National Need (GAANN) Fellowship. He became a visiting scholar at Ohio University in Athens, Ohio, USA in 2010, where he helped establish the Sustainable Energy and Advanced Materials (SEAM) Laboratory. In May 2012, he received his Ph.D. in Chemical Engineering from Missouri University of Science and Technology.

He has published conference and peer-reviewed papers, some of which are listed with the references in this research. Jared Bouquet has been a member of the American Institute of Chemical Engineers (AIChE) since 2006. He has also been a member of Alpha Chi Sigma since 2008.